Institut für Wasserbau · Universität Stuttgart

Mitteilungen

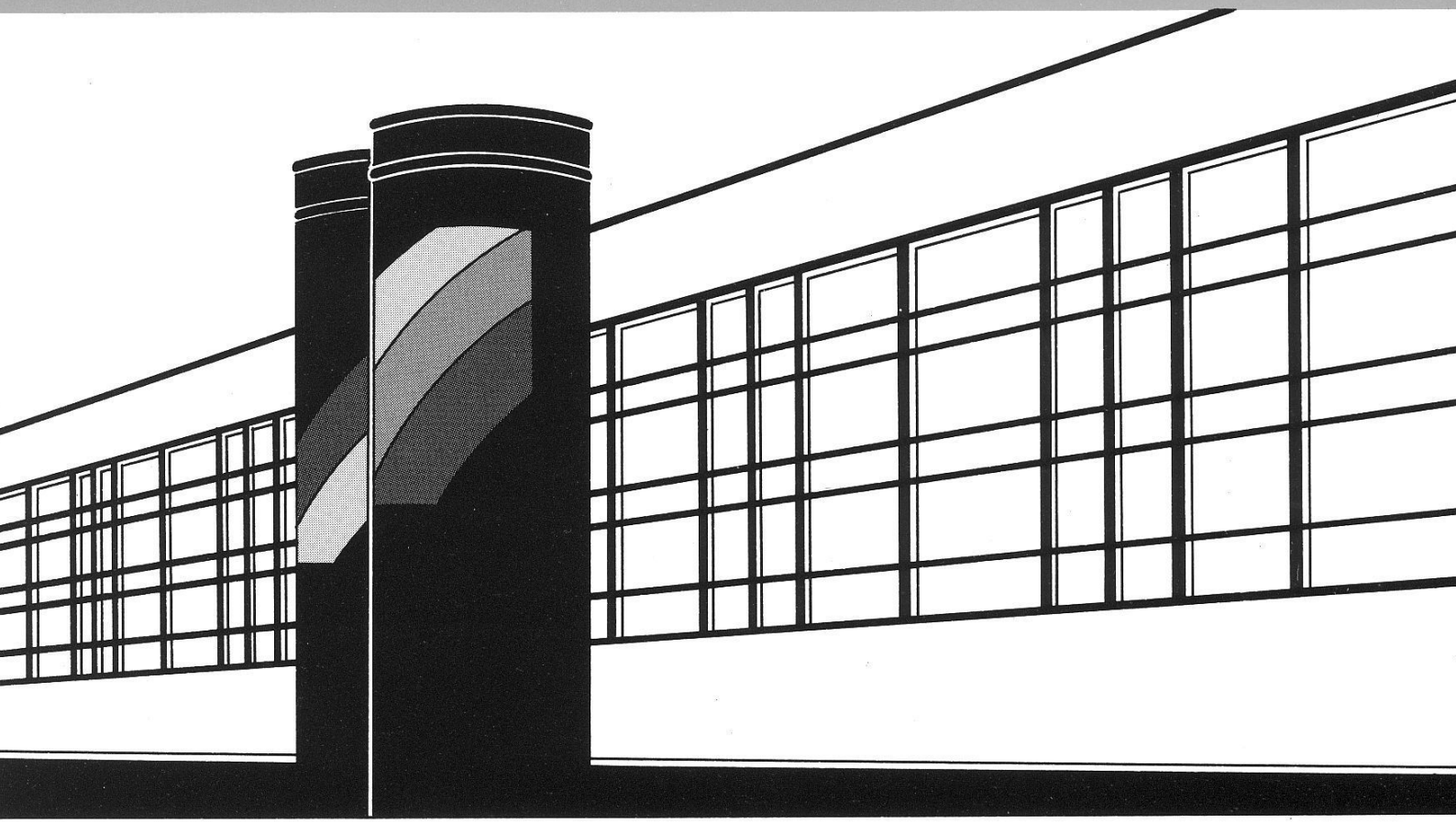

Heft 164 Jens Götzinger

Distributed Conceptual Hydrological Modelling - Simulation of Climate, Land Use Change Impact and Uncertainty Analysis

Distributed Conceptual Hydrological Modelling - Simulation of Climate, Land Use Change Impact and Uncertainty Analysis

Von der Fakultät Bau- und Umweltingenieurwissenschaften der Universität Stuttgart zur Erlangung der Würde eines Doktor-Ingenieurs (Dr.-Ing.) genehmigte Abhandlung

Vorgelegt von

Jens Götzinger

aus Landstuhl

Hauptberichter:	Prof. Dr. rer. nat. Dr.-Ing. András Bárdossy
Mitberichter:	Prof. Dr. Taha B.M.J. Ouarda, Ph.D.

Tag der mündlichen Prüfung: 19. Juli 2007

Institut für Wasserbau der Universität Stuttgart
2007

Heft 164

Distributed Conceptual Hydrological Modelling - Simulation of Climate, Land Use Change Impact and Uncertainty Analysis

von
Dr.-Ing.
Jens Götzinger

Eigenverlag des Instituts für Wasserbau der Universität Stuttgart

D93 Distributed Conceptual Hydrological Modelling -Simulation of Climate, Land Use Change Impact and Uncertainty Analysis

Titelaufnahme der Deutschen Bibliothek

Götzinger, Jens:
Distributed Conceptual Hydrological Modelling - Simulation of Climate, Land Use Change Impact and Uncertainty Analysis / von Jens Götzinger. Institut für Wasserbau, Universität Stuttgart. Stuttgart: Inst. für Wasserbau, 2007

(Mitteilungen / Institut für Wasserbau, Universität Stuttgart: H. 164)
Zugl.: Stuttgart, Univ., Diss., 2007)
ISBN 3-933761-68-9
NE: Institut für Wasserbau <Stuttgart>: Mitteilungen

Herausgegeben 2007 vom Eigenverlag des Instituts für Wasserbau
Druck: Sprint-Druck, Stuttgart

Acknowledgements

During the preparation of this thesis I have become indebted to too many people to mention them all in this section. The first is my supervisor Prof. Dr. rer. nat. Dr.-Ing. András Bárdossy who has given me the chance to work in his group and has supported me with enough ideas for at least another Ph.D. thesis. Second, Prof. Dr. Taha B.M.J. Ouarda, Ph.D. for accepting to co-supervise my thesis and the interesting discussions we had, not only about hydrology, during his time in Stuttgart.

Many thanks are due to all co-workers in RIVERTWIN for the good atmosphere and cooperation; especially to Thomas Gaiser for managing this extremely diverse consortium and keeping us all on track and in time; to Johanna Jagelke and Roland Barthel who have developed the groundwater model for the fruitful teamwork; to Andreas Printz and Hans-Georg Schwarz-von Raumer who solved many GIS problems and provided the land use scenarios and other datasets and to Martha Fernandez for the irrigation water demand time series.

Jürgen Brommundt, Ferdinand Beck, Jan Bliefernicht and Christian Ebert have helped a lot by proof-reading and giving valuable suggestions which improved the final version. The help of Michelle Bester with the English language is also gratefully acknowledged. Furthermore, thanks to all colleagues at the Institute for Hydraulic Engineering for the overall good working atmosphere and the indispensable coffee breaks.

Most of the research this thesis is based on was funded by the European Union in the Sixth Framework Program through the project RIVERTWIN. Data was kindly provided by the State Institute for Environmental Protection Baden-Württemberg and the Direction de l'Hydraulique, Benin.

Last but not least, I want to thank my partner Caro for her continuous support, help and understanding during this project.

Contents

List of Figures

List of Tables

List of Abbreviations

Abbreviation	Meaning
m.a.s.l.	above sea level
ASECNA	Agency for Air Navigation Safety in Africa and Madagaskar
BFI	Baseflowindex
BMBF	Federal Ministry for Education and Research of Germany (Bundesministerium für Bildung und Forschung)
CASIMIR	Computer Aided Simulation System for Instream Flow Requirements
DGE	Directorate General for Water of Benin (Direction Générale de l'Eau)
DKRZ	German High Performance Computing Centre for Climate- and Earth System Research (Deutsches Klimarechenzentrum)
DWD	German Weather Service (Deutscher Wetterdienst)
EU	European Union
FORTRAN	Formula Translator (Programming language)
GIS	Geographical Information System
HBV	A Swedish rainfall-runoff model
IAHS	International Association of Hydrological Sciences
IPCC	Intergovernmental Panel on Climate Change
IWRM	Integrated Water Resources Management
LARSIM	Large Area Simulation Model
LUBW	State Institute for Environmental Protection Baden-Württemberg (Landesanstalt für Umwelt, Messungen und Naturschutz)
MODFLOW	Modular Three-dimensional Finite-difference Groundwater Flow Model
MOSDEW	Model for Sustainable Development of Water Resources
NN	Normalnull (mean sea level)
PUB	Predictions in Ungauged Basins
RIVERTWIN	A Regional Model for Integrated Water Management in Twinned River Basins
SMHI	Swedish Meteorological and Hydrological Institute
SRES	Special Report on Emissions Scenarios (by IPCC)
SRTM	Shuttle Radar Topography Mission by NASA
SVAT	Soil-Vegetation-Atmosphere-Transfer
WEAP	Water Evaluation And Planning System

List of symbols

Symbol	Definition	Unit
α	Exponent of non-linear reservoir	$[-]$
β	Non-linearity parameter of runoff production	$[-]$
$\varepsilon(t)$	Model error	$[m^3/s]$
$\eta(t)$	Normalized model error	$[-]$
$\Phi(x)$	Normal cumulative distribution function	$[-]$
μ	Mean value	[divers]
θ	Model parameter groups	$[-]$
a	Error model coefficient	$[-]$
c	Cell properties	[divers]
D_{test}	Kolmogoroff-Smirnoff D-statistic	$[-]$
$F(x)$	Cumulative distribution function of x	$[-]$
FC	Field capacity	$[mm]$
K	Lipschitz constants	[divers]
k	Index of cell properties	$[-]$
k_i	Recession coefficient of reservoir i	$[-]$
k_{perc}	Maximum percolation rate at soil saturation	$[-]$
L	Number of utilized cell properties	$[-]$
MQ	Mean discharge	$[m^3/s]$
P	Rainfall plus snowmelt	$[mm]$
p	Model parameters	[divers]
P_{eff}	Effective precipitation	$[mm]$
Q_b	Baseflow	$[m^3/s]$
Q_i	Discharge from outlet i of the reservoirs	$[m^3/s]$
$Q_m(t)$	Modelled discharge on day t	$[m^3/s]$
$Q_o(t)$	Observed discharge on day t	$[m^3/s]$
S_i	Water level of reservoir i	$[mm]$
SM	Actual soil moisture	$[mm]$
Std [ ], σ	Standard deviation	[divers]
Var [ ]	Variance	[divers]

Zusammenfassung

Diese Arbeit beschäftigt sich mit der Anwendung räumlich verteilter, konzeptioneller, hydrologischer Modelle zur Simulation der Auswirkungen von Klima- und Landnutzungsänderungen auf den Wasserhaushalt mesoskaliger Einzugsgebiete. Die vier zu beantwortenden Hauptfragestellungen sind:

- Wie lassen sich die Auswirkungen des globalen Wandels auf die Wasserressourcen eines Einzugsgebiets beschreiben und welche Modelle sind notwendig, um diese Effekte abschätzen zu können?
- Wie kann man solche Modelle für die Planung der integrierten Bewirtschaftung von Einzugsgebieten nutzen? Ist es möglich, regionale Modelle verschiedener Sektoren zu verknüpfen, um interdisziplinäre Bewirtschaftungsszenarien zu evaluieren?
- Welche Auswirkungen hat ein sich wandelndes Klima und eine veränderte Landnutzung auf die Wasserressourcen eines Einzugsgebiets?
- Wie kann man die Unsicherheiten solcher Simulationen sinnvoll, mit einem allgemeingültigen Ansatz abschätzen?

Viele der hier vorgestellten Ergebnisse wurden im Rahmen des EU-Projekts RIVERTWIN erzielt. RIVERTWIN steht für "A Regional Model for Integrated Water Management in Twinned River Basins". Projektziel war die Konzeption, Realisierung und Anwendung eines integrierten regionalen Modells zur strategischen Planung der Bewirtschaftung von Einzugsgebieten unter verschiedenen ökologischen, sozialen und ökonomischen Bedingungen im Sinne der EU-Wasserrahmenrichtlinie und der EU-Wasserinitiative. Dieses regionale Modell bildet die Effekte der demographischen und wirtschaftlichen Entwicklung sowie globaler Klima- und Landnutzungsänderungen auf die Wassermenge und -qualität der Gewässer in feucht-gemäßigten, subhumid tropischen und semiariden Gebieten ab. Die Modellintegration wurde zuerst im mitteleuropäischen Neckar-Einzugsgebiet mit guter Datenverfügbarkeit erprobt. Die Übertragbarkeit des Ansatzes auf weitere Regionen mit anderem ökonomischen Niveau, ökologischen Standards und geringerer Datenverfügbarkeit wurde im Ouémé-Einzugsgebiet in Benin (Westafrika) getestet.

Zu diesem Zweck wurde das räumlich aggregierte HBV-Modell in eine rasterbasierte Version umgewandelt. Zur Bestimmung der Modellparameter wurden vier Regionalisierungsmethoden entwickelt und verglichen. Die Verknüpfung mit dem Grundwassermodell MODFLOW wurde durch Austausch der simulierten Grundwasserneubildung und des Basisabflusses realisiert. Die Abschätzung der Auswirkungen des globalen Wandels im Neckar-Einzugsgebiet erfolgte durch die Simulation

von vier Klima- und vier Landnutzungsszenarien. Im Ouémé-Einzugsgebiet kamen zwei Klima- und vier Landnutzungsszenarien zum Einsatz. Im Neckareinzugsgebiet konnten die Ergebnisse mit dem Modell LARSIM der Landesanstalt für Umwelt, Messungen und Naturschutz (LUBW) verglichen werden. Abschließend wurde eine neue Methode zur Analyse der inhärenten Modellunsicherheit entwickelt. Diese stützt sich auf die Aufteilung der Fehler in meteorologische und prozess-basierte Anteile. Die Unsicherheit der Eingangsdaten kann mithilfe stochastischer Methoden beschrieben werden. Die Prozessunsicherheit schließlich wird aus der Modellsensitivität bezüglich bestimmter Parametergruppen abgeleitet. Die Summe beider Teile kann zur Definition eines heteroskedastischen Fehlermodells genutzt werden, das die Kalibrierung hydrologischer Modelle deutlich verbessert.

Daten

Das Neckar-Einzugsgebiet

Das Neckar-Einzugsgebiet liegt in Südwestdeutschland und hat eine Fläche von etwa 14 100 km^2 (Abbildung 0.1). Der Neckar entspringt zwischen Schwarzwald und Schwäbischer Alb und fließt Richtung Norden, um bei Mannheim in den Rhein zu münden. Die Topographie variiert zwischen 93 m ü. NN am Gebietsauslass und bis zu 1022 m ü. NN auf der Schwäbischen Alb. Der im Westen gelegene Schwarzwald besteht hauptsächlich aus kristallinem Grundgestein wohingegen im Osten verkarstete Kalksteinformationen dominieren. Das Neckar-Einzugsgebiet liegt in der feucht-gemäßigten Klimazone. Der jährliche Niederschlag liegt zwischen 700 mm (Tübingen, 370 m ü. NN) und 1680 mm (Freudenstadt, 787 m ü. NN) mit einem Mittelwert von 950 mm. Der mittlere monatliche Niederschlag schwankt zwischen 110 mm im Juni und 66 mm im Oktober. Die Jahresmitteltemperatur beträgt 8.7°C (Minimum 6.4°C in Klippeneck (973 m ü. NN), Maximum 9.1°C in Nürtingen (280 m ü. NN)). Der kälteste Monat ist der Januar (-0.5°C), der wärmste der Juli (17.3°C). Die verwendeten Daten wurden von der LUBW zur Verfügung gestellt. Landnutzungs- (Landsat 1993, Auflösung 30 m), Boden- (Bodenübersichtskarte 200, 1:200 000) und topographische Daten (Auflösung 50 m) wurden auf eine gemeinsame Auflösung von 1 km zusammengefasst. Niederschlags- und Temperaturdaten wurden mit External Drift Kriging (Ahmed and de Marsily, 1987) interpoliert.

Das Ouémé-Einzugsgebiet

Das Ouémé-Einzugsgebiet umfasst etwa 51 500 km^2 und liegt im nördlichen Teil des sedimentären Küstenbereichs und des zentralen kristallinen Teils von Benin (Abbildung 0.1). Die Landschaft wird geprägt durch weitläufige Ebenen, verstreute Inselberge und Plateaus. Der Ouémé durchfließt das Gebiet von Norden nach Süden und mündet in den Lac Nokoué der wiederum mit dem Golf von Benin verbunden ist. Die höchsten Berge im Norden erheben sich bis etwa 617 m ü. NN, wohingegen die Lama Depression im Süden nur wenige Meter über dem Meeresspiegel liegt. Benin liegt im tropischen Westafrika. Die Jahresmitteltemperatur beträgt 27°C, bei Temperaturschwankungen von 5-6°C. Das Land kann in verschiedene Klimazonen eingeteilt werden: die Südsudan-Savannen-Zone mit semi-arider Tendenz und einer einzigen

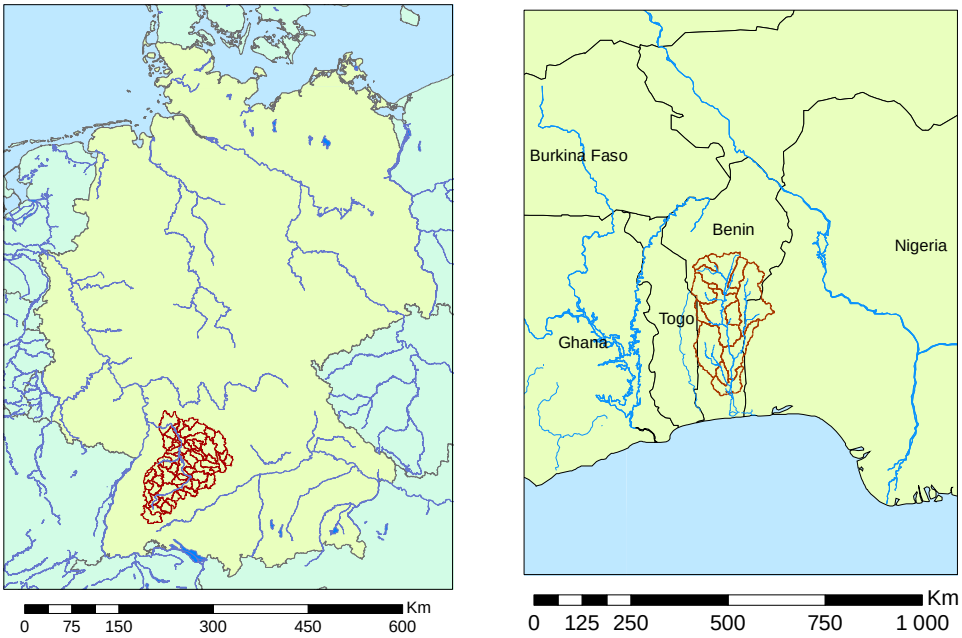

Abbildung 0.1: Lage der Testgebiete: links das Neckar-Einzugsgebiet in Deutschland und rechts das Ouémé-Einzugsgebiet in Westafrika.

Sommerregenzeit in Nord- und Zentralbenin, die subäquatoriale Feuchtsavannen-Zone (Guinea-Savanne) in Zentral und Südbenin und die feuchte subäquatoriale Zone im Süden, die beide zwei Regenzeiten pro Jahr aufweisen (Stahr, 2000). Der mittlere Jahresniederschlag beträgt etwa 1200 mm, die mittlere potentielle Evapotranspiration nach Hargreaves and Samani (1985) jedoch etwa 2800 mm. Meteorologische Daten wurden von der ASECNA (Agency for Air Navigation Safety in Africa and Madagaskar) zur Verfügung gestellt. Landnutzungs- (LANDSAT TM Plus, 2003), Boden (beide 1:200 000) und topographische Daten (Auflösung 90 m) wurden auf eine gemeinsame Auflösung von 3 km zusammengefasst. Niederschlags- und Temperaturdaten wurden ebenfalls mit External Drift Kriging (Ahmed and de Marsily, 1987) interpoliert.

Modelle und Methoden

Zur Simulation des Wasserhaushalts mesoskaliger Einzugsgebiete steht eine große Anzahl hydrologischer Modelle zur Verfügung. Die integrierte Modellierung von Klima- und Landnutzungsänderungen stellt jedoch weitergehende Anforderungen an die verwendeten Ansätze:

- die Verknüpfbarkeit von Modellparametern und Gebietseigenschaften bei der Parametrisierung, um Landnutzungsänderungen abbilden zu können, und
- die Kombinierbarkeit mit anderen Teilmodellen in größeren integrierten Modellkomplexen.

Der erste Punkt wird im Allgemeinen als Regionalisierung bezeichnet und im nächsten Abschnitt näher erläutert. Generell, ist eine hohe zeitliche aber auch räumliche Auflösung wünschenswert. Klimatologische, geographische und auch sozio-ökonomische Daten stehen im Gegensatz dazu jedoch gerade bei der Verwendung von Szenarien oft nur in geringen Auflösungen zur Verfügung. Bei der Modellauswahl muss daher ein Kompromiss zwischen Datenbedarf und -verfügbarkeit getroffen werden. Deshalb wurden in dieser Studie die konzeptionellen Modelle LARSIM und HBV verwendet. LARSIM wird bei der Landesanstalt für Umwelt, Messungen und Naturschutz Baden-Württemberg operationell zur Hochwasservorhersage eingesetzt (Bremicker, 2000). Das HBV Modellkonzept (Bergström, 1995) stammt ursprünglich vom Schwedischen Wetterdienst SMHI und wurde zusätzlich zur räumlich detaillierten Modellstruktur für diese Studie angepasst.

Regionalisierungsverfahren

Vier Regionalisierungsverfahren wurden entwickelt und verglichen:

1. Transferfunktionen
   Dabei werden die Modellparameter, $\boldsymbol{p}$, als lineare oder logistische Funktion von Gebietseigenschaften, $\boldsymbol{c}$, dargestellt und anstelle der Modellparameter die Koeffizienten $\boldsymbol{a}$der Transferfunktionen kalibriert.

$$p = f(a, c) \text{ mit } c \in (Topographie, Landnutzung, Boden, Geologie) \tag{0.1}$$

2. Die modifizierte Lipschitz-Bedingung
   In den Naturwissenschaften wird von ähnlichen Objekten auch ein ähnliches Verhalten erwartet. Diese Annahme kann den Parametern während der Kalibrierung über eine modifizierte Lipschitz-Bedingung aufgeprägt werden:

$$|p_i - p_j| \leq \sum_{k=1}^{L} |c_{ki} - c_{kj}| \cdot K_k. \tag{0.2}$$

3. Die Monotoniebedingung
   Das allgemeine Verhalten unterschiedlicher Teile eines Einzugsgebiets ist meistens bekannt. Die Richtung der Trends der Modellparameter in Abhängigkeit der Gebietseigenschaften kann daher durch das Vorschreiben der Monotoniebedingung während der Kalibrierung vorgegeben werden:

$$\text{wenn } c_{ki} \leq (\geq)\ c_{kj} \quad \text{für alle k, dann } p_i \leq p_j. \tag{0.3}$$

4. Die Kombination der Lipschitz- und Montoniebedingung
   Beide Bedingungen für sich erbrachten keine voll zufriedenstellenden Ergebnisse. Deshalb wurden sie während der Kalibrierung kombiniert.

Modellintegration, Klima- und Landnutzungsszenarien

Die Modellintegration wurde am Beispiel des hydrologischen und des Grundwassermodells demonstriert. Das hydrologische Modell berechnet hierbei Grundwasserneubildungsraten, die als Eingangsdaten in das Grundwassermodell einfließen. Dieses

simuliert unter anderem den Basisabfluss im Gewässer, der wiederum an das hydrologische Modell zurückgegeben wird. Damit kann schließlich der Gesamtabfluss am Gebietsauslass ermittelt werden.

Zur Abschätzung der möglichen Entwicklung des zukünftigen Klimas wurden regionale Klimaszenarien basierend auf Ergebnissen des globalen Klimamodells ECHAM 4 (Roeckner et al., 1996) mit den Emissionsszenarien A2 und B2 des IPCC (Houghton et al., 2001) erstellt. Dazu wurden folgende Methoden angewandt:

- Statistisch-dynamisches Downscaling basierend auf Großwetterlagen (Enke et al., 2005),
- Multivariat-stochastisches Downscaling basierend auf großräumigen Zirkulationsmustern (Yang and Bárdossy, 2005).

Anhand vergangener Entwicklungen und Experteneinschätzungen wurden plausible Landnutzungs- und Benchmarkszenarien für die beiden Einzugsgebiete aufgestellt. Am Neckar ist die Siedlungsentwicklung zu Lasten der Landwirtschaft der Hauptmechanismus der Landnutzungsänderungen. Vorgaben der europäischen Landwirtschaftspolitik könnten zusätzliche Effekte auslösen, die mit den Benchmarkszenarien abgedeckt werden. In Benin ist die Bevölkerungswanderung von Norden nach Süden und die einhergehende Brandrodung der Hauptfaktor. Als Interventionsszenarien wurden darüberhinaus die Errichtung größerer Multifunktionsspeicher betrachtet.

Unsicherheiten der Modellierung

Die meisten Methoden zur Modellkalibrierung und Abschätzung der Modellunsicherheiten setzen normalverteilte Fehler voraus, deren Varianz konstant ist (Homoskedastizität). In den seltensten Fällen ist dies jedoch tatsächlich der Fall, was zur systematisch falschen Einschätzungen sowohl der Parameter als auch der Modellunsicherheiten führt. Deshalb wurde ein neues allgemeingültiges Fehlermodell entwickelt, das zeitlich veränderliche Eingangs- und Prozessunsicherheiten berücksichtigt. Es wird in der Kalibrierung verwendet, um die Fehler zu normalisieren und führt zu realistischeren Konfidenzintervallen des Abflusses als herkömmliche additive oder multiplikative Fehlermodelle. Die Unsicherheit wird aus der Summe der Eingangs- und Prozessunsicherheiten bestimmt. Zur Bestimmung der Unsicherheit des Abflusses durch die räumliche Repräsentation der Eingangsdaten (Temperatur und Niederschlag) dienen stochastische Simulationen dieser Eingangsgrößen.

Die Bestimmung der Prozessunsicherheiten wird anhand einer Sensitivitätsanalyse durchgeführt. Es wird angenommen, dass der Modellfehler durch Prozessunsicherheiten proportional zur Sensitivität ist. Die Gesamtfehlervarianz kann aus den stochastischen Fehlern und den Abflusssensitivitäten bestimmt werden. Die Koeffizienten des Fehlermodells werden gemeinsam mit den Modellparametern bestimmt. Diese Methode führt zu normalverteilten Fehlerzeitreihen, die die variable Dominanz verschiedener Prozesse und Daten repräsentieren. Damit sind die Annahmen der Standardkalibrierungsverfahren erfüllt.

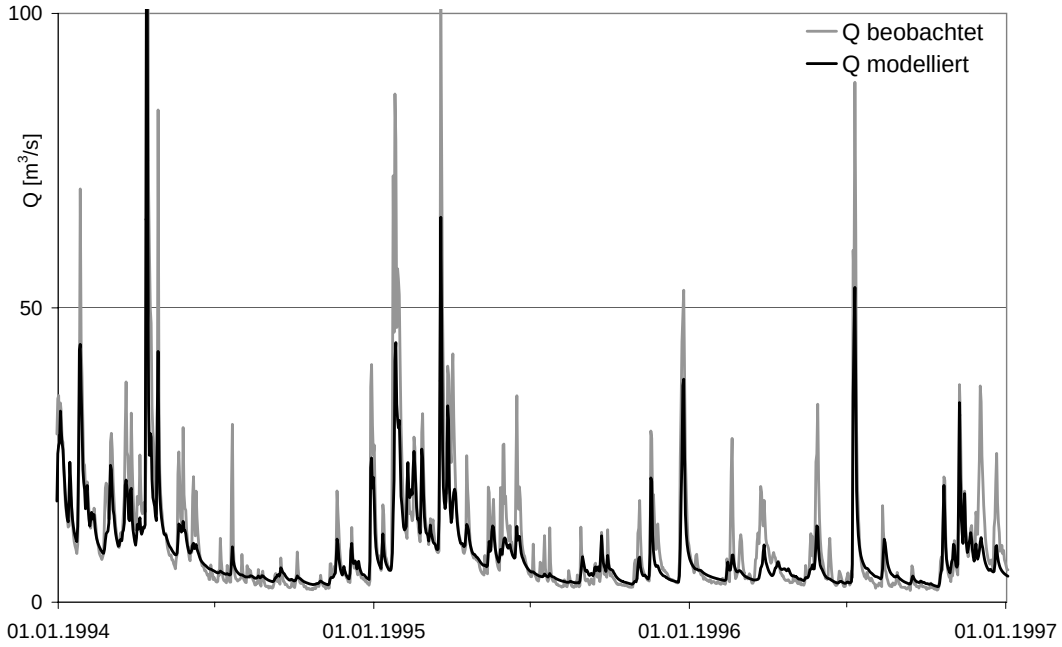

Abbildung 0.2: Beobachtete und simulierte Abflüsse in Gaildorf (Kocher) aus der Kombination von Lipschitz- und Monotoniebedingung (NS = 0,70).

Ergebnisse

Die Modellparameter im Neckar-Einzugsgebiet konnten erfolgreich regionalisiert werden. Abbildung 0.2 zeigt ein Beispiel der Anwendung des Regionalisierungsverfahrens auf ein Teileinzugsgebiet des Neckars. Die Kombination der Lipschitz- und Montoniebedingung führte zu physikalisch kohärenten Parametern und einer mittleren Nash-Sutcliffe Modelleffizienz aller Einzugsgebiete von 0,5 (Tabelle 0.2).

Im Ouémé-Einzugsgebiet konnte in der Validierung eine mittlere Nash-Sutcliffe Modelleffizienz von 0,49 erreicht werden. Allerdings konnte die starke Saisonalität der Abflüsse einschließlich Trockenfallen an manchen Stationen nicht zufriedenstellend reproduziert werden (Abbildung 0.3).

Der Vergleich der verschiedenen simulierten Grundwasserneubildungen und Basisabflüsse zeigt, dass bei der Modellintegration noch Forschungsbedarf besteht. Sowohl der Mittelwert als auch die Variabilität der Ergebnisse der drei verwendeten Modelle ist systematisch unterschiedlich (Abbildung 0.4). Obwohl der Einfluss auf die Gesamtabflusssimulation gering ist, wird die Reproduktion der Niedrigwasserabflüsse doch entscheidend beeinflusst.

Die Simulation von Klima- und Landnutzungsänderungen ist trotz langjähriger Forschung immer noch mit einer großen Unsicherheit behaftet. Für das Neckar-Einzugsgebiet ergeben die hier vorgestellten Berechnungen, dass sowohl der Klimawandel als auch die erwarteten Landnutzungsänderungen in der nahen Zukunft keine signifikanten Auswirkungen auf den mittleren Wasserhaushalt haben werden. Es zeigen sich aber Verschiebungen des Jahresgangs und Änderungen in der Vari-

Tabelle 0.2: Mittelwert und Median der Nash-Sutcliffe Modeleffizienz der Regionalisierungsmethoden im Neckargebiet in der Validierungsperiode.

	Transfer funktionen	Lipschitz-Bedingung	Monotonie-bedingung	Kombination
Kalibrierung Mittel	0.35	0.21	0.06	0.47
Kalibrierung Median	0.49	0.41	0.30	0.53
Regionalisierung Mittel	0.47	0.50	0.47	0.47
Regionalisierung Median	0.51	0.53	0.50	0.50

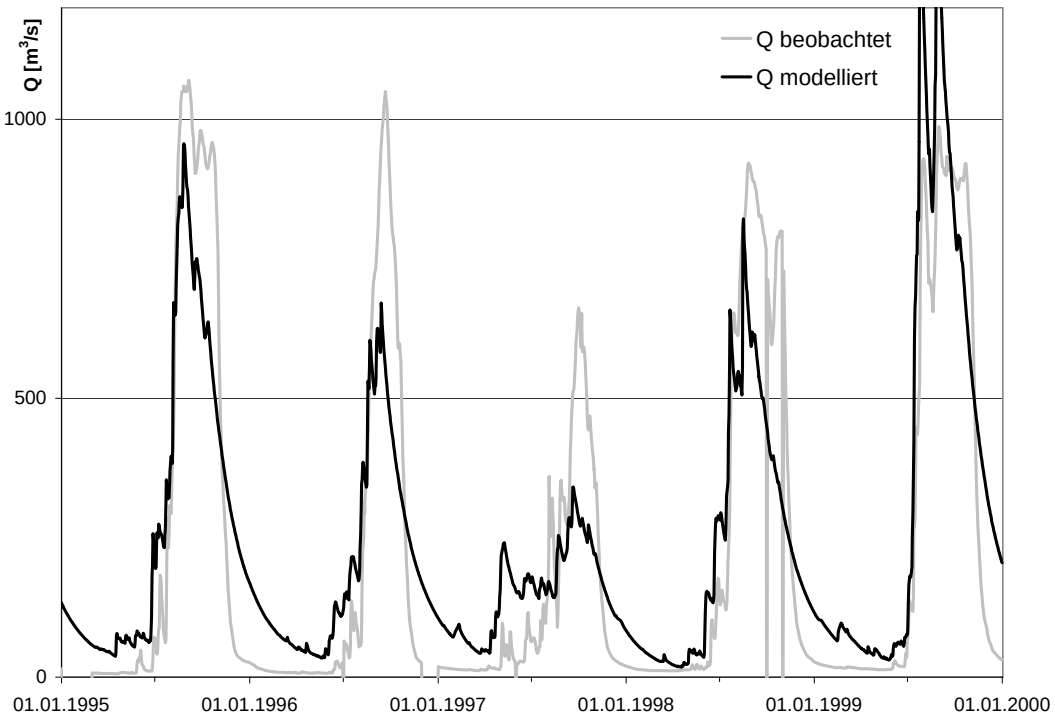

Abbildung 0.3: Simulierte und beobachtete Abflüsse in Bonou aus der Kombination von Lipschitz- und Monotoniebedingung (NS = 0,77).

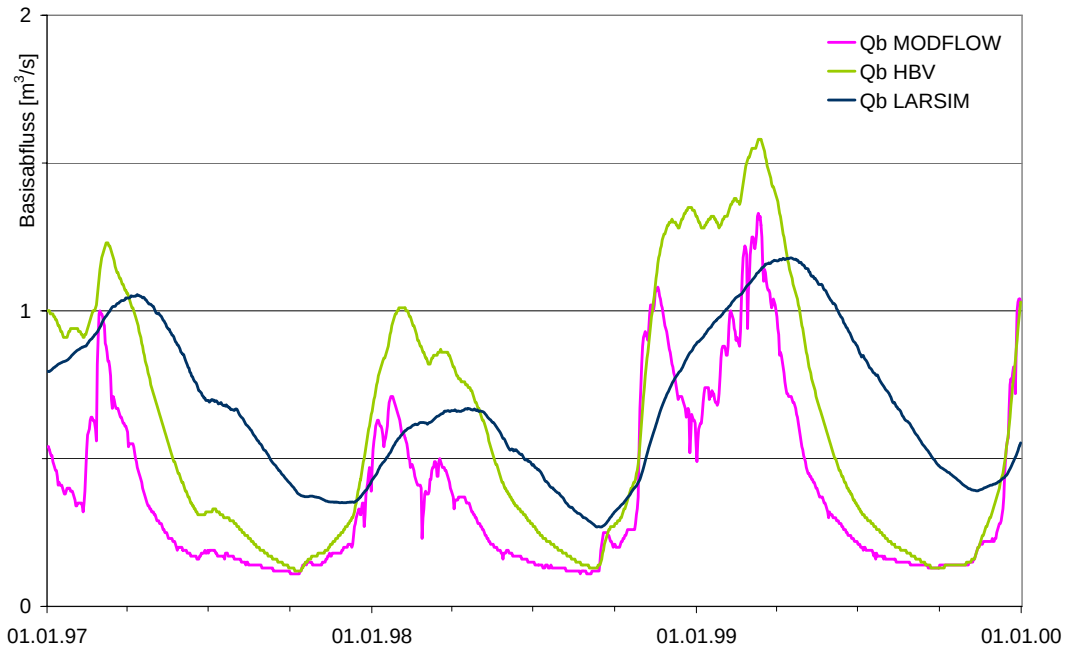

Abbildung 0.4: Mit MODFLOW, HBV und LARSIM simulierte Basisabflussganglinien am Pegel Neuenstadt (1997 - 1999).

abilität, d.h. der Extreme. Dies war jedoch nicht der Fokus dieser Arbeit.

Die Wasserbilanz des Ouémé-Einzugsgebiets wird im Gegensatz dazu schon von geringen Veränderungen in Temperatur und Niederschlag beeinträchtigt, da schon heute im Mittel über 80% des Niederschlags verdunsten. Schon eine geringe Verschiebung dieses fragilen Gleichgewichts könnte daher dramatische Folgen haben. Die Unsicherheiten der Klimamodelle und Downscaling-Methoden ist jedoch noch zu groß, um genauere Aussagen treffen zu können. Die Ausweitung der landwirtschaftlich genutzten Fläche wirkt diesem Trend geringfügig entgegen. Spürbare Verbesserungen der Situation können hingegen nur durch eine erweiterte Wasserspeicherung erreicht werden. Abbildung 0.5 zeigt daher eine Abflusssimulation unter Einbeziehung dreier größerer geplanter Staudämme im Ober-, Mittel- und Unterlauf des Ouémé.

Die Verwendung des heteroskedastischen Fehlermodells in der Kalibrierung führt zu realistischen Konfidenzintervallen der simulierten Abflüsse, die die variable Modellunsicherheit widerspiegeln (Abbildung 0.6). Traditionelle Fehlermodelle ergeben lediglich ein Band konstanter oder relativ zum Abfluss variabler Breite, oder schlagen die gesamte Unsicherheit einer Quelle wie zum Beispiel der Parameterunsicherheit zu. Im Gegensatz dazu gibt das hier vorgestellte Fehlermodell die zeitlich variablen Beiträge der unterschiedlichen Quellen und damit der Gesamtunsicherheit wieder. Die zugrunde liegenden Fehlerverteilungen sind hinreichend normalverteilt und konnten durch Vergleich mit gemessenen Abflüssen validiert werden. Im Unterschied zu den herkömmlichen additiven oder multiplikativen Fehlermodellen, bei denen 93% bzw. 76% der Beobachtungen innerhalb des 80% Konfidenzbereichs liegen, umschließt dieser beim heteroskedastischen Fehlermodell 85% der Messungen.

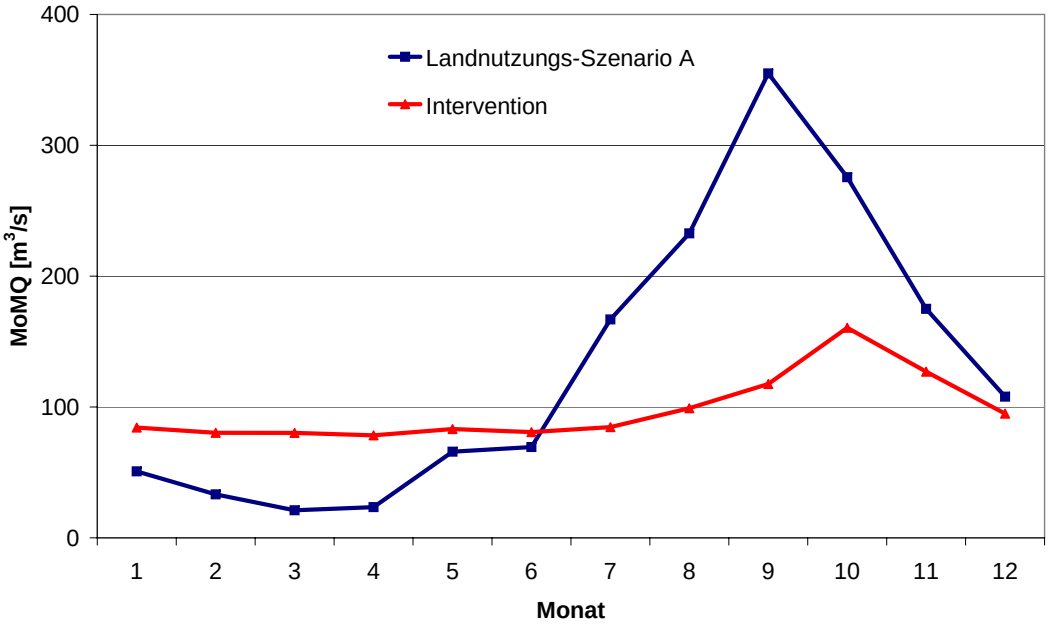

Abbildung 0.5: Mittlerer monatlicher Abfluss in Zagnanado im Interventions- und Landnutzungs-Szenario A.

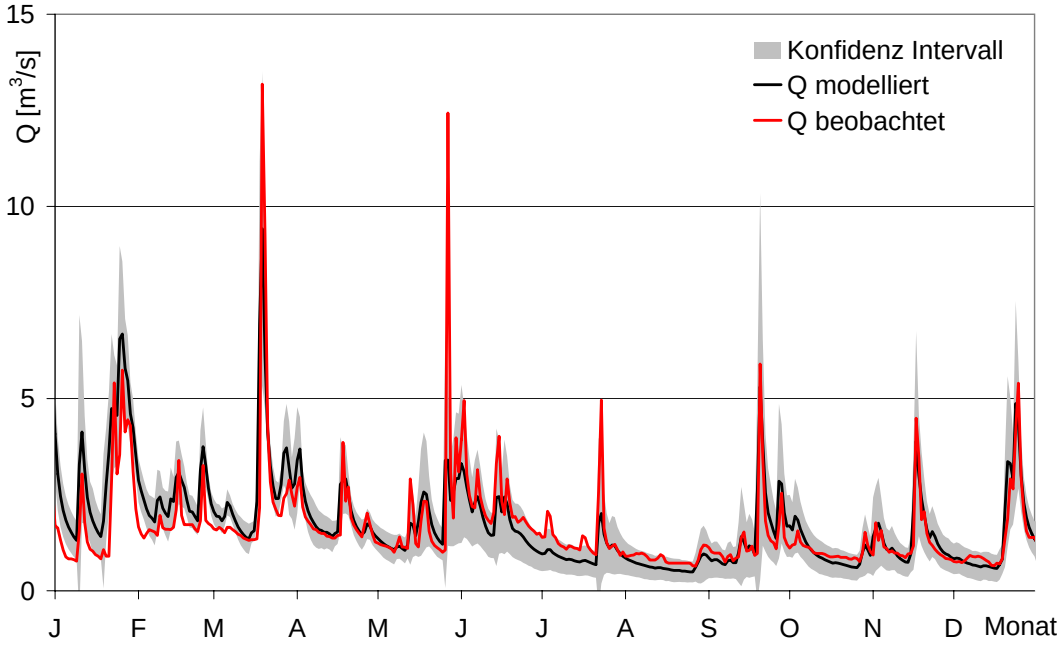

Abbildung 0.6: 80% Konfidenzintervall des heteroskedastischen Fehlermodells für das Jahr 1995 am Pegel Neuenstadt (Maximum-likelihood Kalibrierung).

Schlussfolgerungen

Die Ergebnisse der Regionalisierung von Modellparametern mithilfe der Kombination von Lipschitz- und Monotoniebedingung hat gezeigt, dass die Simulation von Landnutzungsänderungen auch mit konzeptionellen, räumlich verteilten, hydrologischen Modellen möglich ist. Die Verknüpfung mit Gebietseigenschaften reduziert den für die Kalibrierung verfügbaren Parameterraum und somit auch die Unsicherheit des Modells. Die Anwendung am Ouémé hat gezeigt, dass die Methode transferierbar ist und auch in wenig bis unbeobachteten Gebieten die Wasserhaushaltsmodellierung ermöglicht.

Die Modellintegration bietet durch den Abgleich nicht messbarer Größen wie dem Basisabfluss und der Grundwasserneubildung eine zusätzliche Möglichkeit der internen Validierung von Modellen. Dabei wurde offensichtlich, dass noch Forschungsbedarf bezüglich der Repräsentation von grundwassernahen Prozessen (Neubildung und Basisabfluss) besteht. Ein rasterbasiertes Wasserhaushaltsmodell kann in Abwesenheit eines Grundwassermodells immerhin grobe Abschätzungen der Grundwasserverfügbarkeit liefern.

Nach den hier vorgestellten Ergebnissen wird die Wasserbilanz des Neckars in naher Zukunft weder durch Klima- noch durch Landnutzungsänderungen dramatisch beeinflusst. Lediglich größere Eingriffe aufgrund einer veränderten europäischen Landwirtschaftspolitik könnten einen Einfluss auf die mittleren Abflüsse haben. Dagegen könnte der Abfluss des Ouémé signifikant zurückgehen, obwohl durch Brandrodung vermehrt Oberflächenabfluss entsteht. Der Bau größerer Mehrzweckspeicher bietet hier jedoch die Möglichkeit, zusätzlich zur Stromproduktion die starke Saisonalität auszugleichen.

Da die Unsicherheit hydrologischer Simulationen stark von den zu modellierenden Prozessen abhängig ist, sollten diese bei der Kalibrierung und Unsicherheitsanalyse berücksichtigt werden. Dies kann durch die hier vorgestellte Kombination von stochastischen Simulationsmethoden und skalierten Prozesssensitivitäten geschehen. Die Modellparameter und die Parameter des Fehlermodells werden dabei gemeinsam bestimmt. Dieses heteroskedastische Fehlermodell liefert normalverteilte Modellfehler und plausible Konfidenzintervalle der simulierten Abflüsse.

Die vier zu Anfangs eingeführten Fragestellungen sind nur kleine Teilbereiche des jeweiligen Forschungsgebiets und können momentan noch nicht als vollständig beantwortet bezeichnet werden. Neben dem wissenschaftlichen Interesse besteht jedoch auch eine gesellschaftliche Verpflichtung, das Wissen in diesen Bereichen voranzutreiben, um das Streben nach einer nachhaltigen Entwicklung zu unterstützen.

1 Introduction

πάντα ῥεῖ (Panta rhei).
(Everything flows.)

Platon, Greek philosopher (427 to 347 BC)

1.1 Motivation

Water has been identified as one of the key resources for reaching the Millennium Development Goals (UNDP, 2003). Because of limited water availability, these goals can only be achieved by improving the management of water resources. The most problematic regions are found in savannah and steppe regions due to high evaporative demands and land degradation (Falkenmark and Lannerstad, 2005). Models in general and hydrological models in particular have been used for many years in water resources planning. Unfortunately, in most of those arid and semi-arid areas as well as in other climatic regions very few data are available which prevents the use of complex hydrological models. This increasingly problematic limitation has lead to the IAHS initiative "Predictions in Ungauged Basins" (PUB), which focuses on hydrological modelling in areas with few available data or data in low temporal resolution (Sivapalan et al., 2003).

However, water resources management is not the only important task at the moment. The 2006 Elbe and Danube floods and their accompanying consequences have shown again that a deeper understanding of the processes governing the water cycle is necessary. In general, improved management of natural resources and natural hazards is required all over the world. The European Union has made the first steps in this direction. The EU Water Framework Directive introduces the ideas of integrated water resources management into catchment planning. The Floods Directive should lead to a formalized flood risk assessment providing maps that enable the implementation of flood risk management plans for endangered zones.

Finally, the mechanisms of global change should be examined in much more detail for further understanding, in order to prevent any undesired results and to adapt early enough, minimalizing negative impacts on humanity and nature. Therefore, this thesis tries to answer the following questions:

- Can we model the impact of global change on the water resources and what kind of models are necessary to predict the effect of land use change on the water balance of a catchment?
- How can we use these models in the current policy approaches such as integrated water resources management? Is it possible to integrate models on the regional scale to simulate and evaluate interdisciplinary water management scenarios?

- What will be the impact of a changing climate and land use on the water resources of a catchment?
- In general, how can we quantify the uncertainties associated with such simulations in a universally valid framework?

Most of the work which is presented here has been performed within the framework of the EU-funded project RIVERTWIN, an acronym for "A Regional Model for Integrated Water Management in Twinned River Basins". In light of the EU Water Framework Directive and the EU-Water Initiative, this project has dealt with adjusting, testing and implementing an integrated regional model for the strategic planning of water resources management in twinned river basins under contrasting ecological, social and economic conditions. The regional model allows assessing the impacts of demographic and economic development and the effects of global climate and land use changes on the availability and quality of water bodies in humid temperate, subhumid tropical as well as semiarid regions. The existing integration framework was first tested in the European Neckar basin which has high data availability and adequate data density. The transferability of the model to other regions with different economic level, ecological standards and with low data availability was tested in the Ouémé basin in Benin (West Africa) and the Chirchik basin in Uzbekistan (Central Asia). Unlike the Neckar and the Ouémé, the Chirchik was mostly modelled by the Uzbek partners. The project duration was from 2004 to 2007 and all reports as well as more detailed information can be found on the project website www.rivertwin.de.

This thesis is structured in the following way: In Chapter 2, after a short review of hydrological modelling, the basics of regionalisation, integrated water resources management, the two models LARSIM and HBV, and uncertainty analysis in general are introduced. Chapter 3 provides some details on the study sites chosen for this thesis, the Neckar and the Ouémé basin, and the available data. Providing the description of the distributed HBV model, the regionalisation methods, the integration concept and the climate scenarios, Chapter 4 forms the core of this thesis. The results for both basins are presented in Chapter 5. A new uncertainty analysis method is introduced and demonstrated by a case study in Chapter 6. The thesis closes with a summary, some general conclusions, and an outlook on future work in Chapter 7.

2 Hydrological Modelling

Hydrology is defined as the science of water, its properties and states in the atmosphere, on the ground and in the subsurface. It is dealing with the waters interactions with the surrounding media, the water cycle, the distribution above and below the land surface and anthropogenic impacts on these natural systems (DIN, 1996). In all fields mentioned above models can be used to describe the behaviour observed *in situ*. In general, a model is a simplified representation of a more complex natural or anthropogenic system. Therefore, a hydrological model is a mathematical description of a certain part or the whole water cycle. Groundwater models, rainfall models or cryospheric models are examples representing only parts. However, the hydrological models in this thesis are mostly rainfall-runoff models or more specifically water balance models. Rainfall-runoff models are calculating the discharge originating from one or several rainfall events whereas water balance models simulate all major components of the water cycle. A short review of the history and the types of models that are used today is given in the following section.

2.1 Why model?

There are a large number of scientific and operational applications for hydrological models. The former include hypothesis testing, improving our understanding of the system and extrapolating measured data in time and space. Models are mostly used to reproduce the behaviour and processes observed in the field. Generally, they are applied because we cannot measure everything we want to know at every time and at every location.

The latter cover the full range from design applications, forecasting, water management and all aspects of planning for the future. In general, the practical uses can be summarized under the term decision-making (Beven, 2001) to answer questions like "What if...?" or "How much...?". Again, models are used to determine specific values for certain points or future situations which cannot be observed *in situ*.

This diversity of applications may be a reason for the wide variety of hydrological models that have been developed in the past century and are successfully in use around the world. Singh (1995) gives a comprehensive overview of the most popular ones. The field of approaches ranges from the simple Rational Method (Mulvany, 1851) to complex process oriented models like SHE (Abbott et al., 1986a,b). Historically, hydrological models were first applied to calculate flood peaks and volumes at bridges, culverts and reservoirs. The first successful water balance models appeared in the 1960s with the Stanford Watershed model (Crawford and Linsley, 1966). Freeze and Harlan (1969) were the first to design a blueprint of physically based models which simulate the whole water balance based on analytical equations. Nevertheless, it took almost another 20 years before their ideas could be successfully realized by Abbott et al. (1986a,b) and others, mostly because computer power was

still the limiting factor. Nowadays, data limitations and theoretical considerations about their uncertainty are discouraging the further development and large-scale application of highly complex physically-based models, although they have been successfully applied to small and extremely well monitored basins.

From a structural point of view, Beven (2001) classifies hydrological models into five groups:

- The simplest models are runoff coefficients, time transformations and all variations of the unit hydrograph, which are often derived from system theory and formulated in a mostly event-based manner. Examples are the UK Flood Estimation Handbook (IH, 1999) or the FGM Model (Ihringer, 1999). Those models try to simulate individual storm events based on the ratio of runoff to rainfall and temporal retention in the basin. They are mostly purely empirical.

- The further development of system theory has lead to data-based models with regression approaches, transfer functions (Young, 2002) or artificial neural networks (ASCE, 2000a,b). The idea behind all these is to have no prior assumptions about the model structure but to let the data speak for themselves. Their strength lies more in short-term forecasting but because of the danger of overparametrisation, their explanatory power in extrapolating beyond the training range is questioned.

- Process-oriented approaches are the explicit soil moisture accounting models of varying complexity ranging from the Stanford Watershed model (Crawford and Linsley, 1966) to HBV (Bergström, 1995), LARSIM (Bremicker, 2000) and many other examples. These models could also be classified as conceptual models because the physical laws governing the flow of water through the system are not considered explicitly in full detail. Rather, the state of the system is tracked and the subsequent reaction of the dominant processes on this state and the input represents the non-linearity of the catchment. This use of effective or semi-empirical equations requires the calibration of some parameters by simultaneously observed input and output data. The spatial process discretisation can be lumped or partly distributed.

- Complex physically-based hydrological models on the other hand try to simulate all processes which are recognized in the system. The most prominent example is the Système Hydrologique Européen (SHE) by Abbott et al. (1986a,b). These models are often grid- or polygon-based (i.e., hydrological response units) and require detailed information to derive the model parameters. Even in small and very well monitored catchments, some parameters still require calibration because the effective parameter values can not be measured on the desired scale and resolution in the field.

- A compromise between both approaches are models based on distribution functions; the most widely known being TOPMODEL (Beven and Kirkby, 1979) and VIC (Xie et al., 2003). Models of this type use distribution functions to represent the spatial variability of the processes involved. The distribution can be purely statistical or derived from some index of hydrological similarity. Their aim is to model the bulk response at the catchment scale correctly and provide

some approximation of the spatial variability of the system state. Therefore, fewer parameters need to be calibrated than in most physically-based models.

All of these models are useful for certain purposes but also have their specific limitations and weaknesses which are discussed in great detail in recent publications. For the special purpose of modelling the impact of climate and land use change in an integrated framework, some extra prerequisites are necessary.

2.2 Modelling change

The German High Performance Computing Centre for Climate- and Earth System Research (DKRZ) has recently completed new climate simulations which will be part of the fourth Assessment Report (AR4) of the Intergovernmental Panel on Climate Change, IPCC (see www.ipcc.ch). The new simulations show a mean global warming between 2.5°C and 4.1°C until the end of this century (compared with the mean temperature between 1961-1990) - dependent on the emission of greenhouse gases into the atmosphere. The seasonally varying sea ice area decreases between 30% and 50%. One of the consequences of global warming could be a total melting of Arctic sea ice in late summer at the end of this century (DKRZ, 2005). Earlier predictions have lead to significant and continuous effort in simulating the impact of global climate change on the regional hydrological cycle (e.g. Zehe and Bárdossy, 2002; Gaiser et al., 2003; Rieland, 2004; KLIWA, 2006; Stock, 2005). The results are very complex, regionally different and cannot be completely summarized in brevity. A common expectation is the intensification of the water cycle by increased temperatures and a shift in rainfall and discharge regimes. In general, the predictions are still very uncertain depending on the region, time period, downscaling method, and hydrological model.

Land use changes are also transforming the earth's surface at an accelerating pace (Meyer and Turner II, 1992). These changes are closely linked to the issue of sustainability since they affect essential parts of our natural capital such as climate, soils, vegetation, water resources, and biodiversity. Land degradation affects large parts of the developing world and aggravates social tensions between competing users. There is also increased recognition that land use change is a major driver of climate change, through its interaction with ecosystems, biogeochemical cycles, biodiversity and - most importantly - human activities. Land use change, especially deforestation, is considered to be responsible for about 25% of the anthropogenic carbon dioxide emissions (Houghton et al., 2001).

Even more directly, land use change affects the water cycle by modifying interception, evapotranspiration, runoff generation and runoff concentration. These impacts are still largely unknown, although a large body of literature exists describing experimental and theoretical studies. Brown et al. (2005) count a total number of 166 paired catchment studies to determine the change in water yield alone. Although the quality of change was mostly similar, the main limitations for quantitative conclusions were the long time needed to reach a new hydrologic equilibrium, the variability of annual runoff, and sparse information about seasonal impacts. Aside from evapotranspiration, the impact of land use on soil hydraulic properties can be important. Mahe et al. (2005) and Giertz et al. (2005) found that the expansion of agricultural

areas lead to an increase in surface runoff and water yield in two African catchments. Therefore, it is important to consider the change in evapotranspiration and soil hydraulic properties when modelling the hydrological impact of land use change.

Another important aspect is the impact of land use change on floods. In this context, statistical as well as modelling studies have been reported (e.g. Hundecha, 2005; Ashagrie et al., 2006). A notable problem is the differentiating between impacts resulting from climate change, land use change or modifications of the river network. Although this field of research is not investigated further in this study, many common ideas and important analogies can be found.

Modelling the effect of land use change on the water balance requires the model parameters to be linked to catchment characteristics. This methodology is also called regionalisation and finally, the aim is to make predictions in ungauged basins. This challenge is not new to hydrologists. In fact, most catchments worldwide are ungauged (Blöschl, 2005). Even if observations are available somewhere in the region, the temporal length, accuracy or resolution of the data often does not meet the requirements of the current water management issues. This has lead to the PUB initiative focusing on solving this dilemma (Sivapalan et al., 2003). Besides reduction of uncertainty and development of new approaches, the parametrisation of distributed models is one key topic of PUB. Although plenty of literature about regionalisation exists, there has been no universally accepted theory established to date.

Vogel (2005) provides a comprehensive overview of regionalisation studies and approaches. Besides bi- and multivariate regression, clustering, kriging, neural networks and hydrologically homogeneous regions have been used but so far with only limited success. The most significant problem in most of these studies has been the existence of multiple optimal parameter sets which results in weak regression relationships when the regionalisation is carried out after individual calibration.

Parajka et al. (2005) found that a kriging approach and a similarity approach performed best when they tested 17 methods of the types arithmetic mean, spatial proximity, regression and similarity on the HBV model parameters of 320 Austrian catchments. Lee et al. (2005) attempted to find relationships between suitable conceptual rainfall-runoff model structures and catchment types to improve the reliability of model regionalisation to ungauged catchments. They investigated 28 catchments in the United Kingdom and 12 potential model structures but did not find strong correlations to area, baseflow index or annual average rainfall. Maréchal and Holman (2005) developed a catchment-scale rainfall-runoff model parametrised by the British Hydrology of Soil Types classification. They calibrated the model to three distinct catchments and found promising results for the regionalisation of the parameters throughout the UK.

However, scale differences between the variables the relationships were developed for and those they are applied on require additional attention. Xu (2003) found that the parameters of a monthly water balance model could be transferred by regression from 22 meso-scale subcatchments in the NOPEX area to Lake Mäaren basin in Sweden, which is 30 times larger. Nevertheless, for distributed water balance models, regionalisation of the parameters is often the only possibility to reduce the uncertainty from overparametrisation, effective grid scale parameters and the model structure or to find appropriate parameter values at all (Beven, 2001).

Therefore, Engeland et al. (2001) used a Bayesian approach to parametrise the

2 km^2 gridded ECOMAG model for nine catchments of the NOPEX region in Sweden, based on six soil and five land use classes. A limit in the identifiability was reached for three snow-related parameters after data from seven catchments was included. On the other hand, two retention related parameters (depression storage and vertical conductivity) could not be defined appropriately with the available information from all nine catchments. Beldring et al. (2003) calibrated six parameters for five land use classes in a 1 km^2 distributed HBV model of Norway. They ran the model with a daily time step but used monthly mean runoff for calibration in 141 catchments. Although they used 31 parameters to describe the altitude gradients, they found that the major problem was the spatial interpolation of the meteorological input data.

2.3 Integrated water resources management

Traditionally, the management of natural resources was strongly split into thematic sectors such as agriculture, forestry or water management, and spatially subdivided into administrative units which rarely follow the elements of the natural landscape. The idea to overcome this impractical and inefficient situation in the water sector is actually more than 60 years old but had only a dubious record of implementation until recently (Biswas, 2004). The Global Water Partnership (GWP, 2000) defines integrated water resources management (IWRM) as "a process which promotes the coordinated development and management of water, land and related resources, in order to maximize the resultant economic and social welfare in an equitable manner without compromising the sustainability of vital ecosystems."

One of the first legal implementations but certainly with the most far-reaching impact is the EU Water Framework Directive (WFD) (EU, 2000). It forces the member states to report on their water bodies' status, monitoring programs, management plans, measures and goals in a river basin-oriented and integrated way, considering all affected sectors. On the other hand, the EU Water Initiative (www.euwi.net) is promoting these ideas in the developing world as a contribution to the Millennium Development Goals initiative. The need for tools to implement all these initiatives and processes has lead to numerous research activities in the past years (e.g. Refsgaard, 2002; Kämäri, 2005; Harmoni-CA, 2006). A common challenge of these projects is the integration of models from different disciplines. This task, together with the prerequisites to model the impact of global change, builds the framework for the hydrological modelling of this study.

Practically, this means that the models used should enable integration into a larger modelling complex and reproduce the global change signal. In order to properly quantify integrated effects of a changing land use and climate with high spatial and temporal resolution, the models have to fulfil certain criteria: they should be simple enough to work on large scales, with sparse data and future climate scenarios. This is especially important for the application in developing countries. At the same time, the parametrisation should be based on a reasonable representation of the dominant catchment processes and be able to reflect changes in catchment characteristics and forcing data. For these reasons, the conceptual model LARSIM (Bremicker, 2000) and a modified version of the semi-distributed conceptual HBV model (Bergström, 1995) are used in this study.

2.4 LARSIM

LARSIM (Large Area Simulation Model) is operational at the flood forecasting centre of the State Institute for Environmental Protection Baden-Württemberg (LUBW). Furthermore, it was recently used in a regional climate change impact study (KLIWA, 2006). It is a distributed meso-scale model developed to continuously simulate the water balance of large river basins. It incorporates interception, evapotranspiration, water storage in soils and aquifers, runoff generation in the catchment and translation and retention in the river network (Figure 2.1). Snow accumulation and snow melt as well as artificial influences (e.g. storage basins, diversions or water transfer between different basins) are taken into account. LARSIM combines deterministic hydrological model components that are generally applicable and based on available geographic and meteorologic data, such as the Xinanjiang model (Zhao, 1977), or parallel linear storages. LARSIM is generally accepted by the water management agencies in Baden-Württemberg. The version used in this study was provided by LUBW and calibrated manually focussing on flood forecasting. Unfortunately, the required meteorological input data humidity, wind speed, solar radiation and atmospheric pressure are not available in a suitable resolution for the Ouémé basin. To overcome this deficit and to improve the parametrisation strategy, the conceptual model HBV was used in the Neckar and Ouémé basin.

2.5 HBV

The HBV model concept was developed at the Swedish Meteorological and Hydrological Institute (SMHI) in the early 1970s (Bergström, 1995; Lindström et al., 1997). It has conceptual routines for calculating snow accumulation and melt, soil moisture and runoff generation, runoff concentration within the subcatchment, and flood routing of the discharge within the river network (Figure 2.2). The snow routine uses the degree-day approach. Soil moisture is calculated by balancing precipitation and evapotranspiration using the field capacity and permanent wilting point as parameters. Mean monthly potential evapotranspiration is calculated outside the model in this case based on Hargreaves and Samani (1985). The actual daily evapotranspiration is adjusted based on the actual temperature and a calibrated coefficient and reduced linearly below the permanent wilting point. Runoff generation is simulated by a non-linear function of actual soil moisture and precipitation. The runoff concentration is modelled by two non-linear reservoirs representing the direct discharge and the groundwater response. Flood routing between the river network nodes uses the Muskingum method. Additional information about the HBV model version used here can be found in Uhlenbrook et al. (2004), Hundecha and Bárdossy (2004) and Hundecha (2005). Many different implementations of the HBV model concept exist around the world. Based on a semi-distributed version used in the Universitaet Stuttgart the fully distributed model presented in Chapter 4.1 was developed.

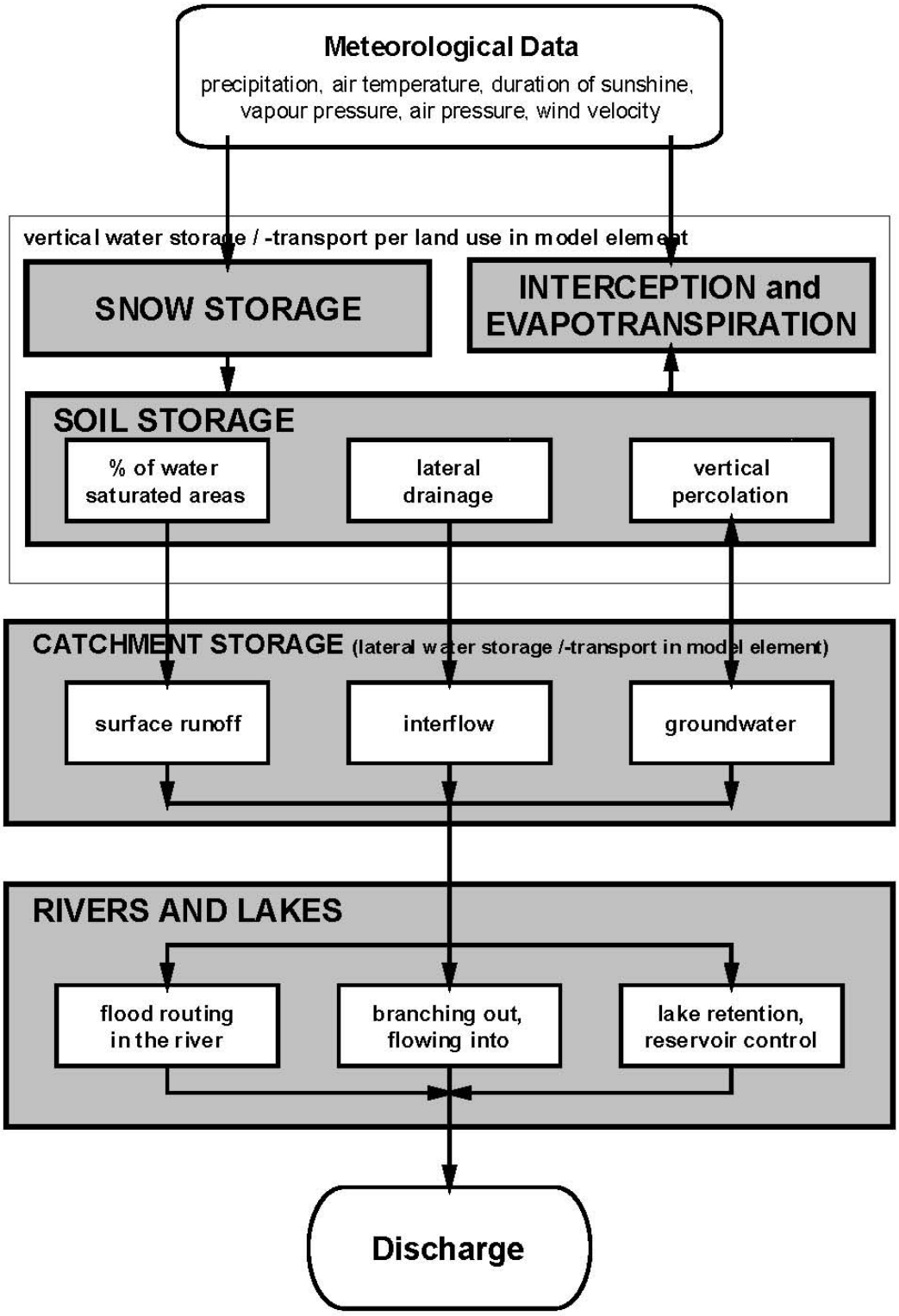

Figure 2.1: Schematic diagram of the LARSIM model (after Bremicker and Gerlinger, 2000).

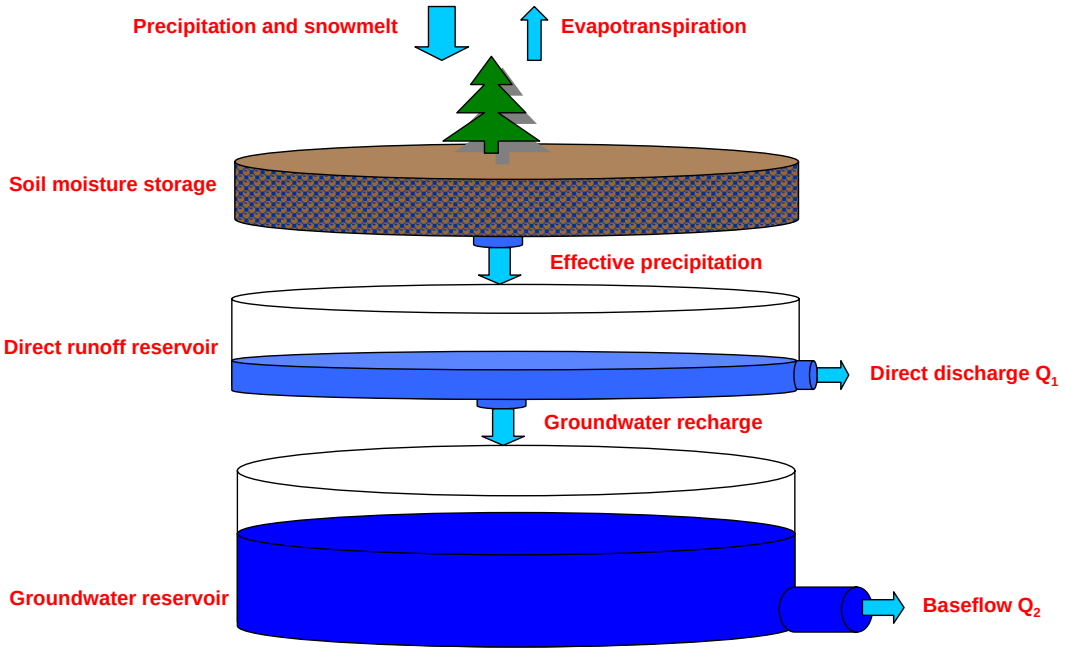

Figure 2.2: Schematic diagram of the original HBV model.

2.6 Uncertainty estimation

Every model by definition is a simplification of a more complex system. The fact that natural processes are described with mathematical equations and the corresponding parameters are derived from observations and experience leads to uncertainties. The main sources are:

1. Input uncertainty: The meteorological input is based on point observations (sometimes combined with indirect measurements such as radar or satellite information). Due to the fact that the exact precipitation, temperature and other input variables are not known at every point of the catchment, uncertainty due to measurement errors and spatial variability, need to be taken into account.

2. State uncertainty: The actual state of the catchment (e.g. moisture conditions, snow cover) is usually not directly observed but calculated using model equations. Due to the fact that the input and the model abstraction are simplifications, the state itself becomes uncertain. Continuous simulations inherit state uncertainty from preceding time-steps.

3. Process abstraction-related uncertainty: The main hydrological processes are described using equations which can only capture parts of the complex natural processes. Parameters of these equations correspond partly to sets of discrete measurements or need to be estimated via calibration. This automatically leads to uncertainties of the corresponding model output.

4. Model structure uncertainty: The formulation of a certain model structure itself leads to uncertainty due to the inherent simplification of the more complex real

system. The discretisation of the landscape into polygons or rasters produces additional errors as the real processes occur on much smaller scales.

5. Output uncertainty: Observed discharge, groundwater level and other observations are also based on rating curves, point measurements, or remote sensing and can be corrupted by measurement errors and neglected spatial variability.

The quantification of these uncertainties is important both for practical decision-making and theoretical modelling. Unfortunately this is neither a straightforward nor simple task. Kavetski et al. (2002); Gupta et al. (2005); Beven (2006); Schaefli et al. (2007) and many others state that, despite the considerable attention that has been given to uncertainty estimation in the recent years, there has been no satisfactory approach to separate all sources of error and to quantify the total uncertainty proposed to date. Singh and Woolhiser (2002) describe this fact as one of the major limitations of current watershed models. Therefore, another purpose of this study was to develop a methodology for the quantification of total model uncertainty considering all relevant error sources.

Even physically-based hydrological models require parameter calibration because subgrid processes can only be parametrised in a lumped way. Effective parameters are required at the model grid scale which can be quite different from field or laboratory measurements despite being lumped with one another (Beven, 1989). This calibration is more difficult than may be expected because of problems associated with the objective function used, parameter interaction, input uncertainty, and the implicitly assumed error model. Kavetski et al. (2002) give a comprehensive overview of these problems and show that objective functions based on least squares or derivatives thereof will yield biased parameter estimates if input and output data are corrupt.

It has long been understood that the choice of a single objective function must lead to biased calibration as each performance criterion is sensitive only to certain characteristics of the hydrograph (Krause et al., 2005). Multi-objective calibration has been proposed to counteract this effect (Yapo et al., 1998; Gupta et al., 2003) and additional information may very well reduce the uncertainty of model predictions. However, the extension of the dimensionality of the optimisation can also increase uncertainty and the approach still suffers from the main shortcomings of standard single-objective calibration. The problem is that most calibration methodologies assume and require that the model errors are Gaussian and that their variance is constant (homoskedastic), which is rarely verified.

Markov Chain Monte Carlo methods are the most popular in uncertainty estimation. The Shuffled Complex Evolution Metropolis algorithm (SCEM-UA) of Vrugt et al. (2003) and the Generalised Likelihood Uncertainty Estimation (GLUE) by Beven and Binley (1992) have been used in numerous studies. The latter has also been criticised for the adoption of "less formal likelihoods", the subjective choice of "behavioural" parameter sets, and the lumping of all sources of uncertainty into a singular parameter uncertainty leading to very wide confidence bounds (Mantovan and Todini, 2006; Kavetski et al., 2002). Perhaps the major concern with both methods is the lack of a specific error model structure acknowledging the properties of input and parameter uncertainties.

Montanari and Brath (2004) propose to use the normal quantile transform in order to make the input and output time series Gaussian and derive a linear regression relationship between the model residuals and simulated river flow. The major drawback of this method is the assumption that the model performance and errors are homoskedastic. Wagener et al. (2003) tackle this commonly ignored feature with a dynamic identifiability analysis (DYNIA). It allows the evaluation of simulated and observed time series with respect to information content for specific model parameters. This analysis can be used to indicate areas of structural failure and potential improvement of the model.

Kavetski et al. (2002) introduce a strict inference scheme called BATEA (Bayesian Total Error Analysis) to analyse the model parameters posterior distribution conditioned to the model, input and output error by Monte Carlo Markov Chains. Considering explicit input and output uncertainty, this method still requires error models of low dimensionality for numerical reasons. Unfortunately, most environmental observation time series show significant heteroskedasticity prohibiting the use of simple multiplicative error models.

Schaefli et al. (2007) use a mixture of two normal distributions to mimic the heteroskedasticity of the total modelling errors of a conceptual rainfall-runoff model applied to a highly glacierized alpine catchment. The two normal distributions represent the error populations during the two very distinct high and low flow regimes. Unfortunately, the approach still assumes normal, homoskedastic and lag-one autocorrelated error distributions for each flow regime and lumps all errors sources into the parameter uncertainty. As the assumptions could not be completely proven by the data, the problem is broken down into two similarly ill-posed cases instead of actually solved.

Gallagher and Doherty (2007) demonstrate the estimation of model predictive uncertainty for a water resource management model consisting of a soil water balance and a groundwater model. Although the chief disadvantage of the method, the assumption that the model is linear, prevents the exact determination of highly non-linear model error, useful approximations of the individual contributions to the overall predictive uncertainty can be given; provided that plausible estimates of the individual uncertainty sources like input data or model parameters are available.

Gupta et al. (2005) identify the typical assumptions of normality, constancy of variance and simplicity of the correlation structure of the underlying error model as the major drawbacks of current uncertainty estimation schemes. Therefore, the methodology presented in Chapter 6 explicitly addresses these important properties: it produces error series which represent the varying importance of different processes in time and are normally distributed. It is based on a scaled composition of plausible error contributions from different uncertainty sources which represents the time-variant importance of different processes. The hydrological model and the corresponding error model is calibrated simultaneously. The uncertainty time series are used as a weighting factor to normalize the model residuals during calibration so that the assumptions of least squares optimization are fulfilled. The methodology is demonstrated by an example application to the distributed HBV model of three watersheds of the Neckar basin.

3 Data

The presented study was performed in two different basins to test the transferability of the model concept to the developing world. A brief overview of the basin characteristics is given in Table 3.1. Additional details about the data used are presented in the following sections.

Table 3.1: Comparison of the Neckar and the Ouémé basin.

	Neckar	Ouémé
Country	Germany	Benin
Climate zone	Temperate humid	Tropical, subhumid
Population	5.5 Mio.	1-2 Mio.
Area (km^2)	14 100	51 500
Data availability	High	Low
Water management problems	Water quality, hydromorphology, flooding	Water quality, flooding, water supply (in dry season)

3.1 The Neckar basin

The Neckar basin, located in south-western Germany, covers an area of about 14 100 km^2. It drains the lowlands between the Black Forest, the Swabian Jura and the Odenwald from South to North and flows into the Rhine River at Mannheim. The Neckar is intensively used for navigation and transportation on a length of 164 km, but also for energy supply through a number of hydro- and thermal power plants. The elevation in the catchment varies from 93 m.a.s.l. at the catchment outlet to about 1022 m.a.s.l. in the Swabian Jura in the South of the catchment (Figure 3.1). The Black Forest on the western border consists of crystalline bedrock whereas karstic limestone is frequently found in the eastern part of the catchment. Both hill chains are characterised by steeper slopes and soils with low storage capacity. The river valleys and plains in the northern part mostly consist of thick, fertile soils. The climate can be characterized as temperate humid, with a long-term average annual precipitation of 950 mm, ranging from 700 mm (Tübingen, 370 m.a.s.l) to 1680 mm (Freudenstadt, 787 m.a.s.l). The precipitation regime shows a weak seasonality with a moderate maximum in June (110 mm) and a minimum in October (66 mm). The average daily temperature in the catchment is 8.7°C with a minimum of 6.4°C in Klippeneck (973 m.a.s.l.) and a maximum of 9.1°C in Nürtingen (280 m.a.s.l.). The coldest month is January (-0.5°C), the warmest is July (17.3°C).

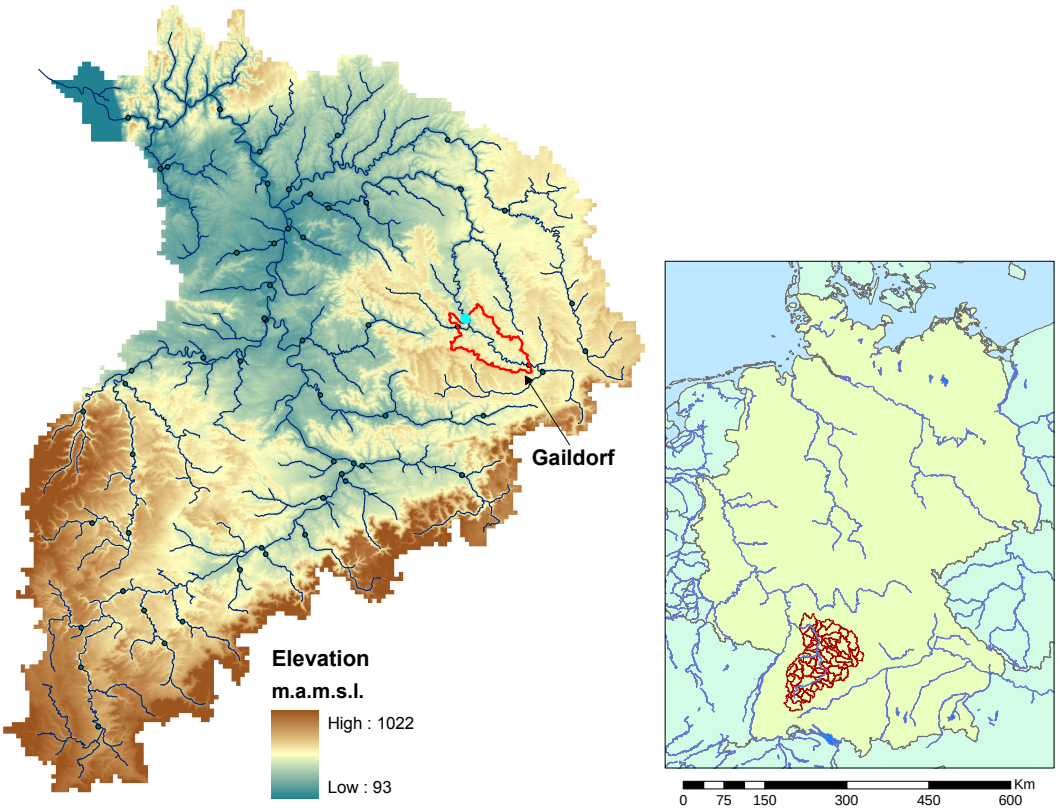

Figure 3.1: Topography, gauging stations of the Neckar catchment and location of the subcatchment Gaildorf (Kocher); Inset: Location of the Neckar catchment in Germany.

All data that was used in this study was provided by the State Institute for Environmental Protection Baden-Württemberg. Landuse (Landsat 1993, resolution 30 m), soil (Bodenübersichtskarte 200, scale 1:200 000) and topographic data (resolution 50 m) were aggregated to a common raster resolution of 1 km. Precipitation and temperature data for model input was interpolated from observation station data using external drift kriging (Ahmed and de Marsily, 1987). Discharge data from 58 gauging stations was used for model evaluation (compare to Figure 3.1). The average, maximum and minimum discharge at the gauge Plochingen, which is the outlet of the 4000 km^2 large upper Neckar catchment, are 46.3 m^3/s, 1150 m^3/s and 3.7 m^3/s, respectively. Approximately 20% of the average discharge originate from large distance drinking water supply from the Danube catchment and Lake Constance to the Neckar catchment. Further downstream at the gauge Laufen (8000 km^2 drainage area) average, maximum and minimum discharge are 88 m^3/s, 1650 m^3/s and 14.1 m^3/s, respectively.

Due to topography and land use a mixture of vegetation types has developed in the Neckar basin, typical of the densely populated parts of Western Europe (Figure 3.2). Large forests are found in the West of the basin (Black forest), in the South-West on

Table 3.2: Land use distribution in the Neckar basin (2000).

Land use class	Area in %	Land use class	Area in %
Dense settlement	0.34	Intensive grassland	0.44
Industry	0.94	Extensive grassland	20.19
Loose settlement	8.87	Coniferous forest	11.19
Farmland	27.24	Windthrow	0.82
Viniculture and orchards	1.08	Deciduous forest	12.66
Open orchard grassland	2.62	Mixed forest	13.23
Fallow land	0.04	Water	0.21
Areas without vegetation	0.09	Wetlands	0.04

the Swabian Jura and in the far North (Odenwald). Different forest types also were the natural vegetation but nowadays about half of the area is used agriculturally as farmland or grassland and only less than 40% is still covered by forest (Table 3.2). The centre of the basin is the Greater Stuttgart Region, which is one of the top ten richest regions in Europe. Large industry factories and associated businesses create jobs which attract people and induces urbanization pressure. In contrast, the population in more rural parts of the basin is shrinking.

The following model input was derived from the available data: areal mean permanent wilting point, field capacity and hydraulic conductivity of the upper two soil layers were calculated for each raster cell from soil maps and samples by Thomas Gaiser and Andreas Printz. Field capacity and permanent wilting point were calculated according to Rawls et al. (1982); Gaiser et al. (2000) and Tomasella and Hodnett (1998). Saturated hydraulic conductivity was estimated after Tomasella and Hodnett (1997). Figure 3.3 gives an example of the spatial distribution of one of the mentioned soil properties. The permanent wilting point shows a similar spatial structure whereas the local differences in mean hydraulic conductivity are much smaller. The data shown here were calculated from the specific field capacity (dimensionless) by multiplying with the soil depth yielding values in mm to be used in HBV. Two striking features are the relatively high storage capacities along the foothills of the Swabian Jura and in the north-western plains and the extremely low values in the Black forest (West) and Odenwald (North). Those characteristics also dominate the water balance of these respective regions. Aside from soil hydraulic properties, the conductivity of the underlying aquifers significantly influences the hydrological behaviour of a catchment, especially throughout low flow periods. The conductivity of the uppermost geological layer was also derived from maps and other hydrogeological information in a resolution of 1 km by Johanna Jagelke. Figure 3.4 shows the spatial distribution of the dominant hydrogeological formations.

Because the geological layers underlying the area are slightly dipping towards the South-East, different strata with quite distinct properties are found at the surface throughout the study area which causes the striped pattern seen in Figure 3.4. Most significant for the hydrology of the watershed are the extremely high conductivities on top of the karstic Swabian Jura and in the incised channels along with the comparatively low values on its slopes. The karstic areas and dipping layers lead to inter-basin transfer of groundwater in certain regions. An important outcome of the

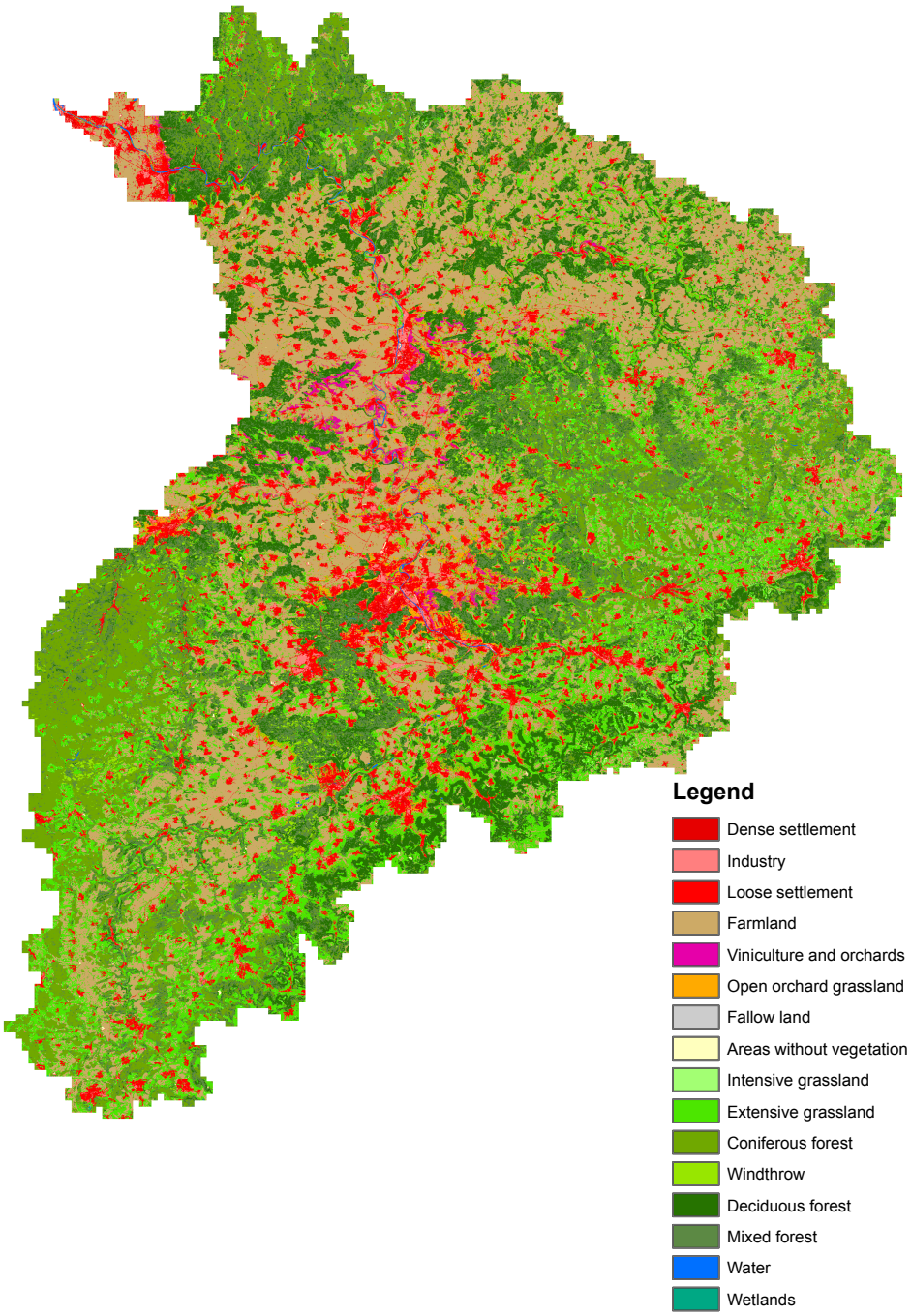

Figure 3.2: Spatial land use distribution in the Neckar basin (2000).

integration of surface and groundwater models was the identification of these regions for consideration in future modelling studies.

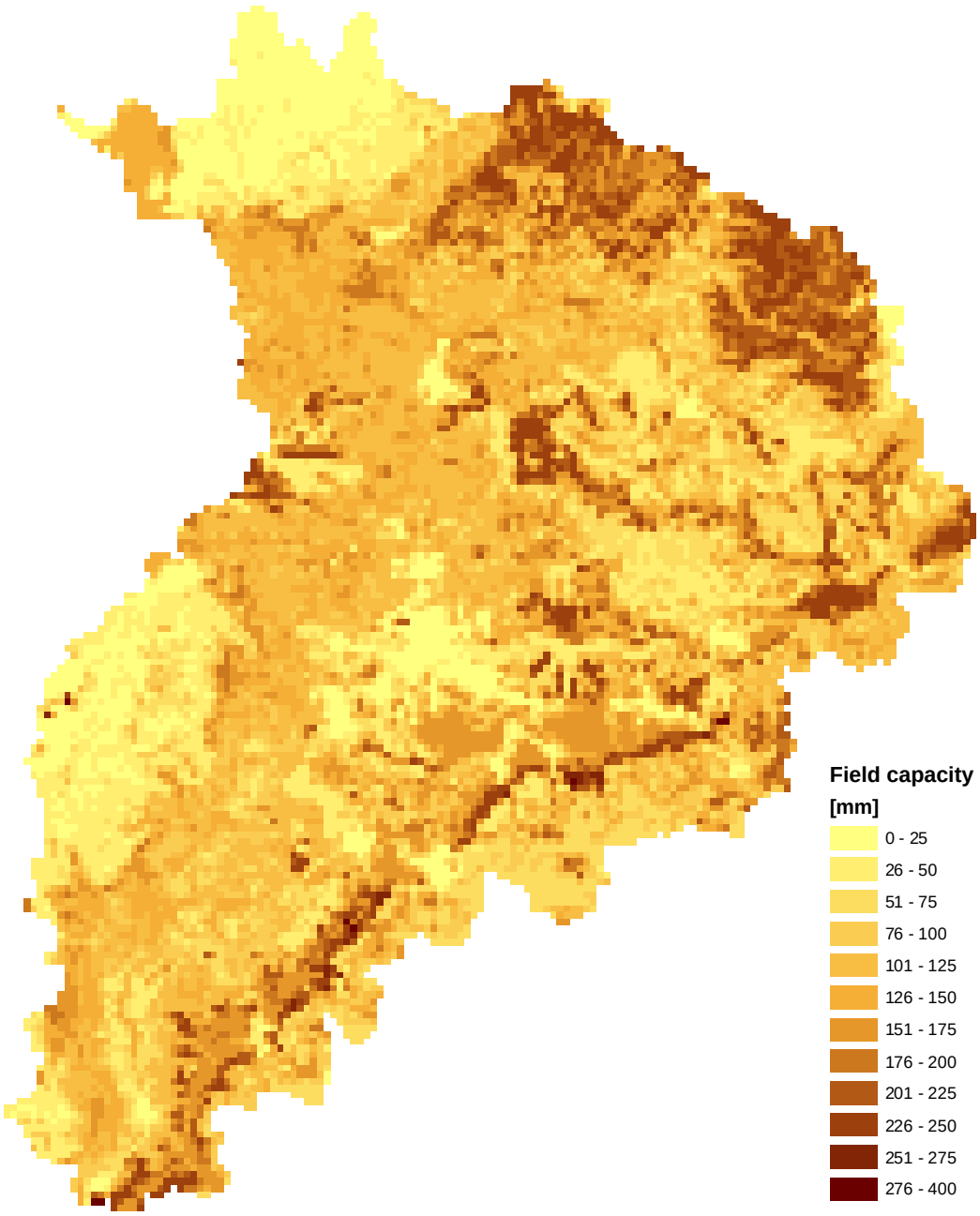

Figure 3.3: Spatial distribution of estimated field capacity in the Neckar basin.

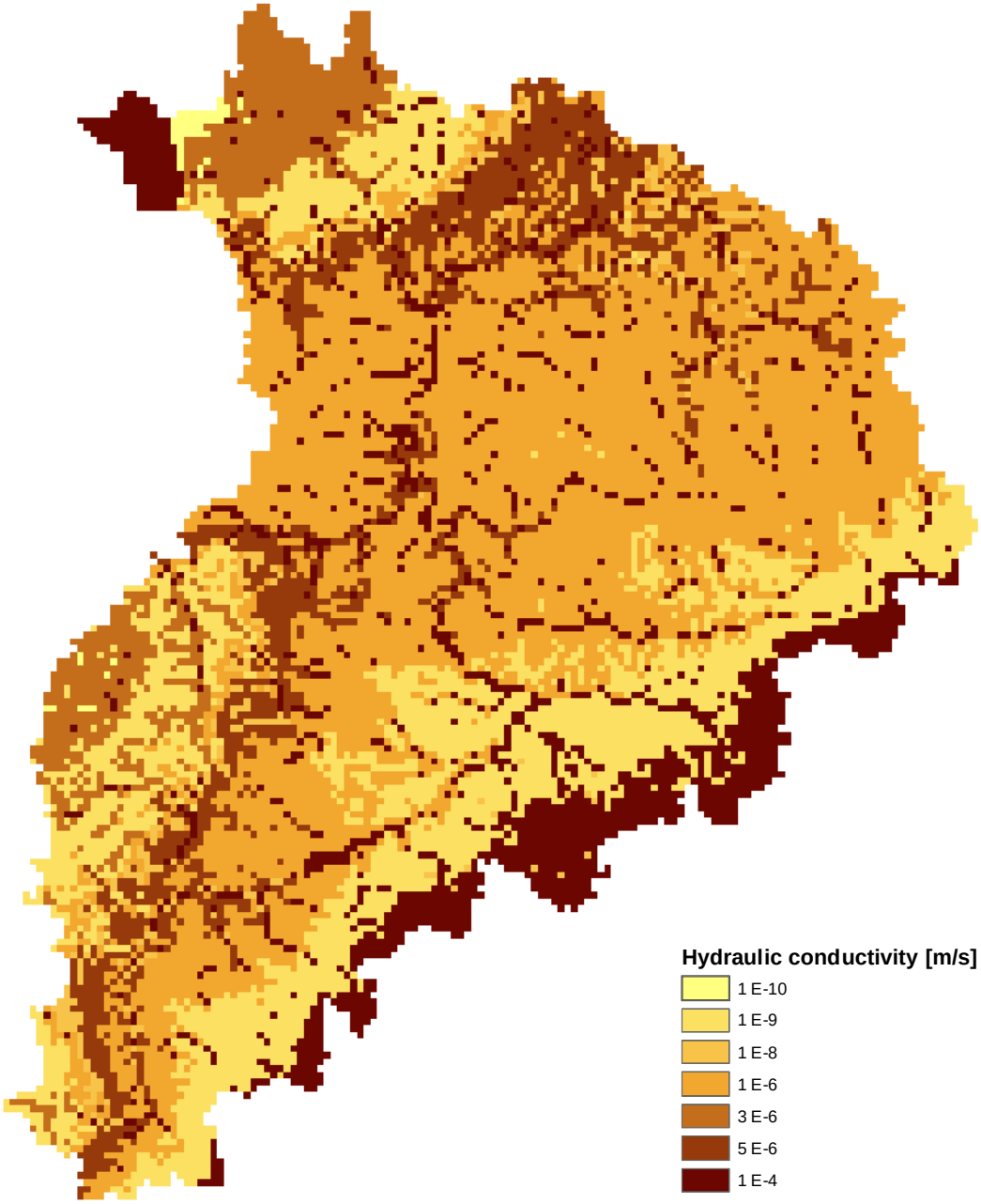

Figure 3.4: Spatial distribution of aquifer hydraulic conductivity in the Neckar basin.

3.2 The Ouémé basin

The Ouémé basin in its entirety covers about 51 500 km^2 and is situated in the northern part of the continental terminal area and the Precambrian crystalline basement of Benin (West Africa). The landscape is characterized by peneplains with scattered inselbergs and plateaus. The Ouémé River crosses the basin from North to South and flows into Lac Nokoué which empties into the Gulf of Benin. Important tributaries are the Okpara (NE) and the Zou Rivers (NW). The southernmost gauging station Bonou marks the outlet of the basin and the border of the study area. North-South oriented mountain chains occur at the towns of Dassa, Gobada, Logozohe, Tchetti, Savalou, Lanta, and Badagba. The highest summits of up to 617 m.a.s.l. are found in the Northwest of the basin. To the South, the terrain gently drops to only a few meters a.s.l. in the Lama depression in the southern part of the Ouémé basin (Figure 3.5).

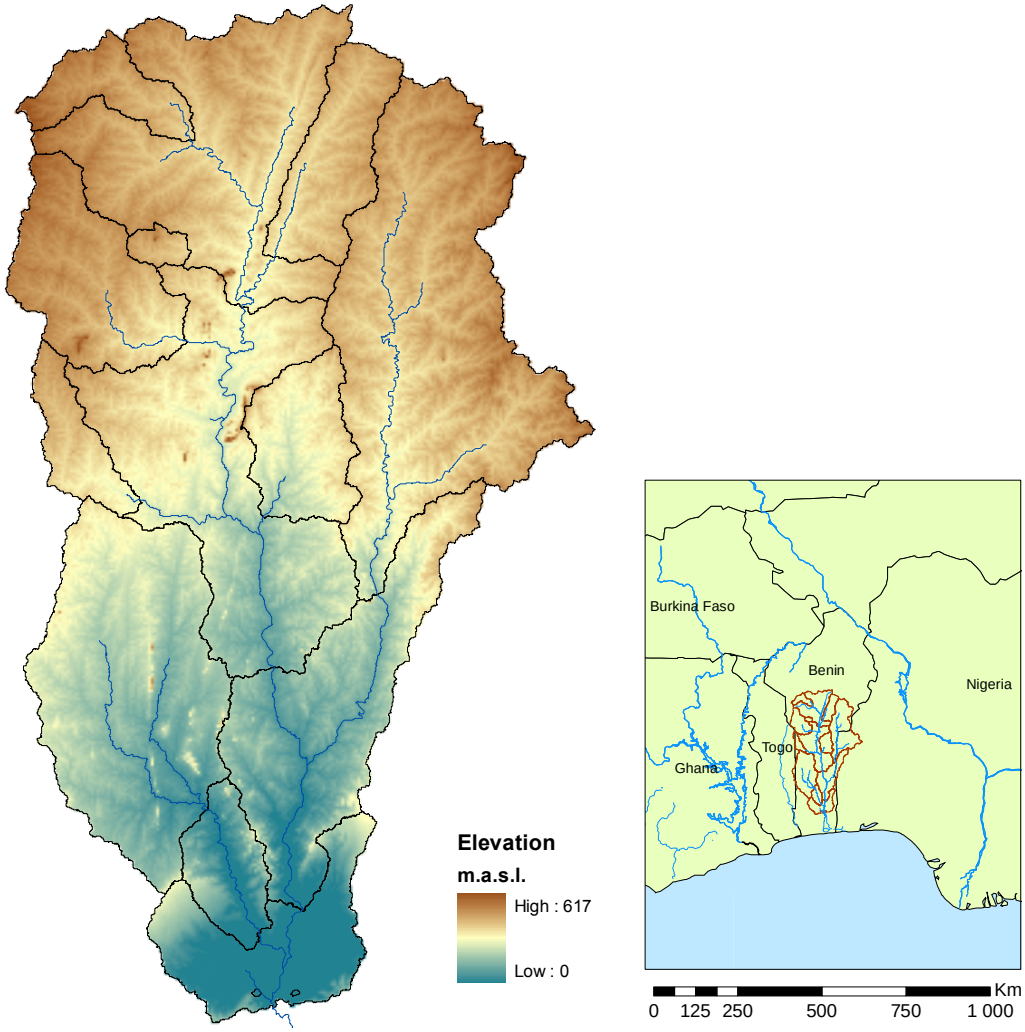

Figure 3.5: Topography and sub-basins of the Ouémé catchment; Inset: Location of the Ouémé catchment in West Africa.

Table 3.3: Land use distribution in the Ouémé basin (2003).

Land use class	Area in %
Gallery forest	3.98
Dense semidecidual forest	2.76
Swamp woods	0.04
Humid areas/floodplains	0.24
Open semidecidual forest and tree savannah	15.20
Floodplain Savannah	0.50
Tree and shrub savannah	38.99
Rocky Savannah (incl. Inselbergs)	0.71
Humid floodplain Prairie/Savannah	0.03
Cropland and fallow	31.03
Cropland mixed with Cashew	0.07
Cropland mixed with Palm trees	2.69
Large scale plantation	0.29
Small scale plantation	2.74
Bare soil and rock outcrops	0.01
Settlement	0.63
Water bodies	0.11

The climate is of typical monsoon type which is characteristic for the large sub-humid Savannah zones of the world. Average annual temperatures are approximately 27°C, with temperature amplitudes of 5-6°C. However, different climatic zones can be found throughout the country: the Southern Sudan Savannah zone with semi-arid tendency and a single summer rainy season in Northern and Central Benin; the subequatorial moist savannah zone (Guinea-Savannah) in central and southern Benin, and the humid subequatorial zone in the South, which both show bimodal rainfall patterns (Stahr, 2000). The mean annual areal precipitation is about 1200 mm, however, the mean annual potential evapotranspiration according to Hargreaves and Samani (1985) is approximately 2800 mm. Meteorological data was provided by ASECNA (Agency for Air Navigation Safety in Africa and Madagaskar). The vegetation is dominated by tree and shrub savannah intersected with a mosaic of cropland and bush fallow (Table 3.3).

Population migration from North to South is the major drive for land use change in the basin. Close to villages and roads, the savannah is converted to cropland by slash and burn methods at an astounding velocity. Figure 3.6 shows the land use distribution derived from satellite images taken in the year 2003.

The majority of the soils in the Ouémé is highly weathered due to the time length of soil formation. The main characteristic of these soils is their high clay content and low water storage capacity. In general, the soils in the southern sedimentary part are deeply weathered and offer a large rooting volume. In the northern crystalline zone, the majority of the soils are less developed and have a smaller water storage capacity. Topographical data (SRTM) was obtained from NASA (2006). Landuse (from LANDSAT TM Plus, 2003), soil (both scale 1:200 000) and topographic data (resolution 90 m) were available.

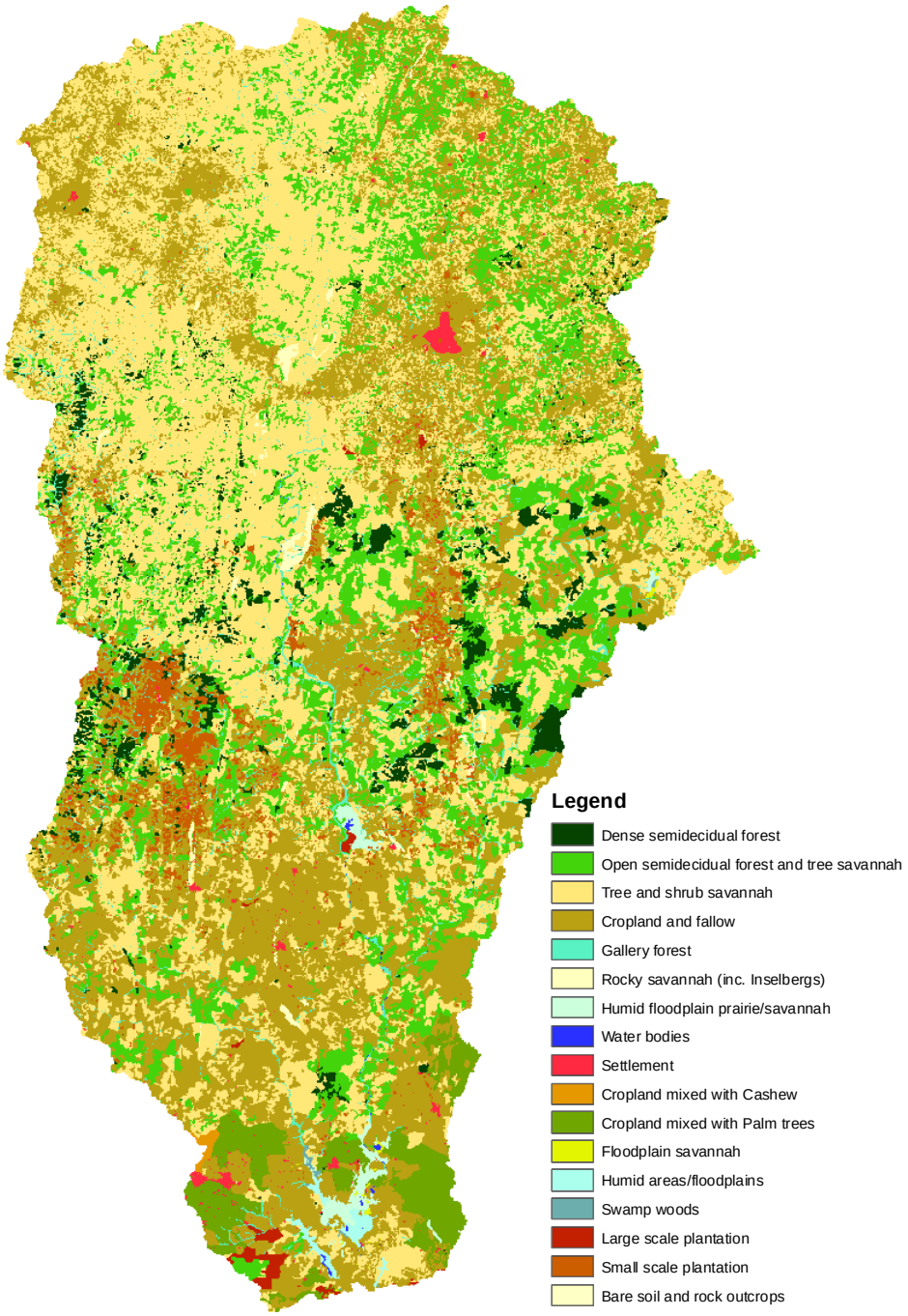

Figure 3.6: Spatial land use distribution in the Ouémé basin (2003)

As in the Neckar basin, they were aggregated to a common raster resolution of 3 km. Precipitation and temperature data for model input was also interpolated by external drift kriging (Ahmed and de Marsily, 1987). Discharge data from 13 gauging stations provided by the Directorate General for Water (DGE) was used for model evaluation. The sub-basins in Figure 3.5 were derived from these gauging stations.

As in the Neckar basin, the areal mean permanent wilting point, field capacity and hydraulic conductivity were derived by Thomas Gaiser and Andreas Printz according to Rawls et al. (1982); Gaiser et al. (2000) and Tomasella and Hodnett (1998, 1997). Figure 3.7 shows the spatial distribution of field capacity which is again strongly correlated with the permanent wilting point. Both variables were calculated from the specific values (dimensionless) by multiplying with the soil depth to produce data in mm for the hydrological model.

Major features are the relatively high storage capacities in the Lama depression (South) and the larger valleys in the centre of the area and the extremely low values along the North-South oriented Kandi fault. This major geologic structure crosses the basin from the central North to the South-West, inselbergs are found on both sides and many streams follow its direction. It is also the most important feature in the spatial distribution of hydraulic conductivity shown for the lower soil layer in Figure 3.8.

As the crystalline basement is only significantly permeable along fractures, the formation of regional aquifers is prohibited and the soil hydraulic conductivity dominates the formation of perched water tables and seasonal baseflow.

Since the early 1970s tropical West Africa has suffered from a prolonged drought that reached its first climax in the first half of the eighties. The average rainfall deficit over 1971-1990 was of the order of 180 mm/year compared with the interval 1951-1970. All climatic zones from the semi-arid Sahel and the sub-humid Sudanese zone down to the humid Gulf of Guinea have been affected. The prolonged West African drought has already brought about a profound deterioration in the economic and social development of West African countries. For example, river discharges in West Africa have decreased by about 40-60% in recent decades, causing shortages in river water availability for domestic and agricultural purposes.

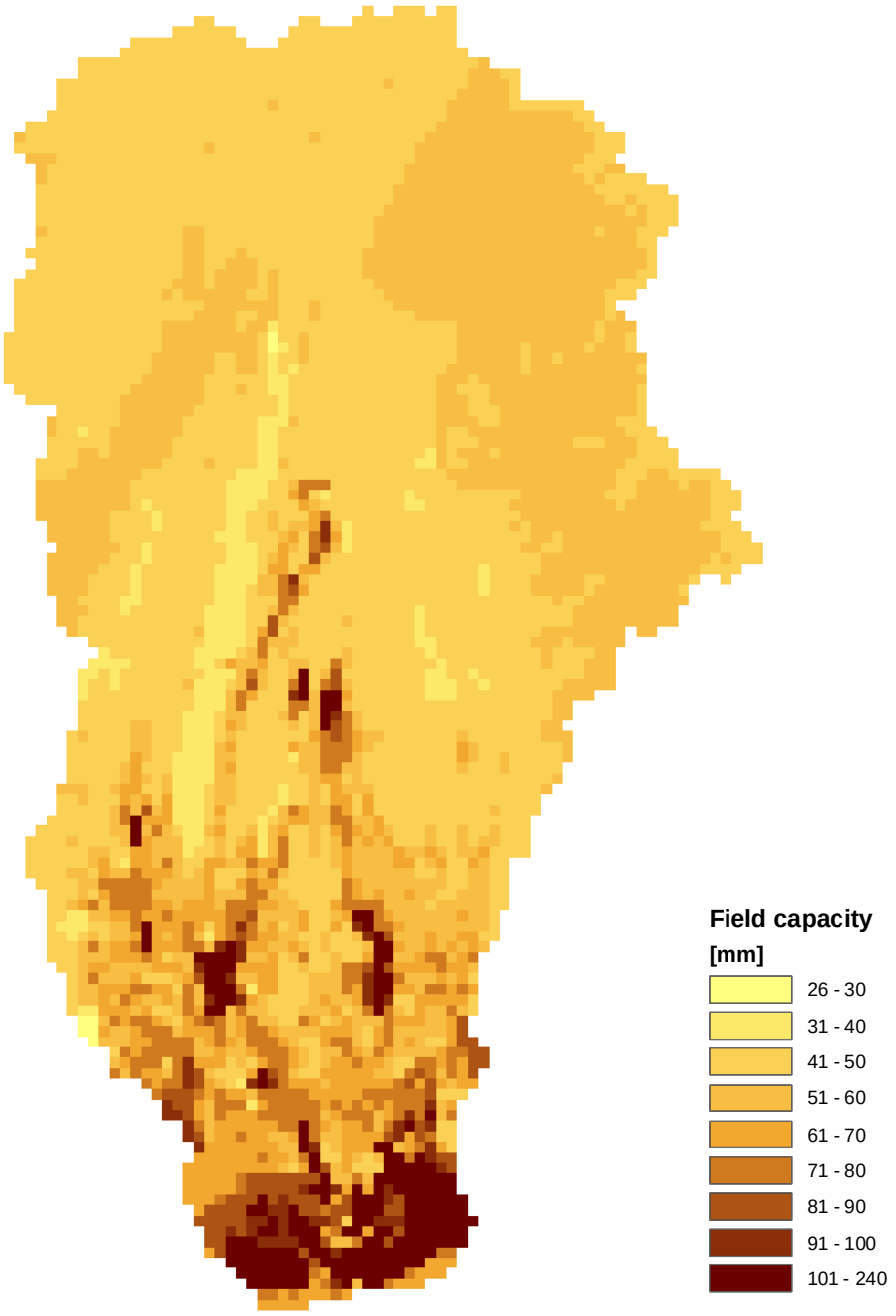

Figure 3.7: Spatial distribution of estimated field capacity in the Ouémé basin.

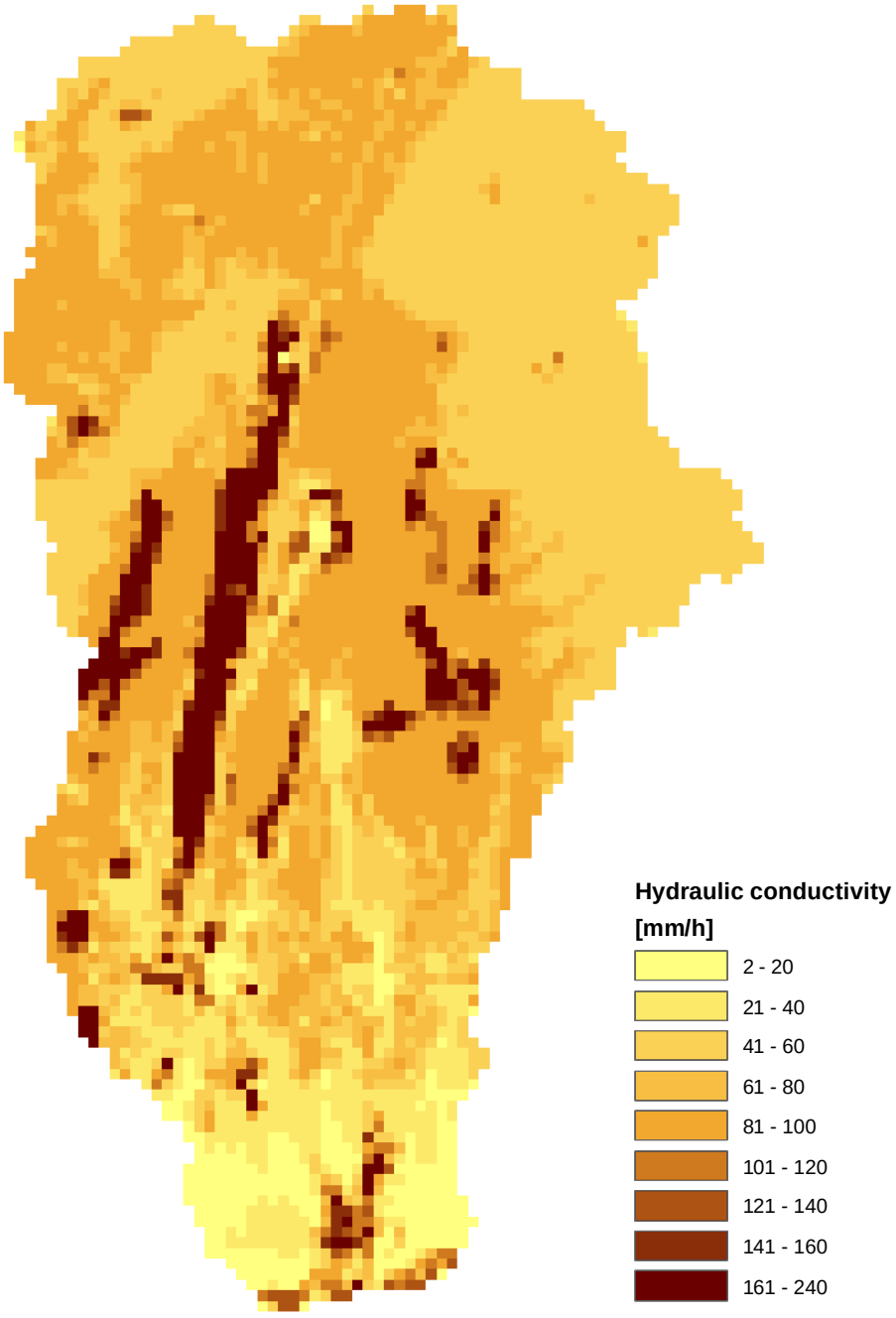

Figure 3.8: Spatial distribution of lower soil layer hydraulic conductivity in the Ouémé basin.

4 Integrated modelling of climate and land use change

In Chapter 2.3, two main requisites for an integrated assessment of the impact of global change on the water balance have been identified:

- Catchment characteristics must be incorporated in the parametrisation to be able to model land use change.
- The models must allow for the linking to other sub models of larger integrated modelling complexes.

The first point is generally referred to as regionalisation and is described in chapter 4.2. In practice, linking models is a similarly complex challenge. The majority of projects face the same problems when models from different disciplines are integrated. The interfaces have to be clearly defined and often compromises have to be made between the demands of the different models, the data availability, and the objectives of the study. Additionally, a common problem is that input and state variables are sparse or missing in the desired resolution. If the fluxes between models cannot be measured at all, innovative solutions have to be found to realistically represent the natural system. In this study, the hydrological model is connected to several other models as shown in Figure 4.1.

Socio-economic and climate scenarios provide the input to the hydrologic, ecologic and economic sub-models, which are loosely linked by exchanging intermediate variables. The final results are stored in a geodatabase that can be queried from a user interface and forms the roots of the decision support system. The hydrological model is connected to other sub-models at three points in the described system. It receives meteorological input data from the climate scenarios, calculates groundwater recharge for the groundwater model (MODFLOW) and stream discharge for the water supply (WEAP), water quality (QUAL2K) and freshwater ecology (CASIMIR) models. The discharge is simulated for relevant points in the river system including the gauging stations used for calibration and validation.

Because soils, land use, topography and other input data such as rainfall and temperature are highly variable in space, a high spatial and temporal resolution is required where applicable. Groundwater recharge varies with climate, soil type and land use. In order to represent these variables as accurately as possible, grid-based hydrological models are used in this study. The second reason for this is even more important: a lumped model can only predict impacts on lumped variables, regardless of the location where the change occurred. To simulate the effects of changes in spatial land use patterns, including the effects of a changed distribution within a subcatchment, a spatially discretised model is necessary. As the LARSIM model of the Neckar basin provided by LUBW runs on a 1 x 1 km raster, the HBV model was modified to operate with a similar discretisation.

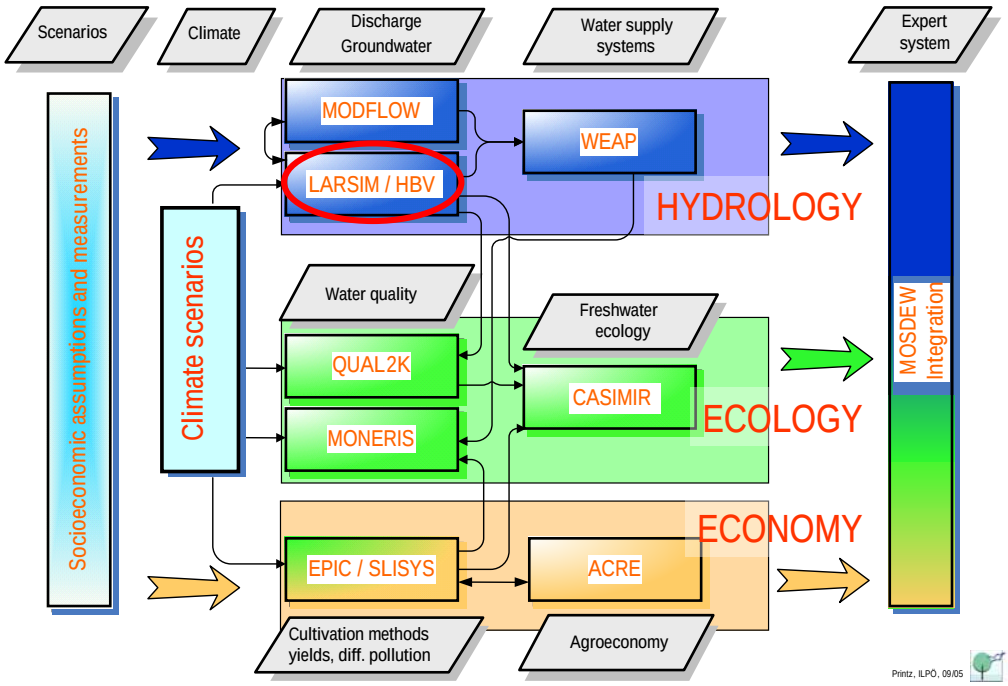

Figure 4.1: Structure and model integration of the decision support system MOSDEW (after Kaule, 2006).

4.1 The distributed HBV model

The main difference between the distributed and the original HBV model is the use of square grid cells as primary hydrological units. Therefore, snowmelt, soil moisture, evapotranspiration and runoff generation are calculated for each grid cell individually. The only exception is one portion of the runoff response which is represented conceptually by reservoirs for direct discharge and baseflow. The baseflow reservoir for the subcatchments is aggregated because the processes in the groundwater systems are taking place on larger scales.

A further improvement is a more physically-based soil moisture module. In the original HBV model, discharge is generated by the soil module based on saturation. The direct runoff reservoir has two outlets. The bottom outlet is considered groundwater recharge and feeds into the groundwater reservoir. The soil moisture is only reduced by evapotranspiration. However, in the new soil module, drainage from the soil to the groundwater system is considered as an additional sink term in the soil moisture balance. The maximum soil moisture storage is defined by the field capacity. Based on actual soil moisture, a variable part of precipitation and snow melt is converted into direct runoff and transferred to the direct runoff reservoir as in the original version. The main difference is that percolation connects the soil moisture storage to the groundwater reservoir, controlled by a maximum percolation rate and the saturation of the grid cell (Figure 4.2).

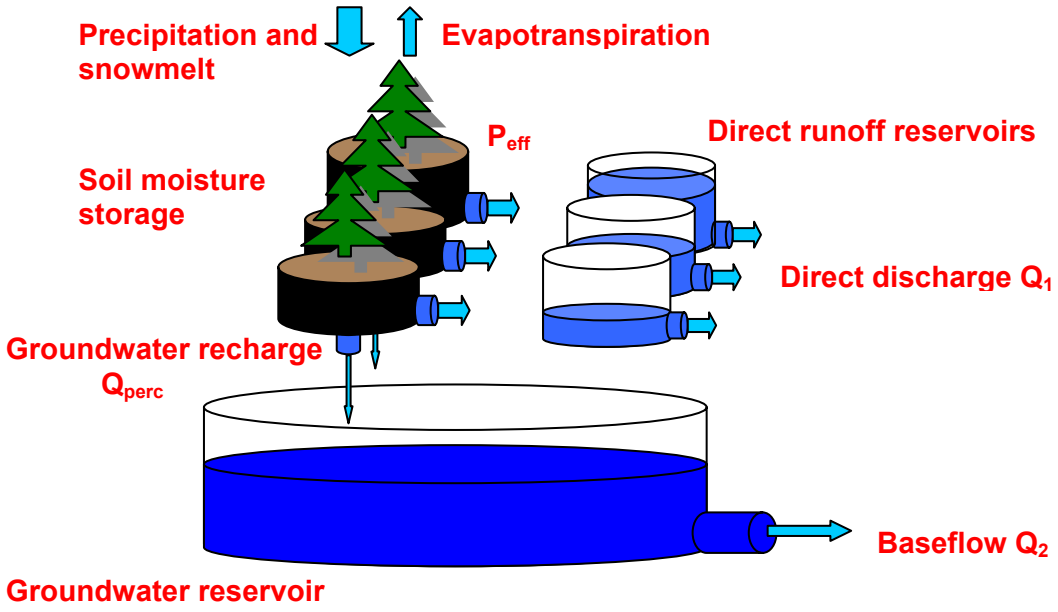

Figure 4.2: Representation of the main processes in the modified HBV model.

The performance of the old and new soil module was not compared specifically. Considering only the efficiency in simulating observed discharges, the fully distributed version with the new soil module was slightly inferior compared to the original version. However, it was used in this study because it provides more information and is supposed to represent the natural system more realistically. This facilitates the regionalisation of parameters because the process description is closer to the processes observed in the field. Despite the large number of parameters, this modified version is expected to produce spatially more reasonable results than the original HBV model because the spatial distribution of the processes is taken into account rather than averaging over larger areas or elevation bands. E.g. Uhlenbrook et al. (2004) obtained better results with a distributed version of HBV than with a semi-distributed. Nonetheless, improved results are contingent on the accuracy of the input data.

Runoff production in the soil (P_{eff}) is calculated using a non-linear relationship between actual soil moisture (SM), field capacity (FC), and rainfall plus snowmelt (P) (Equation 4.1). Direct runoff, percolation from the grid cells, and baseflow from each sub catchment is calculated using the following formulas (Equation 4.2 to Equation 4.4):

$$P_{eff} = \left(\frac{SM}{FC}\right)^{\beta} \cdot P \tag{4.1}$$

$$Q_{perc} = k_{perc} \cdot SM \cdot \left(\frac{SM}{FC}\right)^{5-\beta} \tag{4.2}$$

$$Q_1 = k_1 \cdot S_1^{1+\alpha} \tag{4.3}$$

$$Q_2 = k_2 \cdot S_2 \tag{4.4}$$

with (units adapted by additional coefficients):

P_{eff}	Effective precipitation $[mm]$
SM	Actual soil moisture $[mm]$
FC	Field capacity $[mm]$
β	Non-linearity parameter of runoff production $[-]$
P	Rainfall plus snowmelt $[mm]$
k_{perc}	Maximum percolation rate at soil saturation $[-]$
α	Exponent of non-linear storage reservoir $[-]$
Q_i	Discharge from outlet i of the reservoirs $[m^3/s]$
k_i	Recession coefficient of reservoir i $[-]$
S_i	Water level of reservoir i $[mm]$

Q_i is the discharge from the respective outlet of the reservoirs; k_i is the respective recession coefficient, α is the exponent and S_i is the water level of the reservoirs (Equation 4.3 and Equation 4.4). The non-linearity parameter β describes the variability of the runoff coefficient of the soil at different saturations (Equation 4.1). The percolation is limited to a maximum rate when the soil is saturated (k_{perc}). Below field capacity, the percolation is reduced non-linearly using the same parameter β but with opposite direction and depending on the range of the parameter. In this case, β varies between one and four leading to higher infiltration rates for soils with high β (Equation 4.2). Using β in Equation 4.1 and Equation 4.2 assumes that soils with higher runoff coefficients (small β) will show smaller infiltration capacities. Hence, there is a need for further research in the formulation of the soil moisture module.

Except for field capacity which was derived from soil data, all parameters of the routines described above need to be estimated by calibration against observed discharge data if no other multi-response data is available. Instead of direct calibration, the parameters were regionalised based on catchment characteristics for two reasons:

- calibrating a model with a significant number of free parameters for every grid cell is not reasonable for meso-scale catchments. In an average catchment of 200 km^2 more than 1000 parameters would be calibrated based on one discharge time series; and
- if the model is to reflect changes in catchment properties, then the parameters must be linked to natural features of the basin since calibration for potential future scenarios is not possible.

Therefore, the next sections gives a general introduction to the regionalisation methods developed in this study.

4.2 Regionalisation of distributed model parameters

In this study, five parameters of a 1 km^2 gridded version of the HBV model are estimated based on soil properties, topography and six land use classes. Four different regionalisation approaches were used. The idea behind these four is to reduce the parameter space available for optimization by some form of constraint and therefore be able to find reasonable regression relationships. This avoids the problem of equifinality which often leads to weak correlations between model parameters and

catchment properties (Beven and Binley, 1992). The first approach directly estimates the relationships between catchment characteristics and model parameters. Following the ideas of Hundecha and Bárdossy (2004), transfer functions are defined and the parameters of the transfer functions are calibrated instead of the model parameters themselves. The other three approaches are more general and use prior knowledge about the form of these functions. By imposing conditions on the relationships between model parameters and catchment characteristics, the available parameter space for calibration is significantly reduced. This is demonstrated with a modified Lipschitz condition as a measure of similarity, a monotony condition, and a combination of both constraints. The methods were developed in the central European Neckar basin (Götzinger and Bárdossy, 2007).

4.2.1 Transfer functions

In this method, the model parameters, $\boldsymbol{p}$, are expressed by transfer functions of catchment characteristics:

$$p = f(flowtime, landuse, soilproperties, area, geology) \tag{4.5}$$

Regionalisation was completed by *a priori* assumption of linear or logistic relationships between model and transfer function parameters. The model was then calibrated by adjusting the parameters of the transfer functions instead of the model parameters themselves following the method proposed by Hundecha and Bárdossy (2004). Table 4.1 shows the combinations of catchment characteristics and model parameters used for calibration. The cell properties which are most closely related to the respective model parameters were selected. As several possible alternatives were suitable, the most successful combinations were chosen for further application.

Table 4.1: Regionalised parameters and basis for regionalisation.

Parameter	Regionalised by:	Regression type
β	Upper soil layer permeability, permanent wilting point	Logistic
k_{perc}	Bedrock permeability, lower soil layer permeability	Logistic
k_1	Flow time, land use	Linear
α	Land use, field capacity	Logistic
k_2	Bedrock permeability, catchment area	Linear

The simplest bivariate regression type is a linear equation with three parameters such as:

$$z = a \cdot x + b \cdot y + c \tag{4.6}$$

where x and y are two variables explaining the variable z and a and b are the regression coefficients which have to be found, e.g. by least squares approximation. As the explaining variables often span a much wider range than the dependent variables, a

logistic regression with five parameters (e.g. Equation 4.7) was used in these cases.

$$z = a + \frac{w}{1 + b \cdot e^{-(c \cdot y + d \cdot x)}} \tag{4.7}$$

Here, a, b, c, d and w are the unknown regression coefficients. The function can take the form of a sigmoid curve, a stretched S-curve with two asymptotic limits (a and $a+w$) and a quasi-linear middle portion. Therefore, this regression type can be very useful to describe relationships between variables with strongly differing ranges.

All model parameters not mentioned in Table 4.1 such as the degree-day factor, threshold temperature, and additional evapotranspiration are calibrated directly and held constant throughout the study area. The areal-weighted mean soil properties (field capacity, permanent wilting point, hydraulic conductivity of two soil layers) for the grid cells are calculated from the attributes of the soil classes identified in the catchment. Automatic calibration was accomplished using simulated annealing (Aarts and Korst, 1989), a stochastic optimization algorithm which is based on the analogy with the crystallisation mechanism of metallurgy. With decreasing temperature, fewer possibilities for the movement of atoms during the cooling process are given. By repeated variation of the crystal lattice the optimum state with minimum energy is finally reached. This is translated into reduced degrees of freedom for parameter variation during the course of the optimization. The routine maximizes an objective function composed of Nash-Sutcliffe efficiencies of several temporal aggregation steps. Daily discharges are used to calibrate the runoff concentration parameters (α, k_1, k_{perc} and k_2) which control the retention of the discharge. Weekly and mean annual discharges are used to calibrate the runoff generation parameter β, which controls the water balance.

With this method, a more detailed and realistic representation of the underlying physical processes is achieved with less free calibration parameters than a lumped model approach. The approach was successfully tested in the upper Neckar basin (Götzinger and Bárdossy, 2005). In general, however, the *a priori* definition of the functional form of the relationships is difficult. Furthermore, the method is relatively static and suitable coefficients are hard to find for a larger range of catchment characteristics. Because the results for the whole Neckar catchment were not as good as expected, another methodology was developed.

4.2.2 The modified Lipschitz condition

To improve the efficiency of the regionalisation procedure, another strategy was tested and compared. The same parameters were calibrated directly for the whole catchment. The combinations of parameters and catchment characteristics described in Table 4.1 were also used in this approach. However, in this strategy, the parameters of a selected set of subcatchments were calibrated simultaneously under the condition that similar cell properties must lead to similar model parameters. This assumption can be enforced using the continuity of the regionalisation relationship. In analysis, a function is said to be Lipschitz continuous if Equation 4.8 holds:

$$|f(x_1) - f(x_2)| \leq K \cdot |x_1 - x_2| \tag{4.8}$$

This concept of continuity is widely accepted in natural sciences. It is generally assumed that any entities with similar properties will also behave similarly. This

assumption is utilized in the parameter estimation problem by a modified Lipschitz condition (Equation 4.9):

$$|p_i - p_j| \leq \sum_{k=1}^{L} |c_{ki} - c_{kj}| \cdot K_k \tag{4.9}$$

with:

p	Model parameters
c	Cell properties
k	Index of the cell properties
i and j	Cell indices
K	Lipschitz constants
L	Number of utilized cell properties

where p are the model parameters, c are the utilized cell properties indexed by k, whereas i and j are indices for all the cells of the respective set. K_k is the so called Lipschitz constant for each cell property and L is the number of characteristics used to estimate one parameter. In this study, L is two for all parameters (Table 4.1). During the optimization process, only those parameter sets are accepted which fulfil this condition and yield satisfactory discharge simulations. The functional relationship is enforced by lowering K_k in subsequent calibration simulations until an acceptable regression is found. By excluding all parameters which do not fulfil the Lipschitz condition, only the discharge simulations of those parameters which fall into the corridor defined by K_k are evaluated. Here, and also in the following two approaches, the regression relationships themselves were not evaluated statistically. Nevertheless, their successful application in the regionalisation catchments shows that they are reasonable. Because some of the results of this method were difficult to interpret, another constraint was tested.

4.2.3 The monotony condition

The general pattern resulting from a change of catchment properties is usually predictable, e. g. a higher storage capacity of the soil will generally lead to lower runoff values. This knowledge can be translated into model parameters by prescribing that the relation to catchment properties should be monotonously increasing or decreasing as shown in Equation 4.10:

$$\text{if } c_{ki} \leq (\geq)\ c_{kj} \quad \text{for all k then } p_i \leq p_j \tag{4.10}$$

Again, p are the model parameters, c are the utilised cell properties indexed by k, and i and j are indices for all the cells of the calibration set. All combinations of trends are possible and have been used in this study, e.g. for the recession coefficient of the groundwater reservoir (k_2): A larger bedrock permeability or a smaller catchment area will both lead to a quicker groundwater reaction, i.e. a smaller k_2. The inequalities are adapted to represent the assumed trends in each case. The same parameters were calibrated directly, the same combinations of parameters and catchment characteristics were used and the parameters of the same set of subcatchments were calibrated simultaneously as in the previous Section. Again, only these parameter sets which fulfil this condition and can reproduce the observed discharge

are accepted, and the model is calibrated until a suitable regression relationship is found. By excluding parameters which do not fulfil the monotony condition, only the discharge simulations of those parameters which follow the assumed trends are evaluated. Although this approach ensures the overall trend of the dependencies, it also leads to jumps in the relationships which are difficult to verify from the physics. Therefore, a combination of the last two approaches, the monotony and the Lipschitz condition, was tested.

4.2.4 The combination of both conditions

Using both conditions simultaneously combines their advantages. It ensures that the relationships are sufficiently smooth and follow the trends assumed *a priori*. Therefore, in this last trial only parameter sets which fulfil the Lipschitz and the monotony condition are accepted during calibration. The combination of both conditions ensures that only parameter sets which follow the assumed trends in a smooth way are used in the calibration. By optimizing the simulation efficiencies mentioned above, the model can be calibrated until a useful regression relationship can be derived.

4.2.5 Examples

As can be seen from Table 4.1, each model parameter is combined with two cell properties which results in two-dimensional functions in the case of cardinal features. For classified attributes, a one-dimensional function for each class is defined. As an example, the resulting relationships between field capacity and the exponent α of the non-linear direct runoff reservoir (Eqation 4.3) for the six dominant land use classes of the Neckar basin are shown in Figure 4.3.

Figure 4.3 top left shows the smooth transition of the logistic transfer function from high values of α to lower ones with increasing field capacity. The course of Figure 4.3 top right is quite different. The modified Lipschitz condition defines only the maximum absolute slope of the resulting trend line fitted through the points of the graph. The consequent local maxima, minima, and changes in absolute slope make a physical interpretation difficult. Therefore, the monotony condition was introduced which follows the same transition as the transfer functions but with much more flexibility. The multiple sharp jumps which can be observed in Figure 4.3 bottom left can not be explained physically by threshold behaviour but are likely artefacts of the optimisation routine. Finally, the combination of both constraints (Figure 4.3 bottom right) follows the trend derived from our understanding of the processes but without sharp jumps, which occur when only the monotony condition is used. As mentioned earlier, trend lines can now be fitted through the resulting points of Figure 4.3. Those relationships or the transfer functions themselves can then be applied in ungauged catchments to determine the model parameters from the prevailing catchment properties. The results of this application are presented in Chapter 5.1.1.

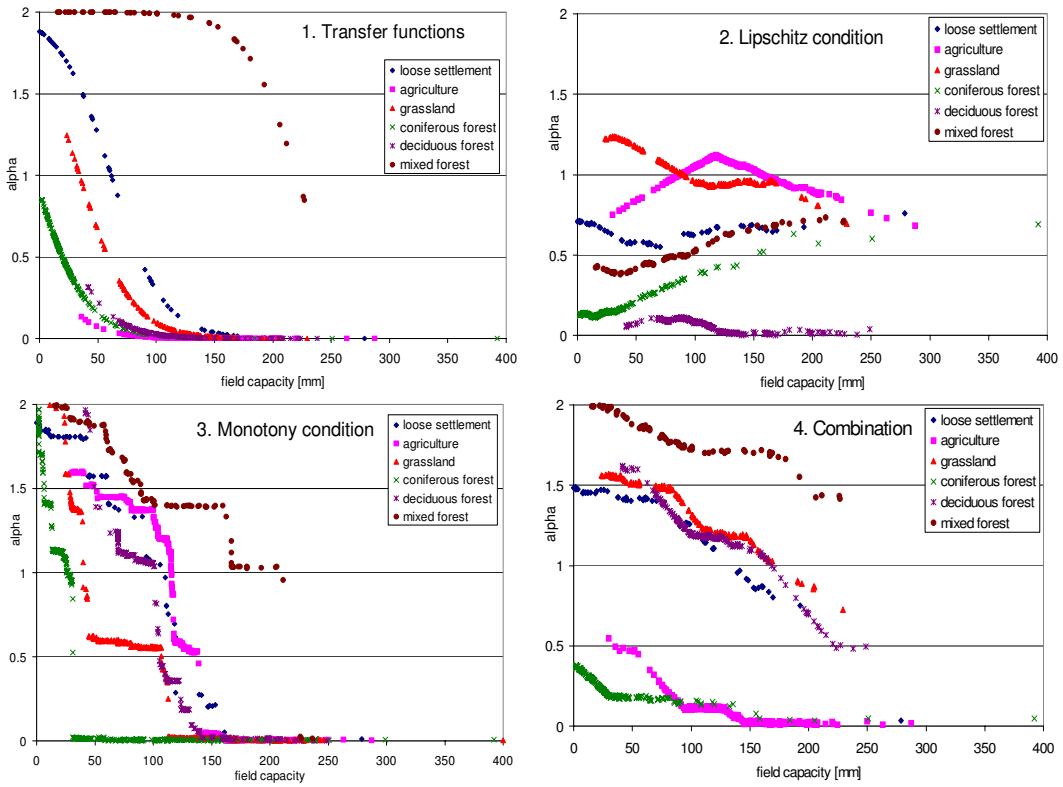

Figure 4.3: Relationships between field capacity and α for six land use classes resulting from the four regionalisation approaches.

4.3 Integration of surface and groundwater models

Model integration has been introduced as a useful tool for integrated water resources management in Chapter 2.3. Besides this rather policy-relevant driver, there are also scientific reasons to pursue this goal. The hydrological cycle is strongly coupled to atmospheric, biological and geochemical cycles. Models that integrate these links may help to improve our understanding of the global cycles and their reaction to perturbations. Bronstert et al. (2005) have shown that the integration of different models is possible for several scales, although associated with significant uncertainty.

As a result of the equifinality discussion (Beven and Binley, 1992), it has been proposed to reduce parameter uncertainty by using multi-response data or multi-criteria calibration. Kuczera and Mroczkowski (1998) observed that augmenting stream flow data with groundwater level data did not improve the identifiability of a nine parameter conceptual model. On the other hand, the use of stream salinity data in addition to stream flow data in the calibration process substantially reduced the parameter uncertainty in their study. Seibert (2000) discovered that the parameters of "HBV light" were significantly constrained when calibrated against stream flow and groundwater level data. For one of the catchments considered in the study, the multi-criteria calibration led to an improvement of the model structure.

As many conceptual hydrological models simulate the groundwater contribution

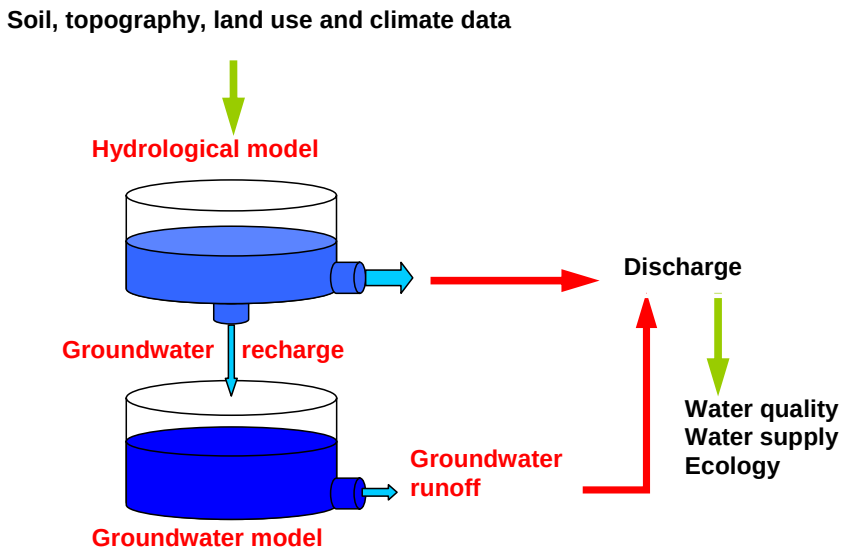

Figure 4.4: Integration strategy of the surface and ground water models.

by a linear storage reservoir, the integration of a physically-based groundwater model should improve the modelling results and lead to more realistic projections for the future. Earlier studies have also shown that uncertainty largely depends on input data, errors in the conceptual model (scale and abstraction), or commensurability issues (Beven and Binley, 1992). Integrating further models enables assumptions and simplifications of conceptual models to be analysed and a multi-response validation of the integrated model to be performed, which may provide more insight and trust in the results. Comparable to the studies mentioned above, the integrated surface and groundwater models in this study are calibrated against runoff and groundwater levels, respectively. However, through the integration concept presented here, they are also conditioned to simulate groundwater recharge and groundwater runoff fluxes which are consistent with the corresponding model. By this indirect check on internal processes, the uncertainty of the modelling complex can be reduced. Some of the problems encountered during the modelling process will be presented and discussed.

The integrated modelling of groundwater recharge and groundwater runoff in the meso-scale Neckar basin are the focus of this Section. Figure 4.4 presents the selected integration strategy: Soil, topographic, land use and climatic data provide the parameters and driving forces of the hydrological model which calculates discharge components and high resolution groundwater recharge rates. The latter serve as input for the groundwater model which simulates groundwater levels as well as groundwater runoff in the stream network. The runoff is then used in the hydrological model as the groundwater component of the discharge. Capillary rise from the groundwater to the root zone on this scale is negligible in the Neckar basin and is therefore not included in the model integration. The simulated total discharge serves as input to water quality, ecological and water supply models. In contrast to the water balance models, no feedback is included between these models.

All models were calibrated individually. LARSIM and HBV were calibrated to fit the observed discharges and to provide a realistic estimate of groundwater recharge.

The groundwater model was calibrated mainly to fit the groundwater levels, but also to minimize the difference between the groundwater runoff simulated by the groundwater model and by the hydrological models. Including this groundwater runoff in the hydrological model decreases the simulation efficiency of the total discharge. Nevertheless, the additional constraints on the individual models (groundwater recharge and groundwater runoff) reduce the degrees of freedom of the system which leads to lower model efficiency but increased confidence in the transferability of the model structure and parameters for predictions. As neither groundwater recharge nor baseflow can be validated by measurements on this scale we have to assume that those processes are well represented. An integrated model may be less efficient in simulating observed data but if the above assumption holds it will be more suitable to predict unobserved states and changes because the physical basis of the system is better represented.

4.3.1 MODFLOW

The physically-based 3D finite-difference groundwater flow model MODFLOW (McDonald and Harbaugh, 1988) was used to model the groundwater flow in the Neckar basin. MODFLOW is a well verified code for mathematical modelling of saturated groundwater flow. It is based on the horizontal and vertical discretisation of the modelling domain and solves the groundwater flow equation - derived from both the law of conservation of mass and Darcy's law - for each discrete point in space and time taking into consideration recharge, pumping and drainage from the given groundwater system. It enables the simulation of leakage between adjacent aquifers and can reproduce flow paths in all three spatial directions. Using the River-Package, MODFLOW also enables simulation of in-/exfiltration into/from rivers. Nine hydrogeologic units are distinguished in the Neckar basin, six of which are classified as freshwater aquifers. The impermeable crystalline rock is considered to be the bottom of the aquifer system. Although the geological structure of the Neckar catchment is characterised by gently dipping formations towards south-east, the orientation of the layers can still be described as quasi-horizontal. However, the dipping layers lead to increasing complexity of the hydrogeological situation due to the fact that different geological formations form the uppermost aquifer in different parts of the basin. More detailed information about the groundwater model can be found in Bárdossy et al. (2006). The set-up, calibration and all simulations were performed by Johanna Jagelke.

4.4 Scenarios of climate and land use change

> *Prediction is very difficult, especially about the future.*
>
> Niels Bohr, Danish physicist (1885 - 1962)

A typical temporal horizon for water resources management planning is 25 to 50 years, however, the lifespan of some hydraulic structures can be up to 80 years or longer. As it is virtually impossible to foresee the exact development of climate and land use for such a long time, scenarios are often used to assess several possible future outcomes. The IPCC (Houghton et al., 2001) defines scenarios as "a plausible

and often simplified description of how the future may develop, based on a coherent and internally consistent set of assumptions about key driving forces (e.g., rate of technology change, prices) and relationships. Scenarios are neither predictions nor forecasts and sometimes may be based on a 'narrative storyline'. Scenarios may be derived from projections, but are often based on additional information from other sources." An important point is the clear distinction between scenarios and forecasts. Scenarios cannot predict the exact temperature or the water demand for a specific day in the future. They can, however, help to estimate how the mean behaviour of a system may change under certain circumstances. Two main drivers must be considered for water resources planning: the climate and the catchment attributes - mainly land use but also other factors such as water abstraction.

4.4.1 Climate change scenarios

In climate research, there are four main SRES families (A1, A2, B1 and B2), which are used to determine the future composition of the atmosphere according to potential socio-economic storylines and emission developments. The letters A and B describe the economic dimension of the global development. The A scenarios exhibit a stronger economic growth and the B scenarios are more oriented towards sustainability and ecologic protection. The numbers one and two indicate the level of international cooperation. One stands for a diverse world focussing on local and regional alliances whereas two means a strong international cooperation and exchange of technologies. Although many different sub-storylines are used in the literature, the box below provides some general details on the four scenario families.

Several global circulation models have simulated these four climate scenarios, unfortunately, with partly contradicting results. As the differences in the near future are comparatively small, only climate scenarios from the climate model ECHAM 4 (Roeckner et al., 1996) and the emission scenarios A2 and B2 are used in this study. ECHAM 4 operates on a horizontal resolution of 2.8 degrees (about 300 km) which requires the downscaling of the meteorological variables to a resolution suitable for hydrological modelling. The results of two downscaling methods have been used in this study:

- Enke: a statistic-dynamical downscaling based on circulation patterns (Enke et al., 2005)
- Yang: a multivariate stochastic downscaling using a different circulation pattern classification scheme (Yang and Bárdossy, 2005)

The first method is used by the water authorities in the Neckar basin (LUBW) in a regional climate change impact program (KLIWA, 2006). Two realisations with the driest and wettest climate were provided by LUBW from the stochastic scenario ensemble which are further denoted by Enke dry and Enke wet. Both are based on the emission scenario B2, the time period 2021 to 2050, and are available only within the Neckar basin. The second method also provides two scenarios based on the socio-economic storylines A2 and B2 which cover the period 2000 to 2030 and are further called Yang A2 and Yang B2 in both basins. The downscaling was carried out by Wei Yang and is described in more detail in Yang and Bárdossy (2005).

In terms of precautionary planning, the Enke scenarios are compared to the Yang scenarios and used together with socio-economic scenarios of earlier time frames although they relate to a potentially later climatic situation. Table 4.2 compares the key figures of the four scenarios in the Neckar basin to a reference period. Obviously, the differences are relatively small especially between the two Enke realisations. All four scenarios show an increase in temperature and precipitation relative to the reference period, which is more pronounced in the case of the Yang downscaling method.

Scenario families of the Special Report on Emissions Scenarios (SRES) (from Houghton et al., 2001)

A1. The A1 storyline and scenario family describe a future world of very rapid economic growth, global population that peaks in mid-century and declines thereafter, and the rapid introduction of new and more efficient technologies. Major underlying themes are convergence among regions, capacity building and increased cultural and social interactions, with a substantial reduction in regional differences in per capita income.

A2. The A2 storyline and scenario family describe a very heterogeneous world. The underlying theme is self-reliance and preservation of local identities. Fertility patterns across regions converge very slowly, which results in continuously increasing population. Economic development is primarily regionally oriented and per capita economic growth and technological change more fragmented and slower than in other storylines.

B1. The B1 storyline and scenario family describe a convergent world with the same global population, that peaks in mid-century and declines thereafter, as in the A1 storyline, but with rapid change in economic structures toward a service and information economy, with reductions in material intensity and the introduction of clean and resource-efficient technologies. The emphasis is on global solutions to economic, social and environmental sustainability, including improved equity, but without additional climate initiatives.

B2. The B2 storyline and scenario family describe a world in which the emphasis is on local solutions to economic, social and environmental sustainability. It is a world with continuously increasing global population, at a rate lower than in A2, intermediate levels of economic development, and less rapid and more diverse technological change than in the B1 and A1 storylines. While the scenario is also oriented towards environmental protection and social equity, it focuses on local and regional levels.

For the Benin test case, the approach was slightly different. As the dependence on circulation patterns is much weaker than in the Neckar basin, a stochastic weather generator was used to generate high resolution climate scenarios from the available global circulation model output (Yang and Bárdossy, 2006). Compared to the control

Table 4.2: Mean temperature and precipitation of the climate scenarios in the Neckar.

	Temperature	Precipitation
1988 - 1999	9.3 °C	1074 mm
Enke dry	10.9 °C	1162 mm
Enke wet	10.9 °C	1220 mm
Yang A2	12 °C	1208 mm
Yang B2	11.9 °C	1311 mm

Table 4.3: Mean annual potential evapotranspiration and precipitation of the climate scenarios in the Ouémé.

	Potential evapotranspiration	Precipitation
1980 - 1999	2818 mm	1186 mm
Yang A2	2840 mm	1073 mm
Yang B2	2855 mm	1078 mm

simulation both climate scenarios show an increase in temperature, and therefore, potential evapotranspiration. Precipitation increases in the North but during the rainy season, decreases in the South (Table 4.3). The climate scenarios are still affected by a large uncertainty, thus results must be used with caution.

4.4.2 Land use change scenarios

Estimating the future land use of a basin is associated with much more uncertainty than the future climate because it depends on a multitude of local factors. As in the socio-economic storylines of the SRES scenarios, political, economic, technical and natural boundary conditions need to be considered. Following these global frameworks, regional scenarios for both basins have been developed by an interdisciplinary scenario group in RIVERTWIN. Using expert judgements, historical trends have been extrapolated into the future under the following premises: In the Neckar basin, the main process could be the conversion of farmland into residential areas. Forests are protected and grassland is stronger subsidized by the EU Common Agricultural Policy. As the Neckar basin showed a substantial economic and population growth in the past compared with other regions in Germany, two scenarios of settlement growth according to the SRES storylines and two policy interventions were defined:

- A10: stronger economic development (6% settlement growth per year, dense settlements with less green space)
- B20: more ecology-oriented development (5% settlement growth per year, loose settlements with more green space)
- 50% grassland: conversion of half of the farmland into grassland (evenly distributed)
- 100% fallow: complete abandonment of intensive agriculture and conversion to fallow

Table 4.4: Total area [km^2] of the major land use types in the Neckar basin in 2000 and for the four socio-economic scenarios.

Land use class	2003	Scenario A10	Scenario B20	Scenario 50% grassland	Scenario 100% fallow
Dense settlements	49	463	15	49	49
Loose settlements	1 281	937	1 158	1 781	1 281
Farmland	3 937	4 640	4 764	1 839	0
Fallow	6	99	100	7	3 943
Grassland	2 918	2 903	2 972	4 575	2918

The last two scenarios should be seen as maximum benchmark scenarios for potential EU policy programs. As farmland is the main source for diffuse pollution of surface- and groundwater, interventions reducing the agricultural area are plausible. These two extreme scenarios can show the maximum expected impact on the water balance from such a policy. They were developed together with the Environmental Ministry Baden-Württemberg. The settlement growth is implemented according to observed trends of the past. Cities and villages were growing uniformly into areas where settlements already existed close-by. According to these assumptions, land use grids for the socio-economic scenarios have been designed by Hans-Georg Schwarz-von Raumer. Key figures are presented in Table 4.4.

The land use maps have been constructed on a finer resolution and then classified according to the prevailing land use of the km^2 grid cells. Therefore, the areas of the land use types vary in the scenarios although they were not modified directly.

In the Benin case, the major driver for land use change is population growth and subsequent conversion of the natural savannah vegetation into settlements, roads and a mosaic of fields by slash and burn. Together with stakeholders, two socio-economic scenarios have been set up:

- A: optimistic, stronger economic development, controlled urbanisation, two large-scale irrigation schemes (3.2% population growth per year)
- B: pessimistic, weak national economy, uncontrolled settlement and farmland development (3.5% population growth per year)

These scenarios are also used in the national planning administration of Benin. For each scenario, the population growth has been translated into a specific demand for settlements and agricultural area according to the development of the national framework. This demand has been satisfied in a similar way as in the Neckar basin: according to the proximity to roads and existing villages, new settlements and agricultural areas have been created leading to the land use distribution shown in Table 4.5 and summarized in Figure 4.5.

The Directorate General for Water has identified several potential sites for the construction of multi-purpose reservoirs. Therefore, scenario A contains in addition to the present reservoirs two of the finally selected dam sites (Bétérou and Assanté) which supply two large scale irrigation schemes. These reservoirs have a volume of

Table 4.5: Total area [km^2] of the major land use types in the Ouémé in 2003 and for the two socio-economic scenarios.

Land use class	2003	Scenario A	Scenario B
Forest	9 510	5 308	3 058
Savannah	19 350	10 799	6 222
Gallery Forest	2 114	1 903	1 480
Rocky Savannah	332	332	332
Mosaic of fields	16 303	25 893	35 005
Tree plantations	1 349	3 982	2 277
Water	47	109	47
Settlement	281	960	865

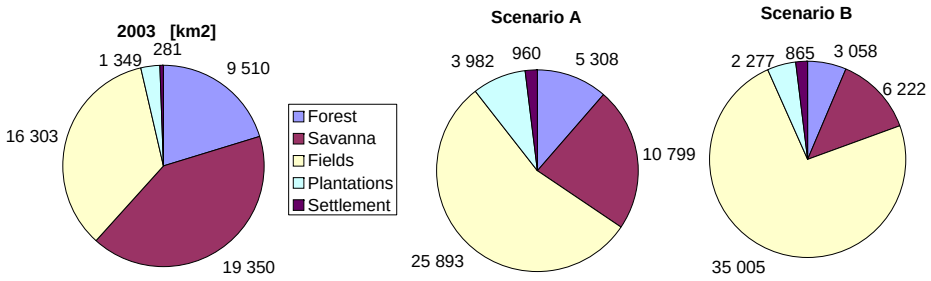

Figure 4.5: Summarized land use distribution in the Ouémé basin for the reference year 2003 and the two scenarios.

24 Mio. m^3 and are kept full as long as possible to provide irrigation water during the dry season. This operational rule has been incorporated into the hydrological model. The water demand for irrigation has been modelled with WEAP by Martha Fernandez and included into HBV as monthly time series.

In an additional intervention scenario, these two reservoirs are extended with the help of foreign investors to a volume of 500 Mio. m^3. Together with another planned dam in Kétou, they could provide more than 100 MW of electrical energy to the region. The planned volume and operational discharge of the proposed dams are given in Table 4.6.

Table 4.6: Key figures of the investigated hydropower reservoirs.

Site	Volume	Regulated minimum discharge
Bétérou	500 Mio. m^3	30 m^3/s
Assanté	500 Mio. m^3	30 m^3/s
Kétou	2000 Mio. m^3	100 m^3/s

The Kétou dam is planned as a pure hydropower project with 2 billion m^3 storage volume. Operation of all three would be slightly different from a single-purpose irrigation scheme. The water level is kept at its maximum as long as possible, however, a regulated minimum discharge of 30 and 100 m^3/s for the two smaller and the one larger dam, respectively, are maintained during the dry season for energy

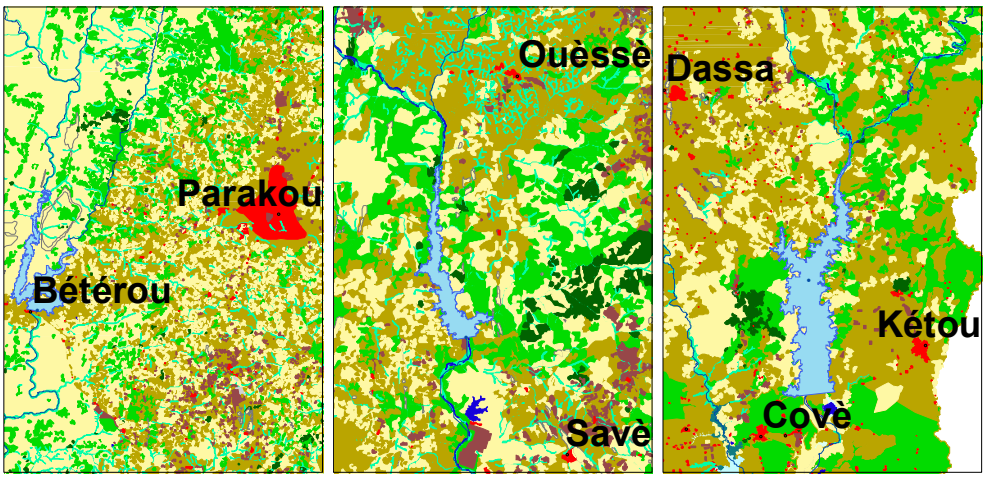

Figure 4.6: Surface area of the hydropower reservoirs planned as intervention in Bétérou, Assanté and Kétou.

production. If the inflow to the reservoir is higher and the reservoir is full, then the discharge is kept at the inflow minus the irrigation demands in Bétérou and Assanté. For the intervention, these operational rules together with the irrigation demands have been incorporated into the hydrological modelling.

The artificial lakes cover areas of 41 and 208 km^2, respectively, when they are at full capacity. Therefore, the land use map, the potential evapotranspiration, and the model parameters were updated accordingly. Three extracts of the land use map are given in Figure 4.6 for visualisation. In addition to the higher potential evapotranspiration from water bodies, the actual evapotranspiration from lake surfaces must also be adapted because this water is available for evaporation as long as the reservoir is not empty. Therefore, lake evaporation has also been included as an additional sink term in the mass balance of the water volume stored in the reservoirs.

5 Results

5.1 Regionalisation of distributed model parameters

5.1.1 Neckar basin

In this case study, six subcatchments with areas from 45 km^2 to 340 km^2 were used to calibrate the model on rainfall, temperature and runoff data from 1980 to 1989. The subcatchments were selected in order to cover the whole range of available catchment characteristics. The regionalisation relationships determined in the calibration were then validated in the remaining 51 subcatchments of the Neckar basin. As an example of the application of the presented methodologies, the simulated and observed hydrographs from the 140 km^2 subcatchment Gaildorf (Kocher) are shown in Figure 5.1 to Figure 5.4.

The model could not be calibrated successfully to the smallest subcatchment (Schwaigern, Lein) with any of the methods. Only the combination of Lipschitz and monotony condition produced discharge simulations which were better than the mean measured values (Nash-Sutcliffe model efficiency > 0). The subcatchment was still included in the calibration set to account for the smaller subcatchments in the regionalisation set. Table 5.1 shows the mean and the median of the daily Nash-Sutcliffe model efficiencies of the four methods for the calibration and the regionalisation subcatchments. The average regionalisation model efficiency of the Lipschitz method is slightly better than the other approaches. All four methods were able to produce reasonable parameter sets for most of the 51 regionalisation catchments. The calibration efficiency of the monotony condition is lower than the others because the method could not fit the discharge hydrograph of one other calibration subcatchment. But the developed regression relationships could still be used to generate reasonable parameter sets for the regionalisation subcatchments.

As expected, all four methods failed to reproduce the observed discharge (Nash-Sutcliffe model efficiency < 0) in karstic areas and in heavily modified or regulated river basins, which indicates their sensitivity to catchment characteristics. The transfer functions failed in eight subcatchments (16%) and the Lipschitz and monotony condition in 15 and 16 subcatchments (29% and 31%), respectively. This shows that the transfer functions are more robust in producing the general flow behavior of catchments. The Lipschitz and monotony condition are more flexible and are adjusted specifically to the calibration catchments. They are therefore also more sensitive to the characteristics of the landscape they are applied in.

The combination of Lipschitz and monotony condition also failed in eight subcatchments. This shows that the combination of both constraints is more robust than both methods individually. It can also describe a wider range of flow behaviour because the developed relationships are not so strictly conditioned to the specific calibration catchments. Six of those eight catchments could also not be simulated with

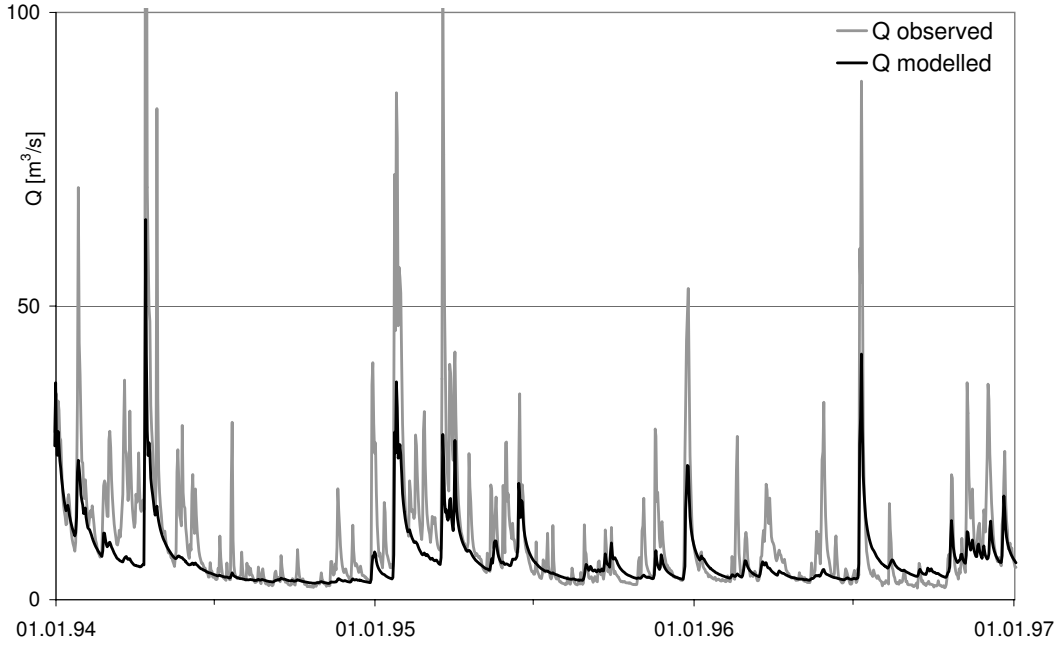

Figure 5.1: Observed and simulated discharge at Gaildorf (Kocher) resulting from transfer functions (mean Nash-Sutcliffe model efficiency in the validation period: NS = 0.69).

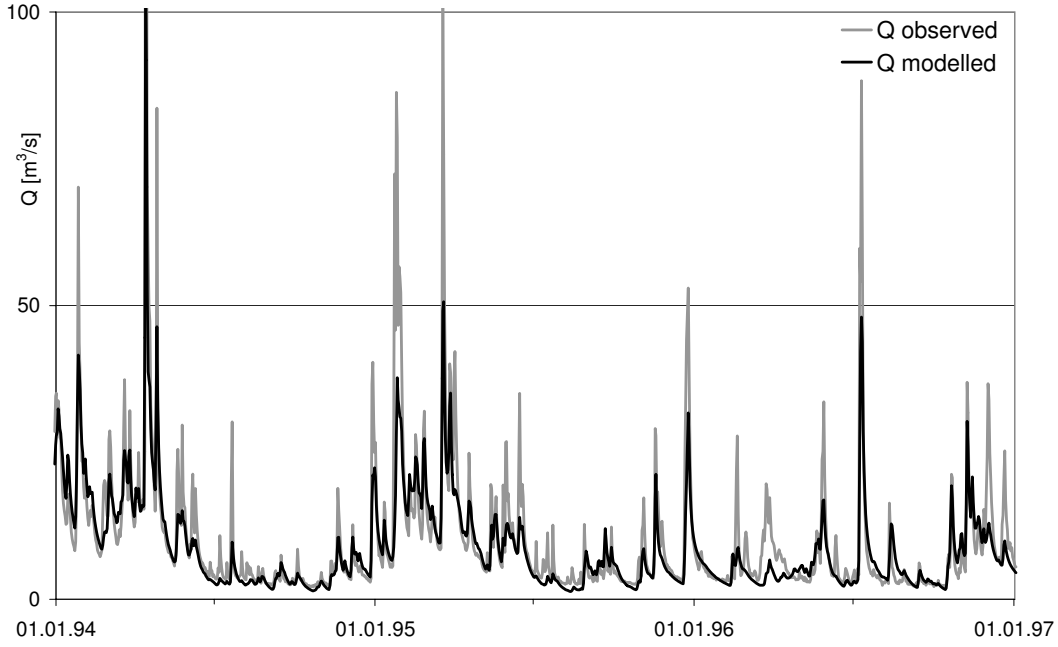

Figure 5.2: Observed and simulated discharge at Gaildorf (Kocher) resulting from the Lipschitz condition (NS = 0.71).

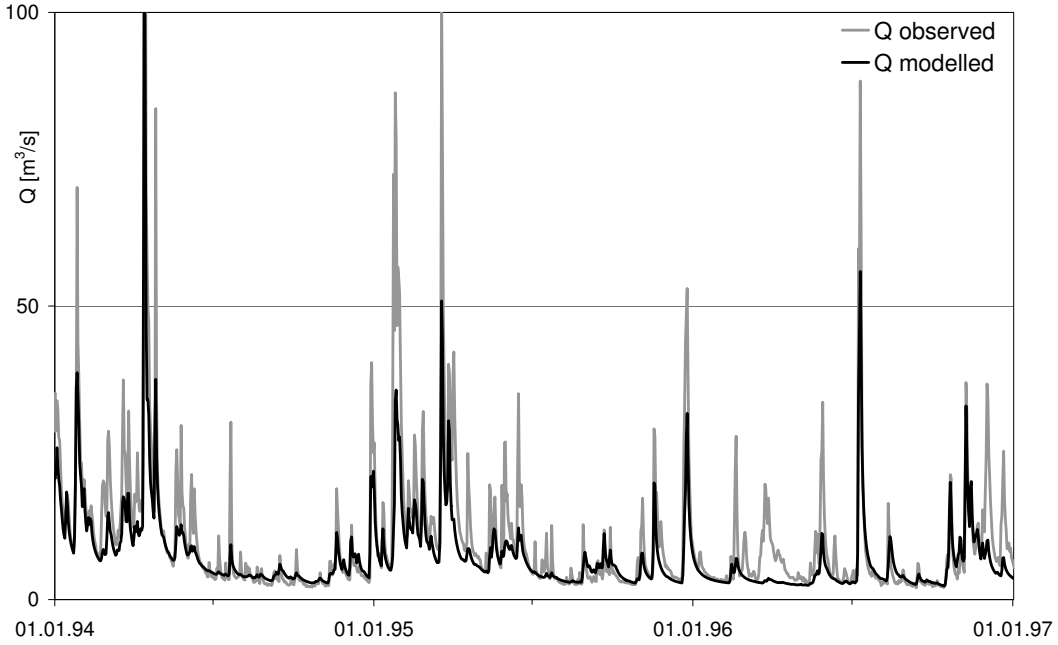

Figure 5.3: Observed and simulated discharge at Gaildorf (Kocher) resulting from the monotony condition (NS = 0.68).

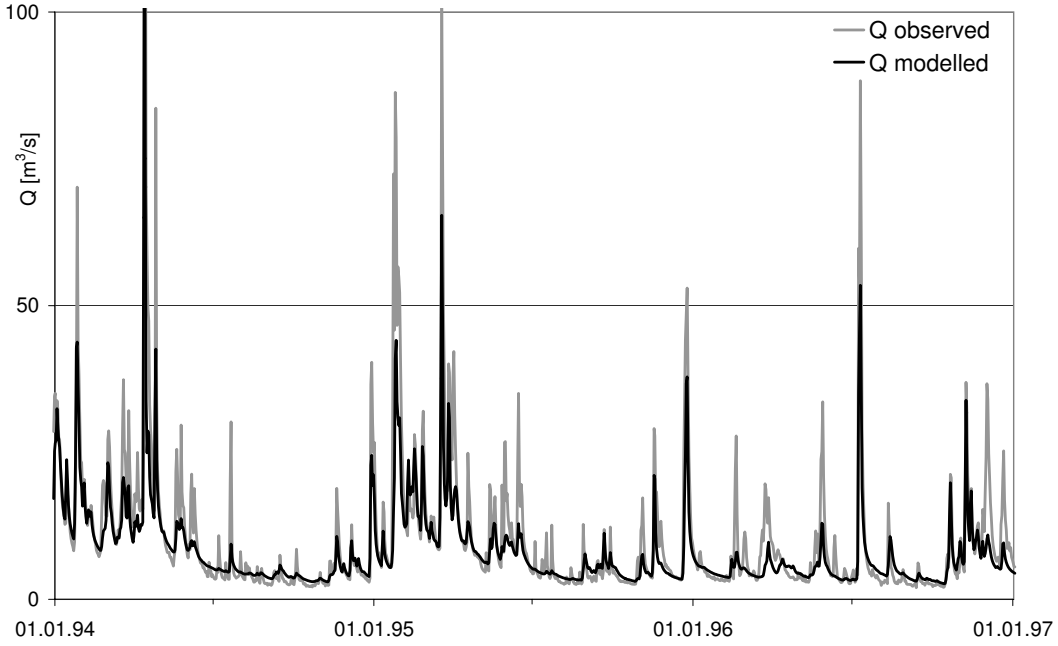

Figure 5.4: Observed and simulated discharge at Gaildorf (Kocher) resulting from the combination of Lipschitz and monotony condition (NS = 0.70).

Table 5.1: Mean and median of the Nash-Sutcliffe model efficiencies of the regionalisation methods in the validation period.

	Transfer functions	Lipschitz condition	Monotony condition	Combination
Calibration mean	0.35	0.21	0.06	0.47
Calibration median	0.49	0.41	0.30	0.53
Regionalisation mean	0.47	0.50	0.47	0.47
Regionalisation median	0.51	0.53	0.50	0.50

the transfer functions. This supports the hypothesis that the methods can not work in karstic and regulated river stretches. Furthermore, the developed relationships are not universally applicable physical laws. They are only valid for the physiographic setting they were calibrated in. Therefore, they also had to be estimated again based on available observations for application in the Ouémé basins. This test of the methodology is described in the following section.

5.1.2 Ouémé basin

In order to test the transferability of the approach the combination of Lipschitz and monotony condition described in Chapter 4.2 was applied as regionalisation method in the Ouémé basin. Data scarcity and the almost fourfold size of the basin lead to the selection of a spatial model raster resolution of 3 km. Six of the thirteen subcatchments were chosen according to their data quality and to cover most of the range of prevailing catchment characteristics. The regionalisation relationships derived from fitting trend lines to the calibrated data points were then used to estimate the model parameters in the remaining seven subcatchments. Fig 5.5 provides an example of such calibrated data points. An example of the application of the methodology in the Ouémé basin is shown in Figure 5.6. The parameters of the headwater catchment Vossa (1 935 km^2) were calibrated and the above mentioned regionalisation relationships were determined from the resulting dependency between the model parameters and catchment characteristics of the calibration set. The total discharge in this example matches the scale and variability of the observations sufficiently well for water resources management planning. The general seasonal behaviour but not all observed flood peaks can be reproduced. The Nash-Sutcliffe model efficiency for daily discharge at this gauge lies at 0.65. The application of the regionalisation is shown exemplarily for the outlet at the gauge Bonou (51 543 km^2) in Figure 5.7. The comparison of observed and simulated discharge shows the potential of the method but also its weaknesses in coping with scarce and partially also erratic data and the extreme runoff regime which could not be modelled with completely satisfying accuracy (compare also Table 5.2 and Table 5.3). For the total catchment, a slightly better performance is achieved by regionalisation than for the headwater catchment Vossa by direct calibration. The remaining deviations stem from the conceptualization of the processes and uncertainties in model structures and input data. The uncertainty in the discharge observations can be estimated from the frequent missing

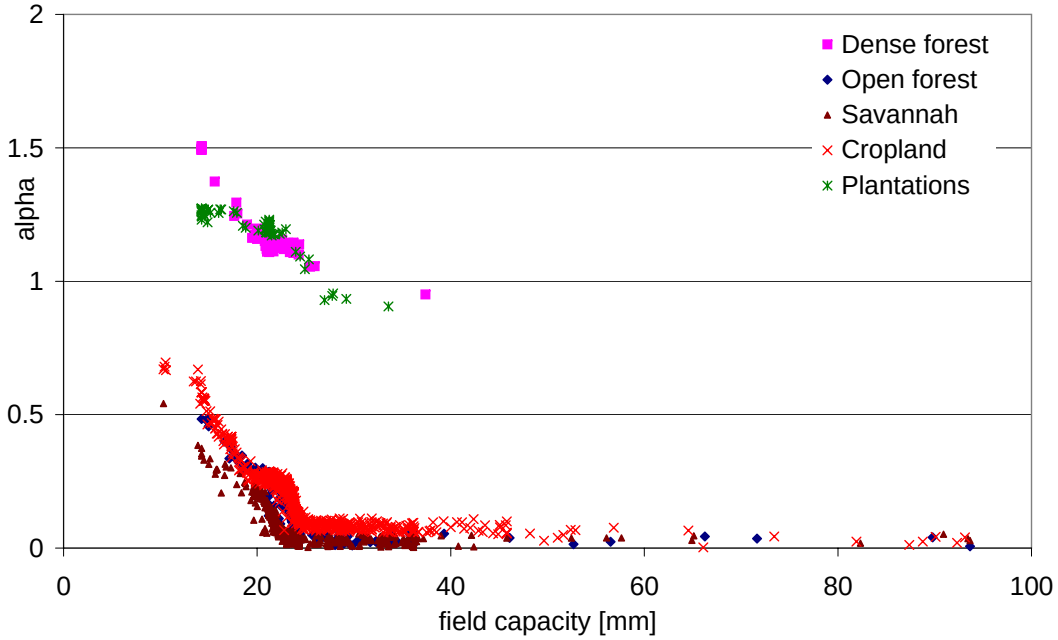

Figure 5.5: Relationship between *alpha* and field capacity for different land use classes derived from the combination of Lipschitz and monotony condition.

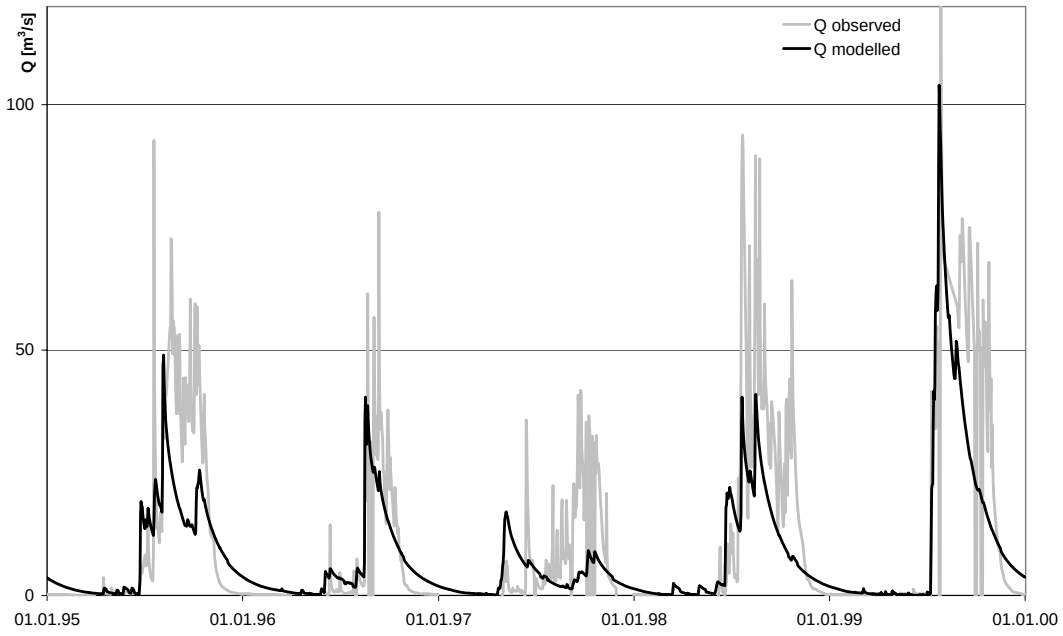

Figure 5.6: Simulated and observed discharge from direct calibration of model parameters at Vossa. Note that missing observations were set to zero in the hydrograph.

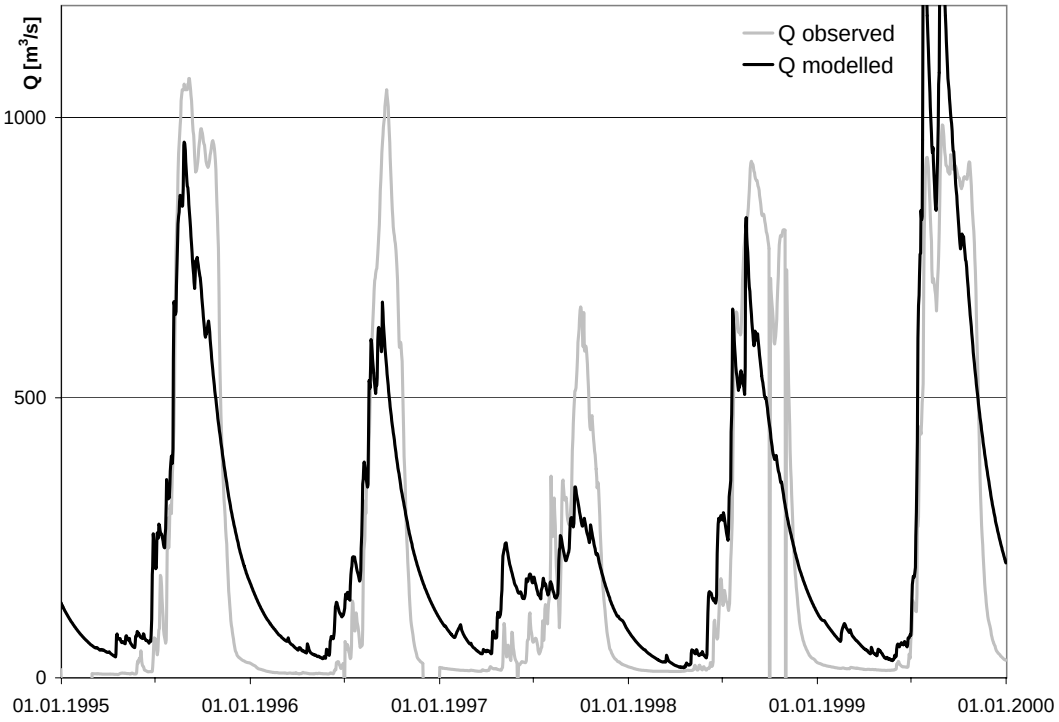

Figure 5.7: Simulated and observed discharge from regionalisation of model parameters at Bonou. Note that missing observations were set to zero in the hydrograph.

observations and erratic behaviour of the discharge. At the outlet the Nash-Sutcliffe model efficiency for daily discharge amounts to 0.77. Considering the available data and their uncertainties, the water balance of the whole Ouémé catchment can be reproduced with satisfactory accuracy. In other subcatchments, the model efficiency is partly better but in some it is also partly worse than these examples. The average Nash-Sutcliffe coefficient of all sub-basins for the validation period is 0.50. Table 5.2 shows the model efficiencies and mean discharges for the subcatchments of the calibration set with which the regionalisation relationships have been determined.

Table 5.2: Model efficiency and mean discharge, MQ, of the calibration set in the validation period (1990-1999).

	Nash-Sutcliffe coefficient	MQ observed [m^3/s]	MQ modelled [m^3/s]
Affon	0.68	11.11	13.34
Wéwé	0.29	3.17	1.79
Cote 238	0.63	21.39	19.31
Vossa	0.65	13.15	10.58
Kaboua	0.42	44.85	49.34
Atchérigbé	0.41	39.27	33.67
Mean	0.51		

Table 5.3 shows the model efficiencies and mean discharges for the subcatchments

Table 5.3: Model efficiency and mean discharge, MQ, of the regionalisation set in the validation period (1990-1999).

	Nash-Sutcliffe coefficient	MQ observed [m^3/s]	MQ modelled [m^3/s]
Barérou	-1.29	9.06	13.55
Bétérou	0.70	76.52	92.62
Banon	0.21	15.49	9.12
Savè	0.44	160.36	141.76
Zagnanado	0.61	135.82	182.58
Domè	0.18	24.96	30.44
Bonou	0.77	202.65	231.5
Mean	0.49		

of the regionalisation set. The parameters of these subcatchments were derived from their characteristics using the regionalisation relationships. For the gauges Barerou and Domè almost no reliable discharge measurements were available. The comparison of the two mean model efficiencies for the calibration and regionalisation set shows that the regionalisation introduces a slight deterioration of the Nash-Sutcliffe coefficient. Partly this may also be due to the lower data quality of the regionalisation set because unreliable discharge series were intentionally excluded from the calibration set. Nevertheless, also in the Ouémé basin the regionalisation procedure can be considered generally successful.

5.2 Integration of surface and groundwater models

5.2.1 Neckar basin

As described in Chapter 4.3 the groundwater component of a distributed HBV model was replaced by the 3D finite-difference groundwater flow model MODFLOW. Both models were calibrated individually for the time period 1980 to 1989. The validation period 1990 to 1999 was slightly warmer and wetter than the 80's. Therefore the presented validation results already provide some insight on the reliability of simulations of a future climate with increased temperature and precipitation. The simulation of daily groundwater recharge by HBV shows a high spatial variability which is dominated by climate, land use and soil type (Figure 5.8). The mean, distribution and large-scale pattern is comparable to simulations performed by the State Agency for Environmental Protection Baden-Württemberg using the Soil-Vegetation-Atmosphere-Transfer model TRAIN-GWN (Armbruster, 2002) which are shown in Figure 5.9. Local differences are obvious, even in the extent and shape of the catchment area, resulting from the different conceptualisation and parametrisation of the models. The variability of the groundwater recharge simulated with LARSIM (Figure 5.10) is smaller than the other two simulations. The parameters of this model were estimated for whole subcatchments based on discharge at the outlet and therefore the variability within a subcatchment is generated only by differing land use and soil properties.

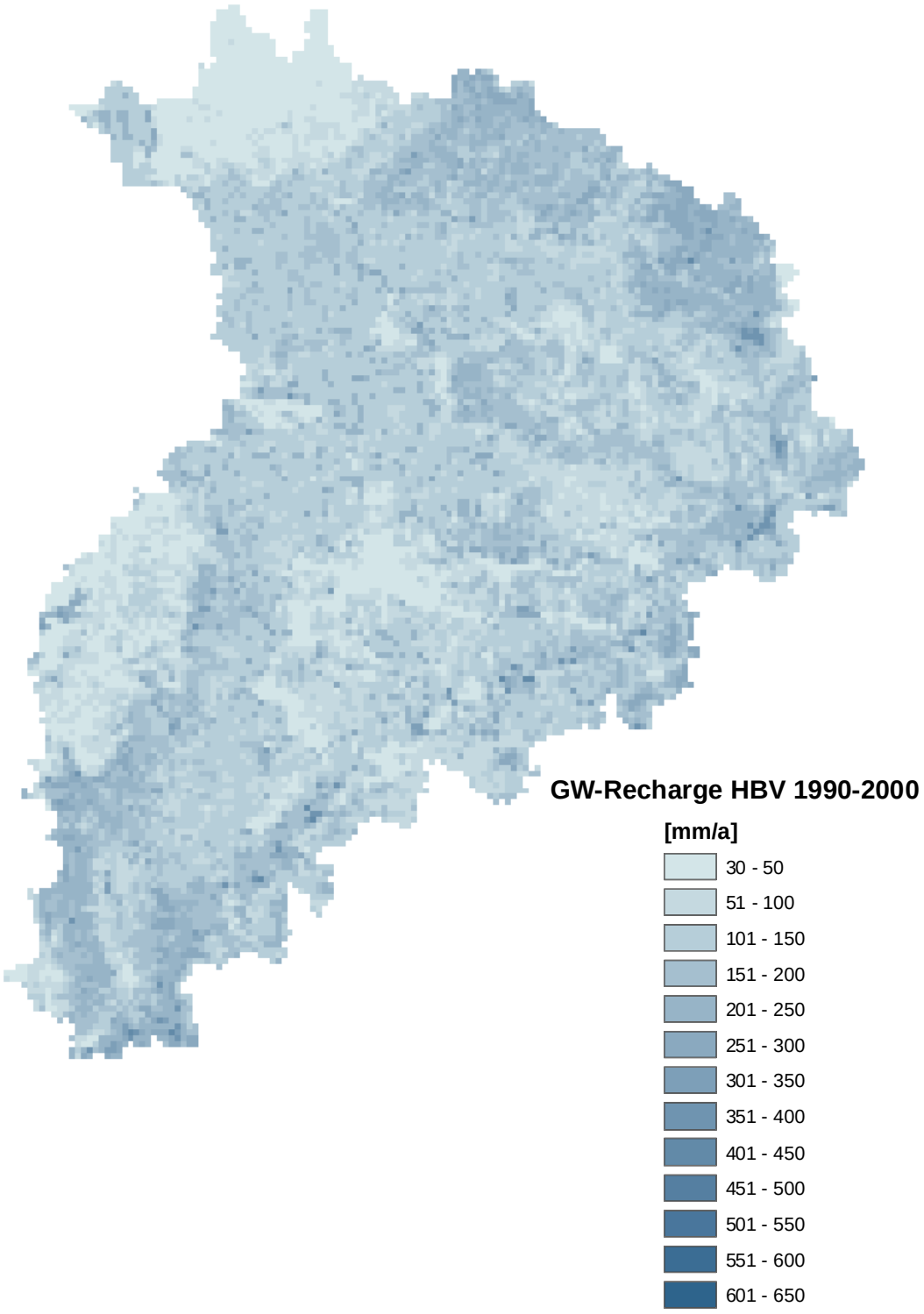

Figure 5.8: Simulated mean annual groundwater recharge in the Neckar basin using HBV.

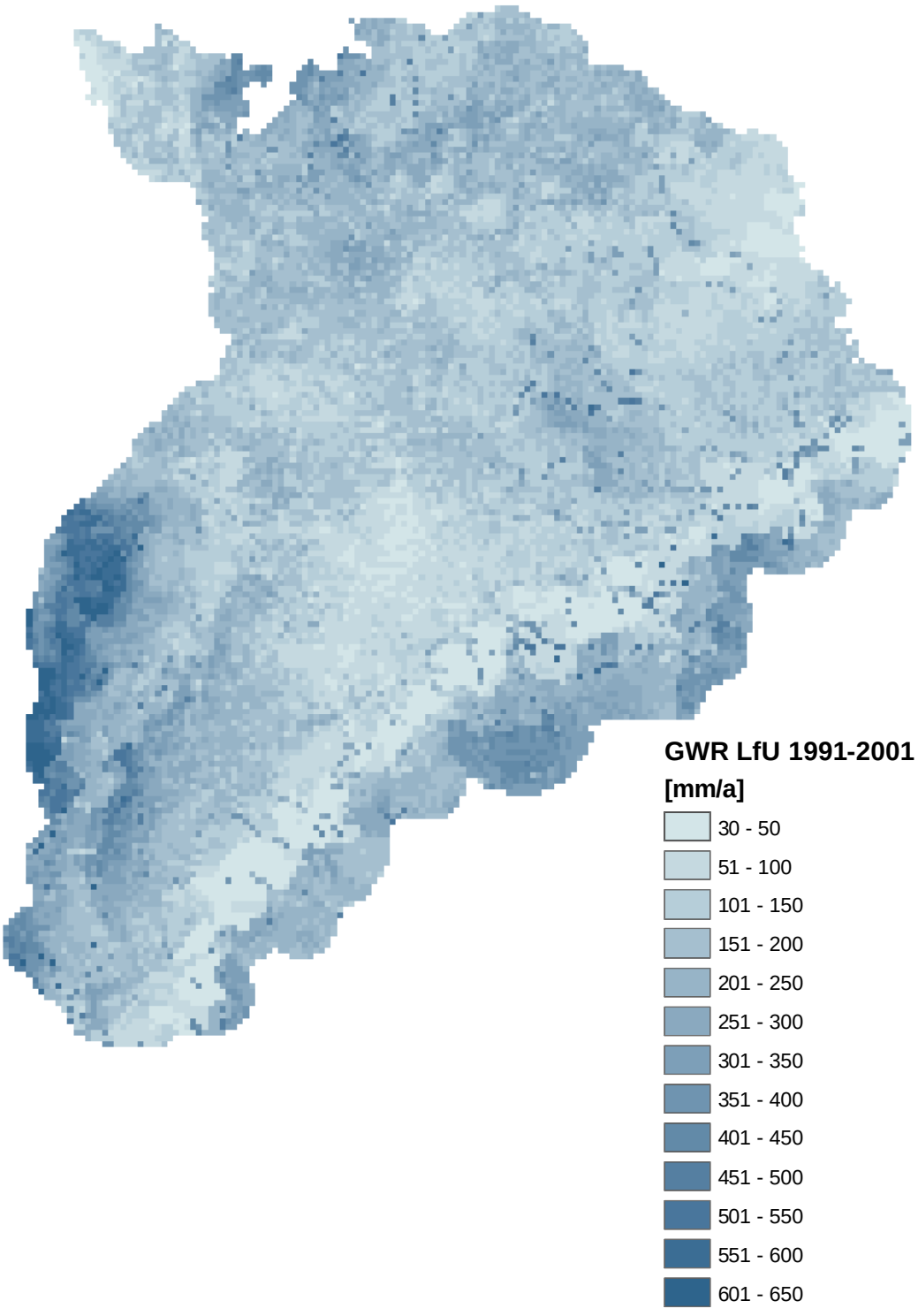

Figure 5.9: Simulated mean annual groundwater recharge in the Neckar basin using TRAIN-GWN.

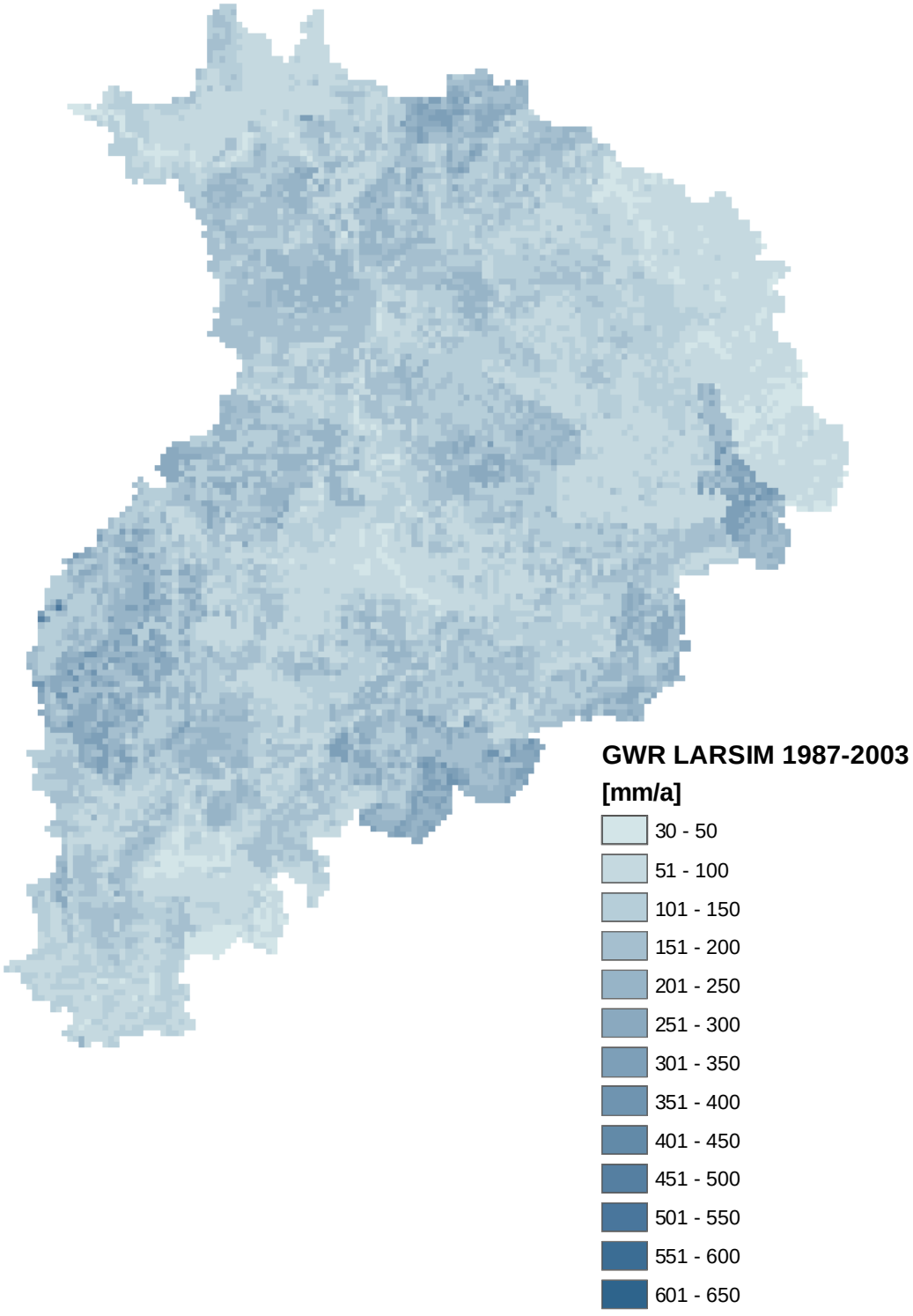

Figure 5.10: Simulated mean annual groundwater recharge in the Neckar basin using LARSIM.

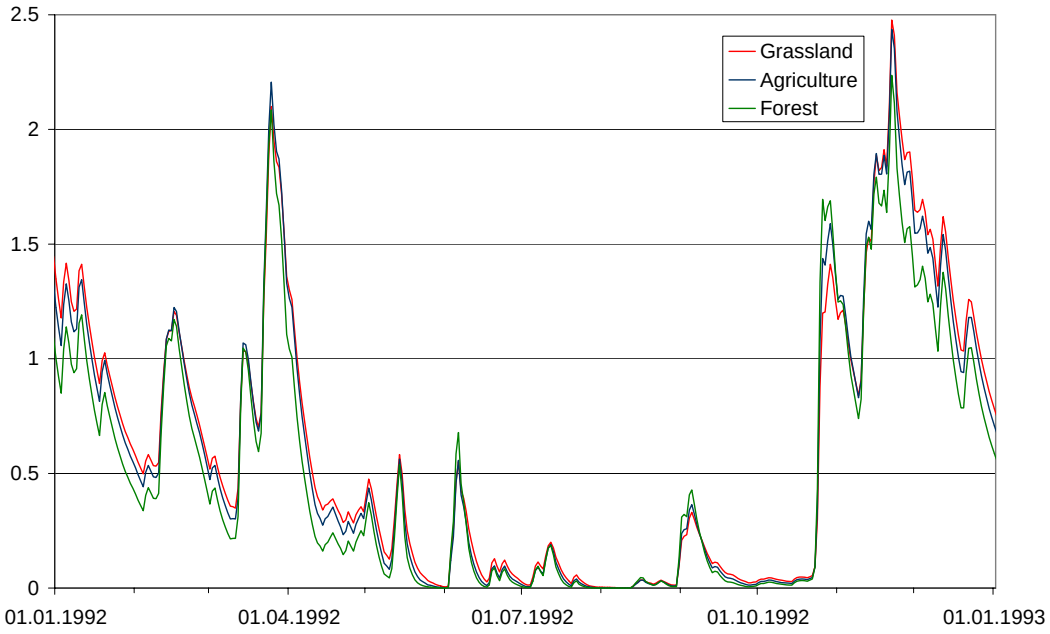

Figure 5.11: Temporal variation of daily groundwater recharge (mm/d) of three land use types, simulated with HBV.

The simulations can not be validated against observations because no lysimeter data is available in the Neckar catchment. Even if such data would be existing, a point measurement is hardly comparable to simulations of a 1 km^2 grid cell. Finally, the definition of groundwater recharge always depends on the scale, purpose and model (Götzinger et al., 2006). The temporal variability of all three models due to fluctuations in rainfall and evaporative demand is also quite high, shown exemplarily by the HBV simulation of three distinct land use types with similar soil properties in Figure 5.11. Using the simulated groundwater recharge the contribution of groundwater to the discharge at any gauge can be estimated with three different models: HBV, LARSIM and MODFLOW (Chapter 4.3.1). TRAIN-GWN is a 1D SVAT model and does not simulate retention and transport of the infiltrated water through the saturated zone towards the stream network. MODFLOW uses the simulated groundwater recharge rates as input to the upper boundary and calculates outflow into the rivers which can be summed up at the basin outlets. A comparison of all three model simulations is given in Figure 5.12. The groundwater runoff simulated with MODFLOW, HBV and LARSIM displays a similar magnitude and variability. But the hydrographs of LARSIM and particularly of HBV are systematically higher than those simulated with MODFLOW. HBV and MODFLOWs dynamic are similar whereas LARSIM reacts a little more delayed and dampened. As expected from a physically based model, MODFLOW shows a much more dynamic response than the linear reservoir models HBV and LARSIM. The differences between the two conceptual hydrological models stem from the varying separation into direct runoff and groundwater recharge as well as from the parametrisation of the groundwater reservoir itself. All three results are plausible compared to base flow separation methods, literature values and process understanding, and could be accepted since

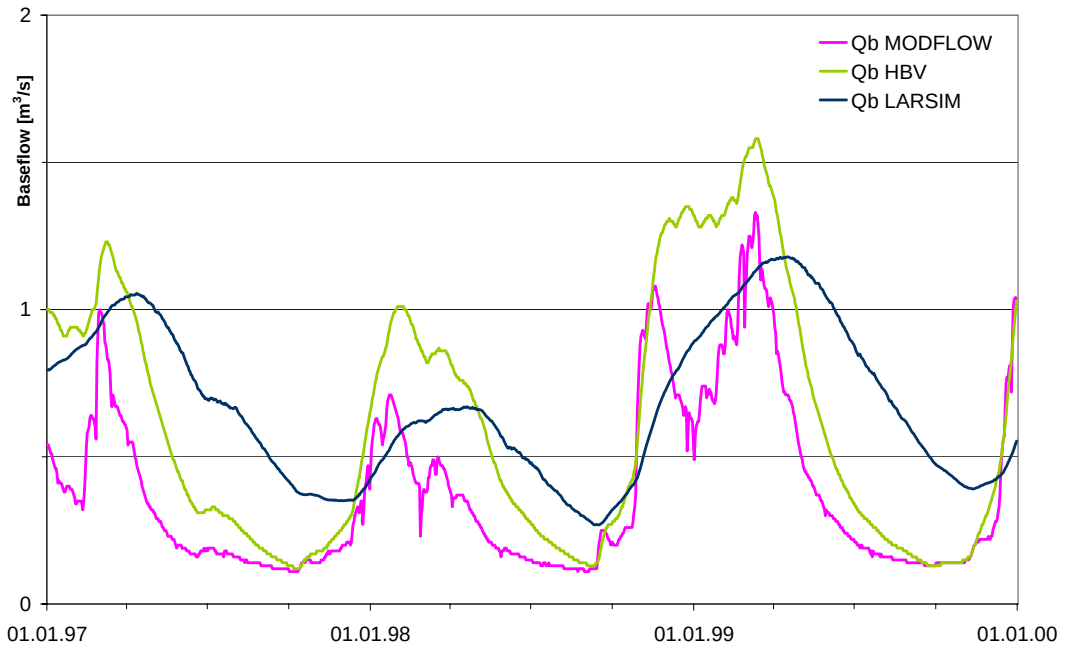

Figure 5.12: Simulated groundwater runoff hydrographs of MODFLOW, HBV and LARSIM at Neuenstadt (1997 - 1999).

the true groundwater runoff cannot be measured directly on this scale. In fact, it is only a conceptual quantity that is always defined with respect to a certain context and scale. Because the simulated discharge in the integrated model is used for river basin management, the groundwater runoff must also primarily serve this purpose. This means that the groundwater runoff should fit well to the other simulated flow components. The hydrographs of the total discharge show that, especially in the low flow periods, the groundwater contribution influences the discharge significantly (Figure 5.13 and Figure 5.14).

The Nash-Sutcliffe model efficiency of the HBV simulations in this basin is 0.57 compared to 0.73 for LARSIM. In this case the integration of the groundwater model baseflow even increased the model efficiency of HBV (0.58 in the integrated model compared to 0.57 in the original simulations). But in most cases it led to a reduced Nash Sutcliffe coefficient (e.g. LARSIM in this basin: 0.67 compared to 0.73). Nevertheless, the loss in accuracy is acceptable given the additional information like groundwater levels and groundwater flows that become available through the integration. The integrated model could potentially be used to simulate the impact of land use and climate change scenarios on the water balance of the Neckar catchment. Nevertheless, the results presented below were achieved with the water balance models alone as they are assumed to provide adequate estimates of the reaction of the water cycle also without the groundwater model. As mentioned above groundwater recharge and baseflow generally can not be validated on this scale and in this case particularly because observations are missing in the Neckar basin. Their plausibility was judged based on model comparison and the aspects observed during the integration process.

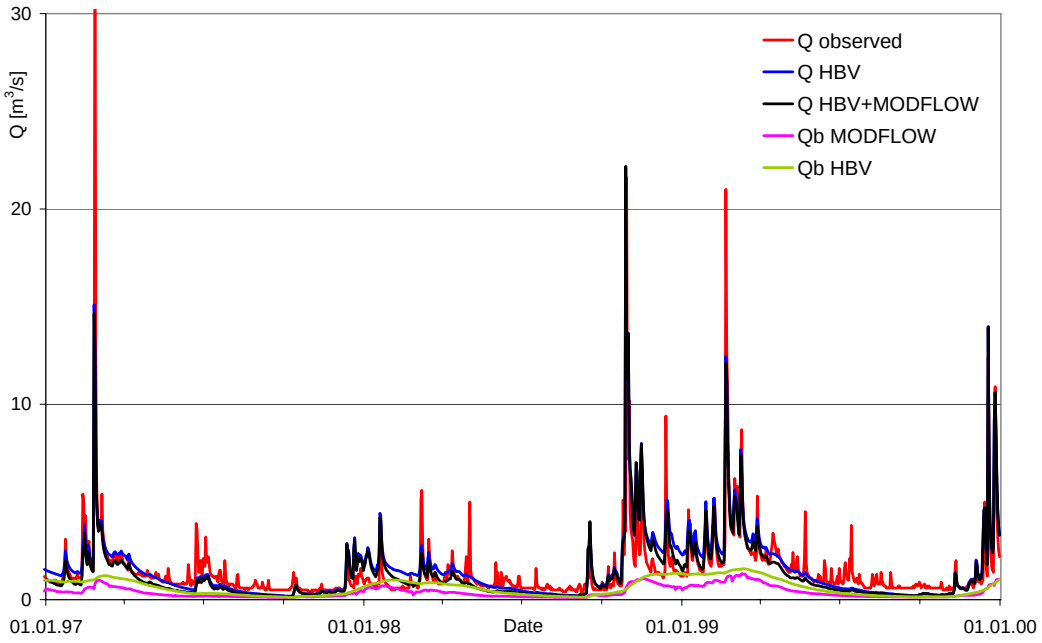

Figure 5.13: Observed and simulated discharge at Neuenstadt (1997 - 1999), red: observation, blue: HBV, black: direct runoff from HBV plus groundwater runoff from MODFLOW, magenta: groundwater runoff simulated with MODFLOW, green: groundwater runoff simulated with HBV.

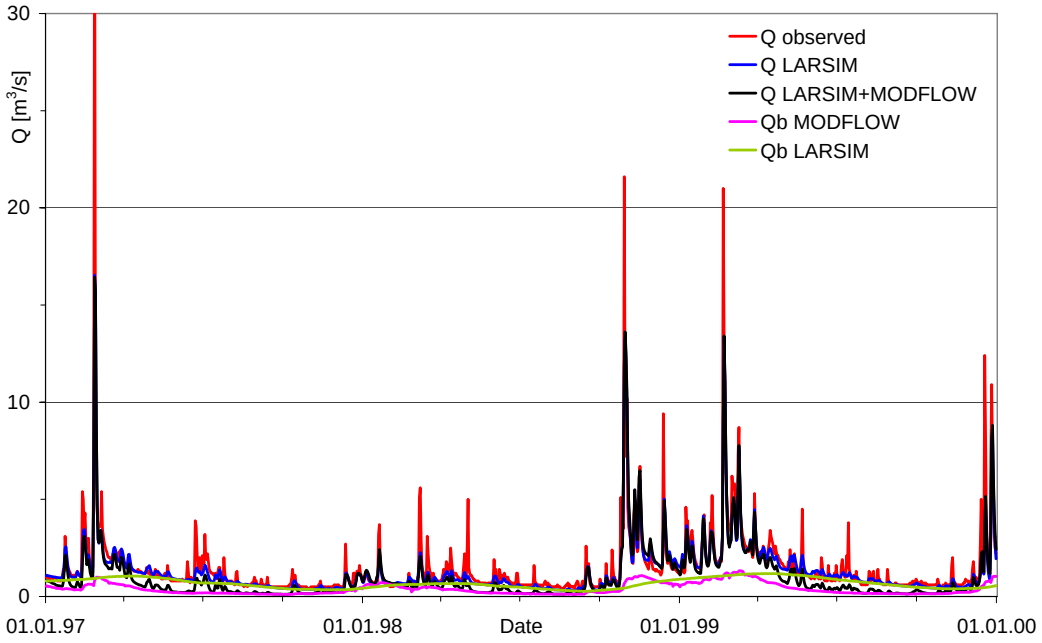

Figure 5.14: Observed and simulated discharge at Neuenstadt (1997 - 1999), red: observation, blue: LARSIM, black: direct runoff from LARSIM plus groundwater runoff from MODFLOW, magenta: groundwater runoff simulated with MODFLOW, green: groundwater runoff simulated with LARSIM.

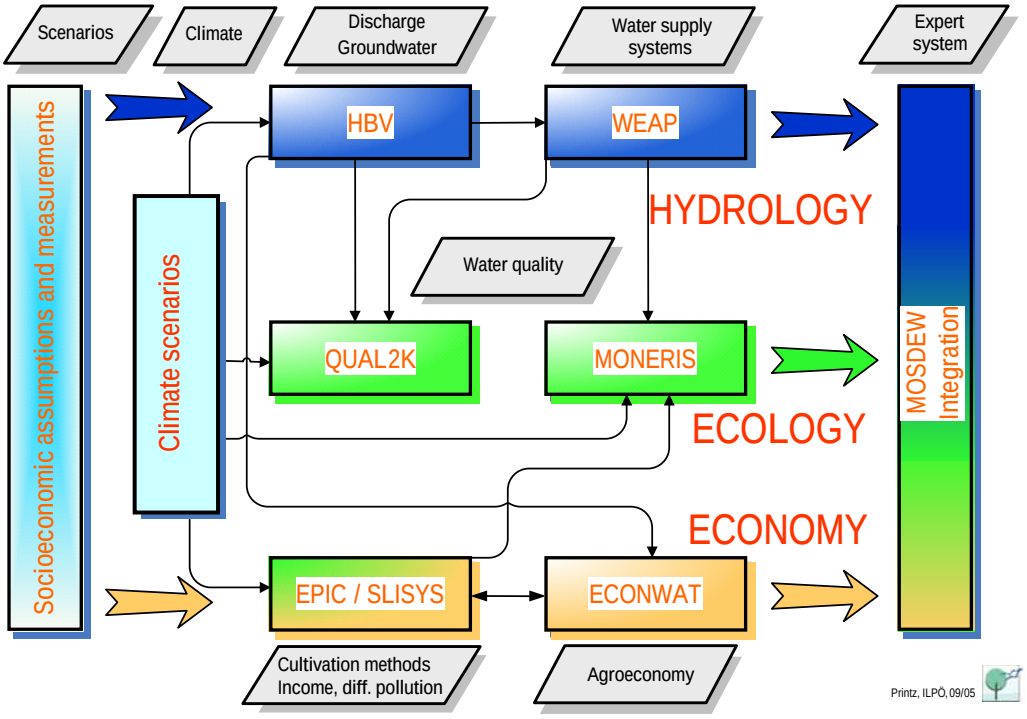

Figure 5.15: Structure and model integration of the decision support system for the Ouémé basin (after Kaule, 2006).

5.2.2 Ouémé basin

Although the general structure of MOSDEW is similar in the Ouémé basin, certain changes had to be made to adapt to the local situation, data availability and purpose of the model (Figure 5.15). The development of a three-dimensional groundwater model as it was implemented in the Neckar catchment was not feasible for the entire Ouémé basin because no regionally connected aquifers exist in the northern, crystalline part. Therefore, the groundwater section of the integrated modelling system MOSDEW for the Ouémé is represented by the groundwater storage module of HBV which has been shown to provide reasonable estimates of groundwater recharge and baseflow. Furthermore, the HBV model provides input to the water demand (WEAP), water quality (QUAL2K) and the agro-economical model (ECONWAT). Whereas the former two use discharge, the latter utilises all components of the water balance, e.g. to estimate the length of the growing period from simulated soil moisture. Therefore the HBV model was calibrated with the threefold objective

- to link the model parameters to catchment characteristics,
- to capture the discharge regime, and
- to give a meaningful estimate of all water balance components that is also reasonably sensitive to changes.

Although the mean Nash-Sutcliffe model efficiencies of the Ouémé basin are tolerable, major drawbacks in modelling the dry season are still visible. Considering the crude input data and the objectives mentioned above the model was nevertheless accepted. Some examples of water balance component simulations are given in Figure 5.16 and Figure 5.17.

The model was calibrated for the time period 1980 to 1989. The validation period 1990 to 1999 was slightly cooler and wetter than the 80s. Therefore the presented validation results already provide some insight on the reliability of modelling a changing climate. The simulation of daily groundwater recharge by HBV shows a moderate spatial variability which is dominated by soil type, land use and climate except for two features (Figure 5.16): Two North-South oriented disturbance structures along the Kandi fault with extremely high soil hydraulic conductivity and several local depressions without drainage exhibit significantly larger recharge values. Furthermore, a North-South gradient with declining recharge values is visible. In the South, clayey layers are found between the sandy quaternary deposits which reduce infiltration, further north these layers have already been eroded.

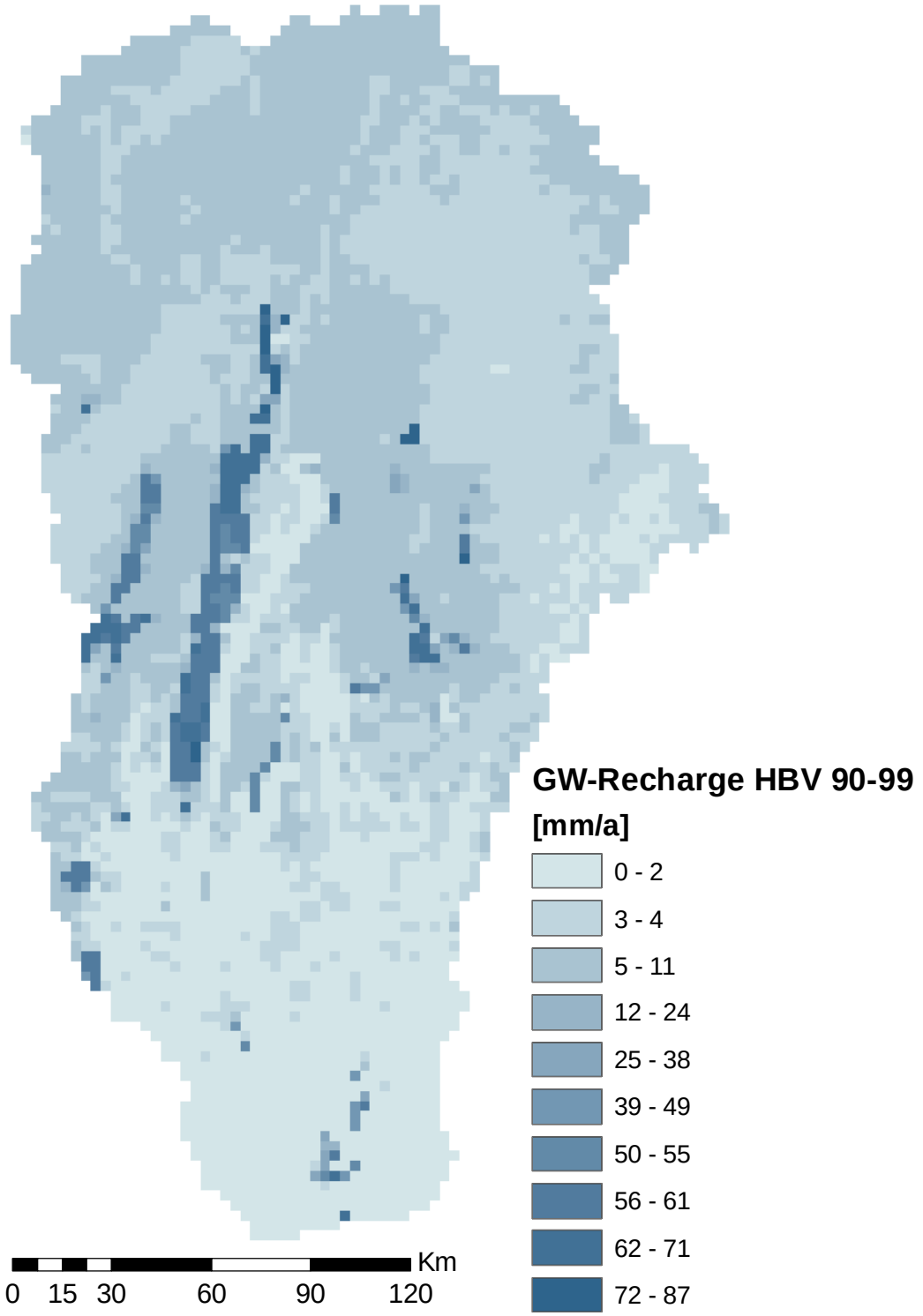

Figure 5.16: Mean annual groundwater recharge in the Ouémé basin simulated with HBV (1990 - 1999).

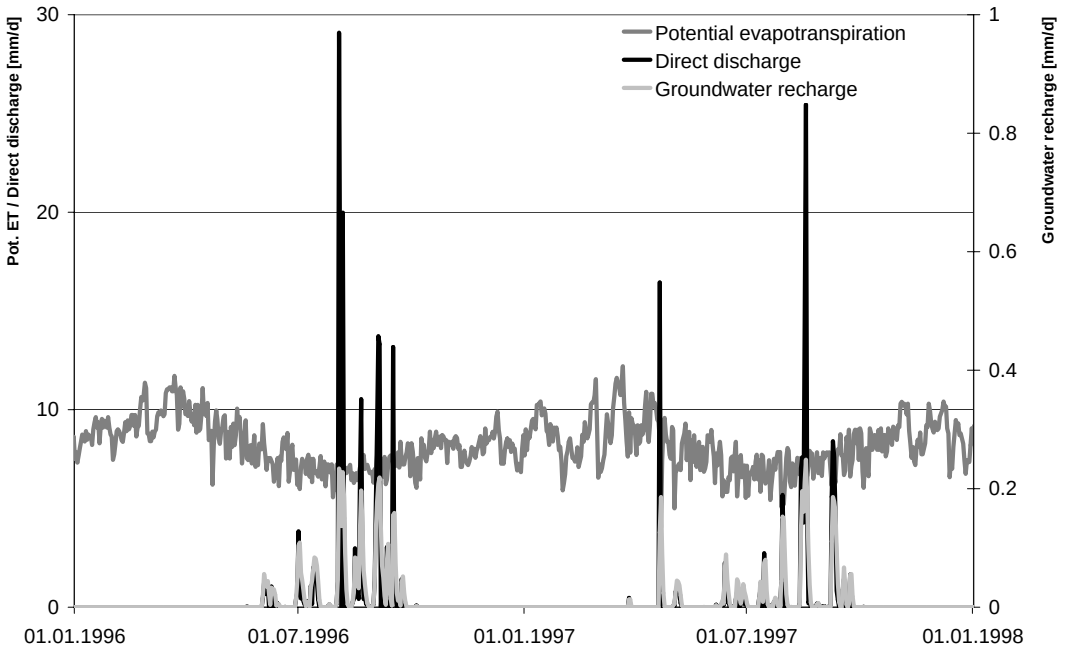

Figure 5.17: Temporal variation of potential evapotranspiration, direct discharge and groundwater recharge in one exemplary grid cell.

On the other hand, the temporal variability of the direct discharge and groundwater recharge is high following the precipitation events, whereas the potential evapotranspiration shows only moderate fluctuations due to the very even temperature (Figure 5.17). It is clearly visible, that runoff generation is limited to a few single precipitation events each rainy season which replenish the soil moisture and initiate direct runoff and groundwater recharge. Obviously, the former is about two orders of magnitude larger which is explained by the lateritic layers which prevent deeper infiltration and lead to horizontal water transport already in the unsaturated zone. The potential evapotranspiration is slightly lowered in the rainy season due to lower temperatures but is still much larger than the runoff if summed up over one year. These water balance components could not be validated directly because they are not measured directly in the study area. Comparison with other studies (Giertz et al., 2005, 2006) nevertheless shows that the order of magnitude and variability can be reproduced. When comparing these point measurements to 3 km^2 grid cells, the commensurability of these values also has to be kept in mind which additionally complicates their evaluation.

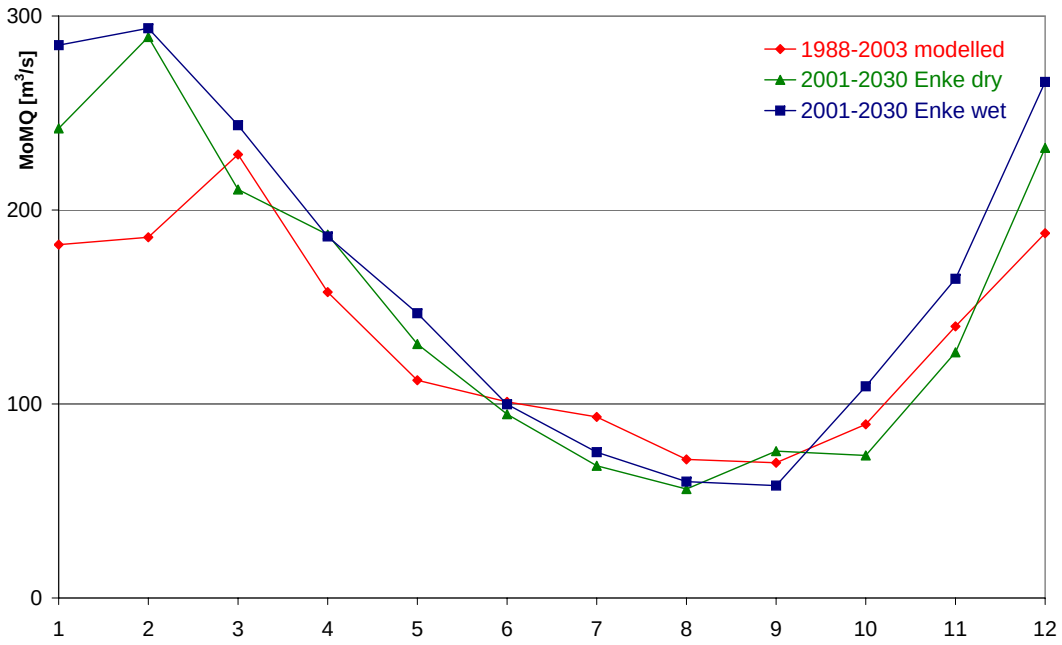

Figure 5.18: Monthly mean discharge at Rockenau simulated with LARSIM, climate scenarios Enke dry and Enke wet compared to a reference period.

5.3 The impact of climate and land use change

5.3.1 Neckar basin

Both climate and land use change are expected to influence the water balance by modifying the input into or the properties of the system. The quantification of this impact has been investigated by running the hydrological models LARSIM and HBV described in Chapter 2.4 and 4.1 with input from the climate scenarios (Chapter 4.4.1). The impact of climate change on the water balance can be evaluated by comparing the simulations of monthly mean discharge, the distribution of daily discharge and the groundwater recharge of a historical period to the climate scenarios. Figure 5.18 and Figure 5.19 show two examples of this comparison. As can be seen, the Enke downscaling scheme predicts an intensification of the discharge regime of the Neckar for both climate scenarios. The mean winter discharges are significantly higher and the mean summer discharges slightly lower than in the reference period. This trend is confirmed by the flow duration curve which shows an increase in the high and medium flows occurring mostly in winter and no change in the usually lower summer flow distribution. The shift is caused by an increase in winter precipitation in both Enke scenarios. The simulations with HBV show a similar impact: The increase in winter is even stronger than with LARSIM, whereas the summer flows remain stable (Figure 5.20). The slight differences between both simulations are caused by the used evapotranspiration methods and their different sensitivity to temperature increases (LARSIM: Penman-Monteith, HBV: Hargreaves-Samani). Another difference is the spatial resolution of input data. LARSIM uses data which are interpolated by inverse distance weighting, HBV uses external drift kriging.

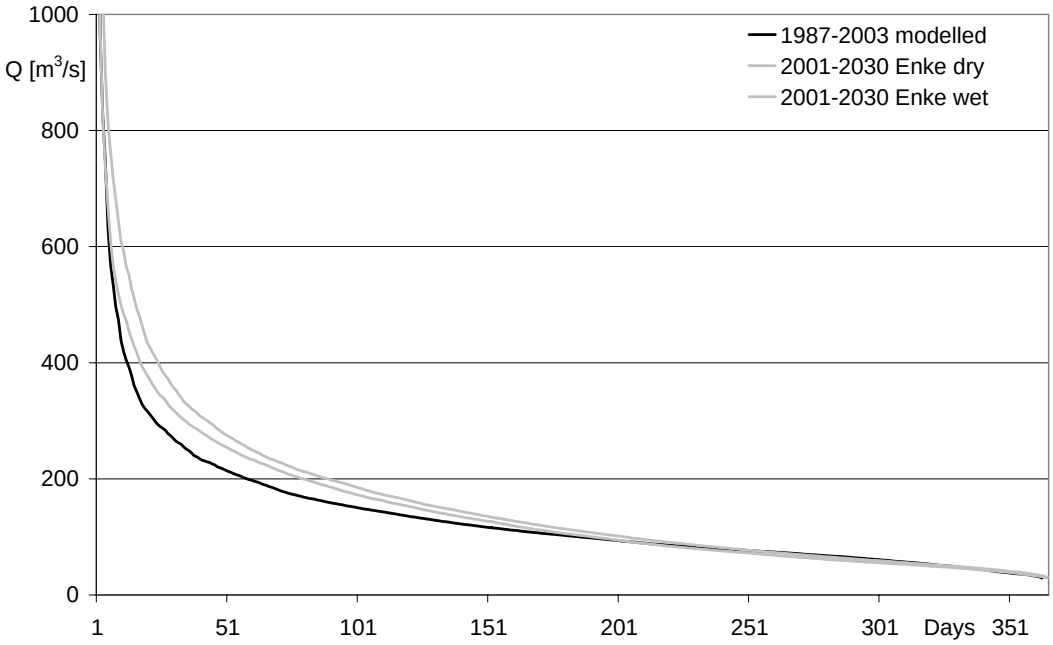

Figure 5.19: Flow duration curve simulated with LARSIM, climate scenarios compared to the reference period.

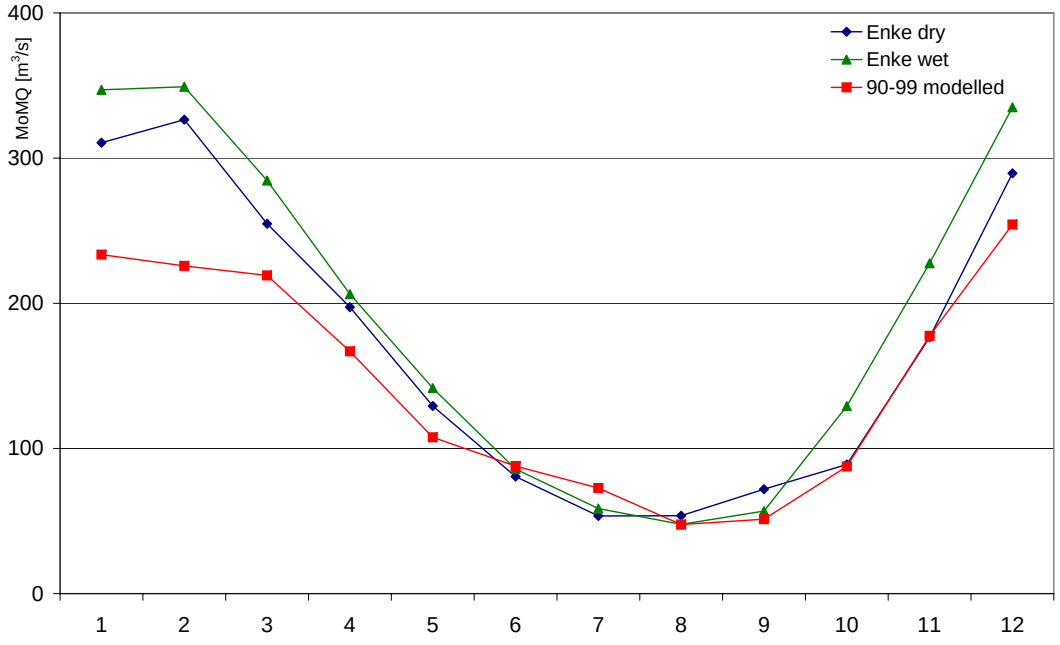

Figure 5.20: Monthly mean discharge at Rockenau simulated with HBV, climate scenarios Enke dry and Enke wet (2001-2030) compared to a reference period.

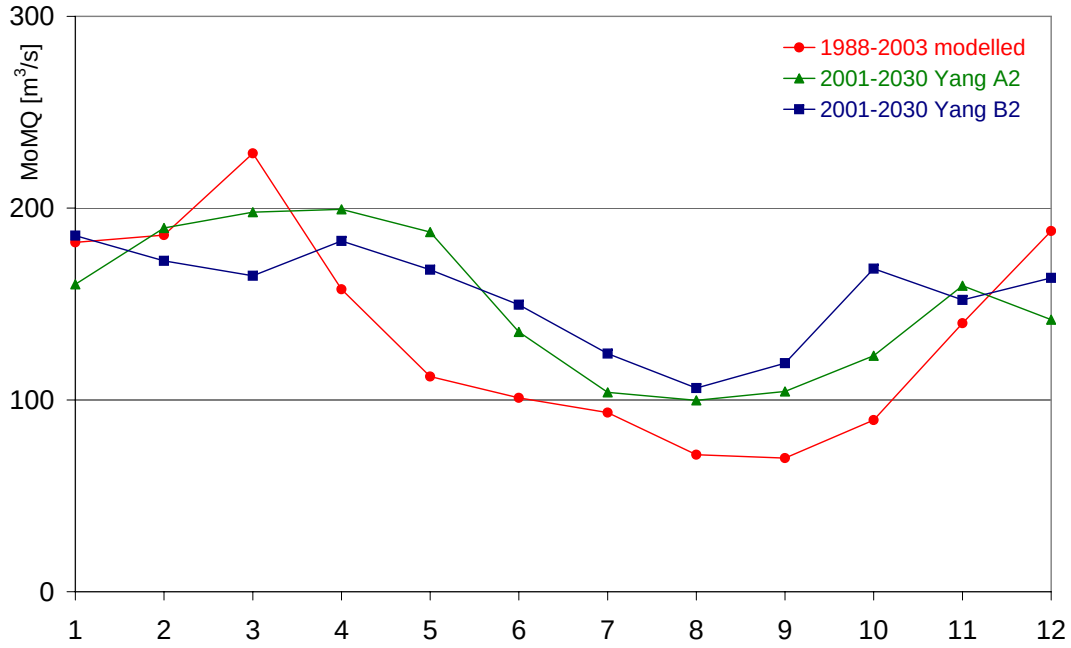

Figure 5.21: Monthly mean discharge at Rockenau simulated with LARSIM, climate scenarios Yang A2 and B2 compared to a reference period.

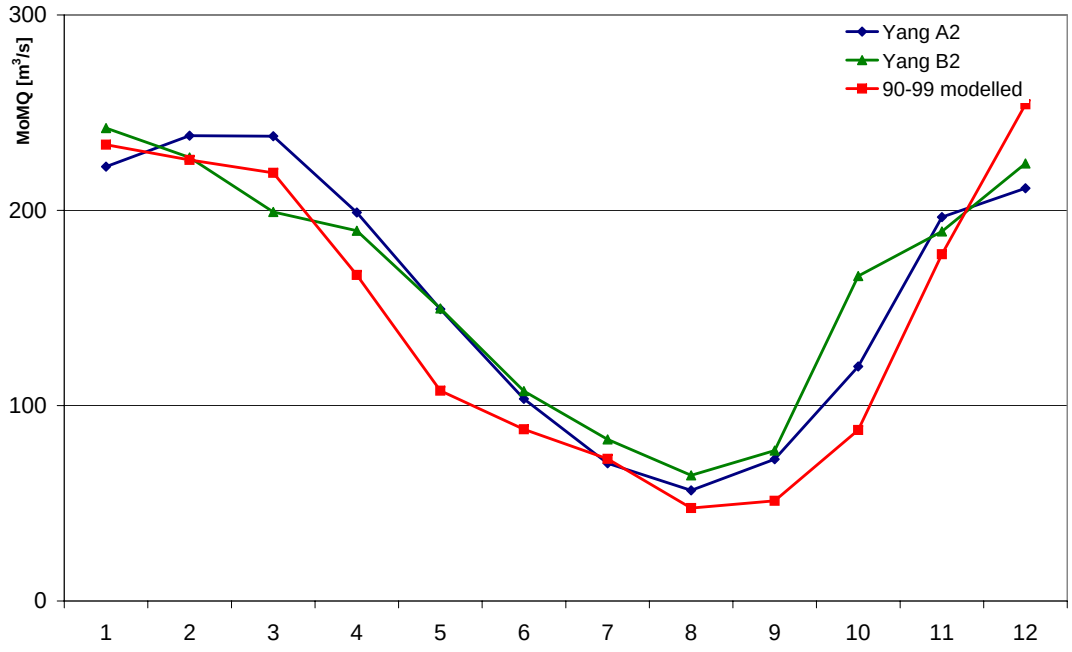

Figure 5.22: Monthly mean discharge at Rockenau simulated with HBV, climate scenarios Yang A2 and B2 (2001-2030) compared to a reference period.

Table 5.4: Mean annual precipitation and simulation of groundwater recharge in the climate scenarios (2021-2030) and a reference period [mm/a].

	Reference period	Enke dry	Enke wet	Yang A2	Yang B2
Precipitation	933.3	938.9	1018.6	1034.1	1075.5
HBV	130.7	116.9	123.5	130.1	133.6
LARSIM	136.6	121.9	130.1	159.5	155.6

The Yang downscaling scenarios show a slightly different picture (Figure 5.21 and Figure 5.22). The simulations with LARSIM project a shift of the discharge regime from winter to summer. The HBV model forecasts an increase in mean discharges throughout almost the whole year. The reason can be found in increased rainfall but also increased winter temperatures. The differences between LARSIM and HBV are due to the data requirements of the models. HBV uses only temperature and precipitation data whereas LARSIM additionally requires barometric pressure, wind speed, relative humidity and solar radiation. The latter are not provided by the Yang downscaling methodology. Constant long-term averages were therefore used for the simulation with LARSIM which causes the visible equalisation of the annual cycle. Hence, an increased uncertainty has to be expected in the combination of the Yang method with LARSIM. The HBV model does not require these additional data and therefore the HBV simulations of the Yang scenarios are assumed to be more reliable.

Simulation of groundwater recharge with both models yields similar results. Table 5.4 compares the last decade (2021 to 2030) of all four climate downscaling scenarios to a reference period which are the years 1990 to 2000 in the case of precipitation and HBV and 1987 to 2003 in the case of LARSIM. The precipitation is given for orientation. Again both models show similar trends. Only in the case of LARSIM and the Yang A2 downscaling scenario and for both models combined with the Yang B2 scenario the increased precipitation also leads to an increased groundwater recharge. In all other scenarios the higher evapotranspiration through higher temperatures compensates or even inverts this effect. For the reasons mentioned above the combination Yang and LARSIM must again be used with reservations. Compared to the reference periods no significant changes could be found in the spatial patterns of groundwater recharge. Overall the impact on the groundwater recharge is smaller than on the discharge. Nevertheless, reduced groundwater recharge could potentially endanger wetlands, groundwater levels and drinking water resources in certain areas. For these questions a detailed 3D groundwater flow model is necessary.

A similar assessment can be performed in the case of land use change. Figure 5.23 shows the comparison of the two socio-economic scenarios A and B with 6% and 5% annual settlement growth, respectively, compared to the baseline simulation of the period 2026 to 2030 of the two Enke scenarios dry and wet. Obviously, the scenarios A and B cannot be differentiated from the baseline simulation, which shows that the impact of the expected urbanisation on the water balance of the whole Neckar catchment is negligible. This result is due to the still comparatively small fraction of settlements compared to the total area. In both scenarios they occupy on average still less than 10% of the total area and the difference in parametrisation is not very large. Nevertheless, the sensitivity to urbanisation is shown by a benchmark simulation in

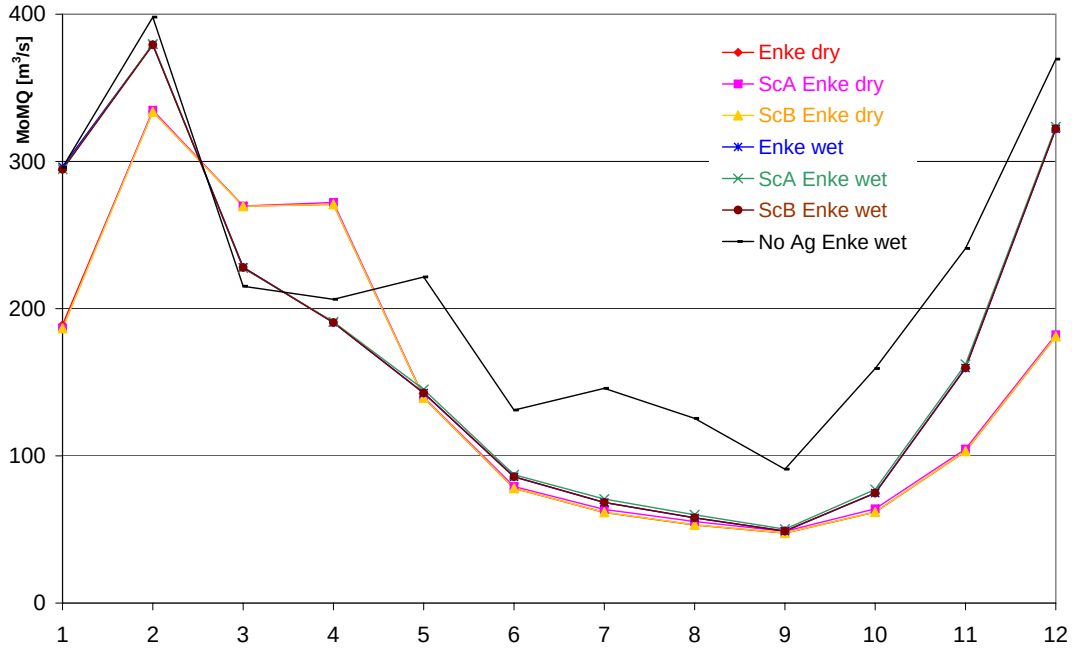

Figure 5.23: Impact of land use change on the monthly mean discharges at Rockenau, simulated with LARSIM (2026-2030): scenario A (ScA), scenario B (ScB), extreme urbanisation (No Ag) and baseline scenario.

which all the agricultural area (about 30%) has been replaced by urban area (No Ag Enke wet). This unrealistic scenario shows that urbanisation will have an impact if certain extreme and probably undesired thresholds are exceeded. Groundwater recharge rates have also been analysed with similar results. Although the increase of settlement area influences the affected cells directly, the overall mean is not changing significantly. The above mentioned trend is confirmed by simulations of HBV and the downscaled scenarios Yang A2 and B2. Figure 5.24 shows the monthly mean discharges of the Yang A2 baseline scenario from 2021 to 2026 compared to the land use scenario A. An implementation of the investigated EU policy interventions for reduction of diffuse pollution would have a greater impact (Figure 5.25). The complete conversion of all farmland into fallow could cut Nitrate leaching by about 67% relative to the land use in the year 2000 (Gaiser et al., 2006). The conversion of 50% of the farmland into grassland would have a similar effect but not as pronounced. However, both interventions would also impact the water balance of the Neckar significantly. Both, fallow and grassland cover the ground also in winter leading to higher interzeption and evapotranspiration rates which reduce winter discharges. Because the evapotranspiration in summer from both land uses is also higher than from farmland, the summer flows are also lower leading to a 15% overall reduction of the mean discharge.

5.3.2 Ouémé basin

The impact of climate and land use change in West Africa is expected to be greater than in Central Europe because the changes are much more dynamic, especially the

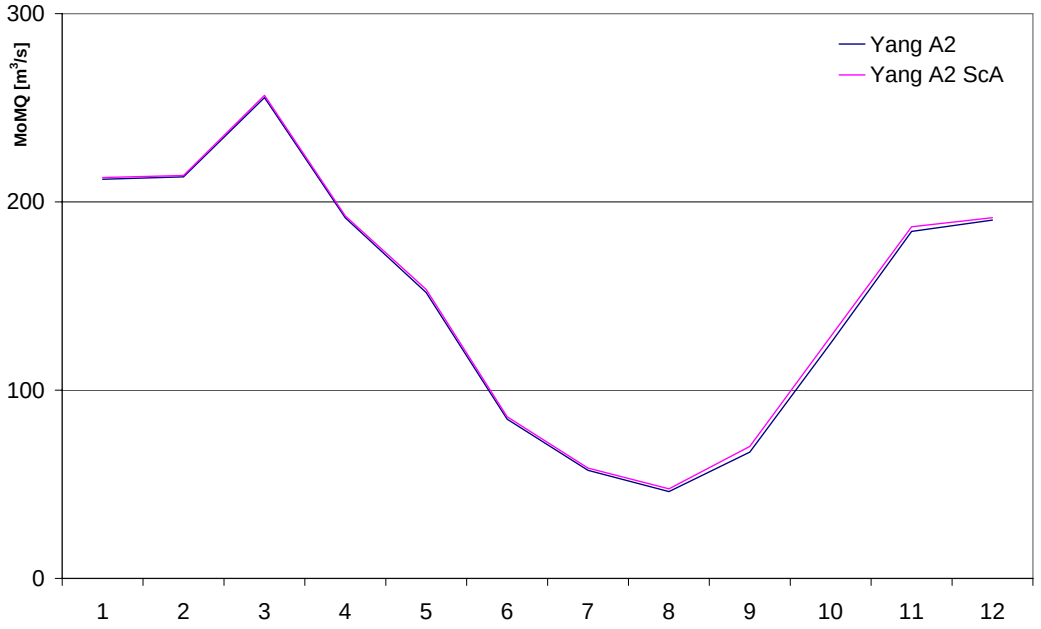

Figure 5.24: Impact of land use change on the monthly mean discharges at Rockenau, simulated with HBV (2021-2026): scenario A (ScA) and baseline scenario.

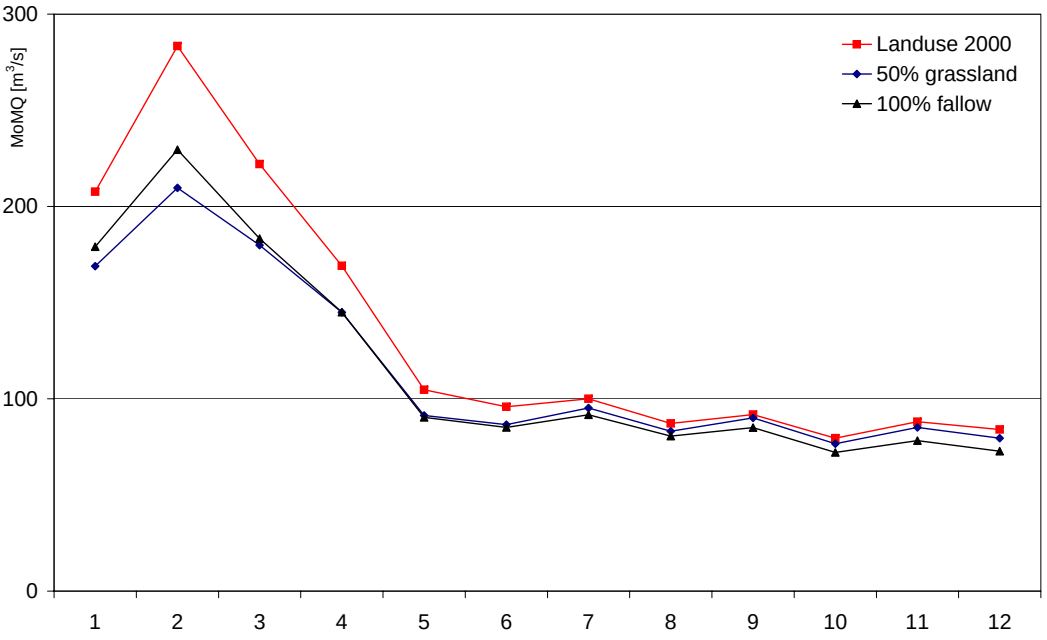

Figure 5.25: Impact of the policy interventions on mean monthly discharges at Rockenau simulated for the year 2000 with LARSIM

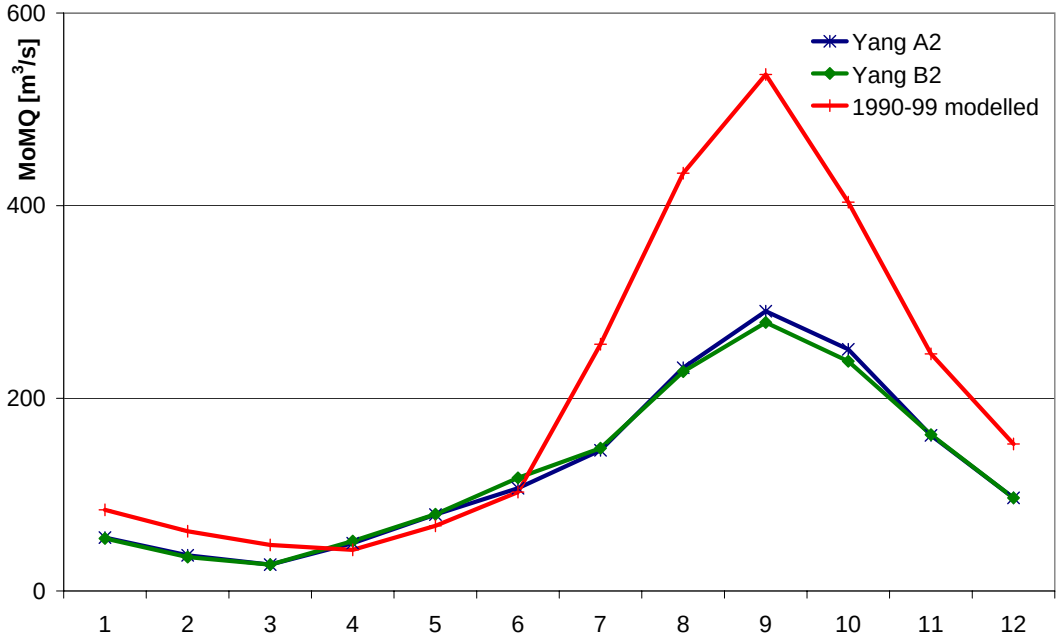

Figure 5.26: Monthly mean discharge at Bonou simulated with HBV, climate scenarios Yang A2 and Yang B2 compared to a reference period.

land degradation from increased settlement pressure. In fact, Thornton et al. (2006) characterise sub-Saharan Africa as one of the most vulnerable regions because societies with relatively low resilience and adaptivity are facing more pronounced changes than many other parts of the world. The quantification of this impact has also been investigated by running HBV (Chapter 4.1) with input from the climate scenarios (Chapter 4.4.1). The impact of climate change on the water balance is again evaluated by comparing the simulations of monthly mean discharge and groundwater recharge of a historical period to the climate scenarios. The reduced precipitation and increased temperature of both climate scenarios also cause the discharge to decrease considerably, especially in the rainy season. The reason for this relatively strong reaction is the vulnerability of the water balance. Because of the high temperature only about 200 mm of the 1200 mm of rainfall are actually turned into runoff. The remaining 1000 mm are evaporating. Therefore a small decrease in rainfall and a small increase in temperature or even a more equally distributed rainfall can significantly disturb the water balance in this climate. Although the exact results of the climate models and downscaling methods and therefore also the impact studies are still highly uncertain, the presented trends must most probably be expected.

A similar analysis with the land use scenarios A and B introduced in Chapter 4.4.2 is shown in Figure 5.27. Because the agricultural area is increasing in both scenarios the discharge is also slightly larger because most crops use less water than the natural vegetation and farmland produces more surface runoff. The irrigation demands can be fulfilled about 92.5% and 95% of the time by the planned irrigation schemes in Bétérou and Assanté, respectively. Compared to the natural runoff these withdrawals are so small that their effect can not be seen in the comparison of monthly mean discharges. As described in Chapter 4.4.2 three hydropower projects were investi-

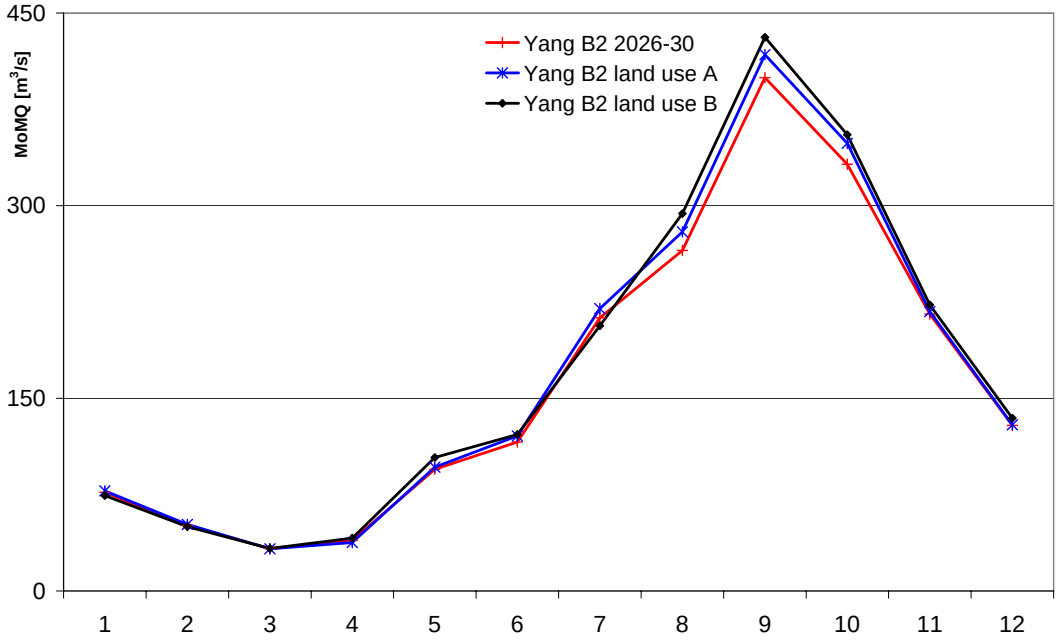

Figure 5.27: Monthly mean discharge at Bonou in land use scenarios A and B compared to the baseline scenario.

gated as a hydrological intervention. Figure 5.28 shows the results of the simulation for the gauging station Zagnanado just downstream of the last reservoir Kétou. As mentioned before, dam operation was modelled in the following way: the reservoirs are filled at the beginning of the rainy season and release their stored water during the dry season at fixed rates. Direct evaporation from the lake surface has to be considered for larger water bodies in this climate. In the case of the multi-purpose reservoirs Bétérou and Assanté this flux represents losses of a similar magnitude than the irrigation demands themselves (on average about 2.6 m^3/s). For the larger dam in Kétou an average evaporation loss of 13.2 m^3/s was taken into account. These losses lead to a lower hydropower production and reliability of the proposed schemes. Bétérou as the reservoir located most upstream of all three can only deliver the planned amount of hydropower energy about 72% of the time. The increased storage volume on the other hand leads to a slightly improved temporal irrigation water availability of 94% despite the larger evaporation losses. With the enlarged reservoir volume, Assanté could provide electricity and irrigation water all the time according to the analysed simulations. The dam in Kétou finally would meet the planned discharge of 100 m^3/s for energy production about 81% of the time under the given assumptions. These estimates show that evaporative losses play a significant role in the feasibility of such projects. An intelligent operation using long term forecasts could improve the situation. Most important anyhow, is a more detailed planning of the exact dimensions and operation rules taking further information into account which is beyond the scope of this thesis. The current study can only provide a general estimate of the given possibilities.

The simulation shows that the storage of water leads to a regulation of the discharge providing many opportunities for improving water supply, fishing, energy

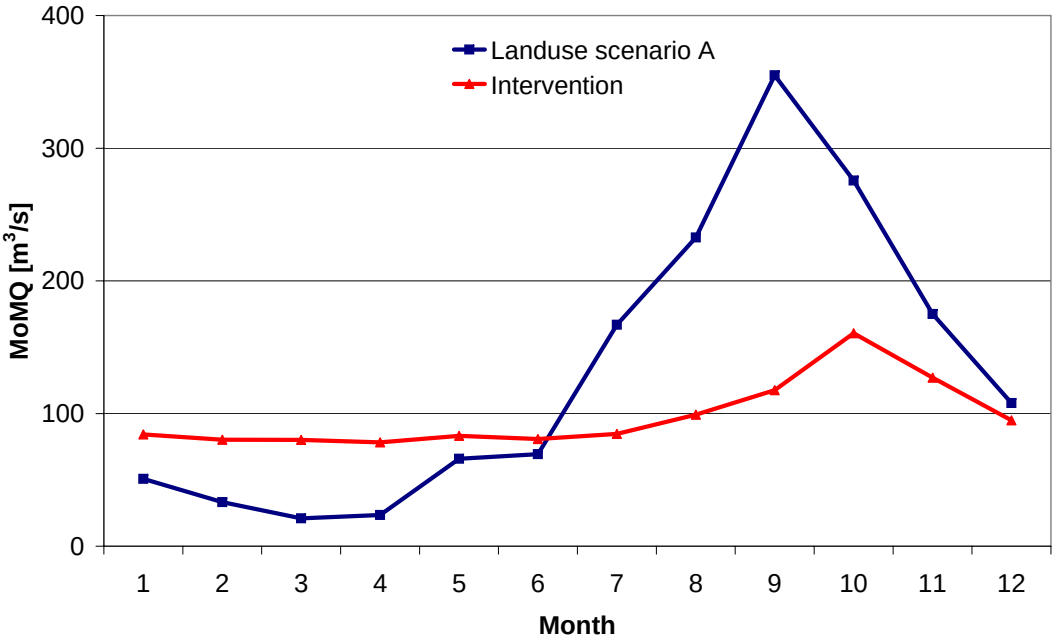

Figure 5.28: Monthly mean discharge at Zagnanado in the intervention compared to the baseline scenario.

production and irrigation. Although the exact results are still uncertain and should not be taken as forecasts the presented general tendencies must be expected for the future. Therefore, it is necessary for precautionary planning to introduce adaptation strategies as early as possible in order to avoid any undesired consequences. The greatest potential is seen in a combination of large and small decentralized storage reservoirs which could be used for multiple purposes. In the end, the integrated management of the scarce resource water in this environment is essential for a truly sustainable development.

6 Uncertainty Analysis

Many calibration techniques, including the one presented in Chapter 4.2 rely on least squares optimization or derivatives thereof (like the Nash-Sutcliffe coefficient) although the underlying assumptions are often not fulfilled. Input errors are significant; model residuals are seldom normally distributed and are affected by heteroskedasticity as different processes are dominant at different times. Simulating discharge correctly is much more difficult for a hydrological model when temperature is around 2°C than during the rest of the year when no snow melt is present (Figure 6.1).

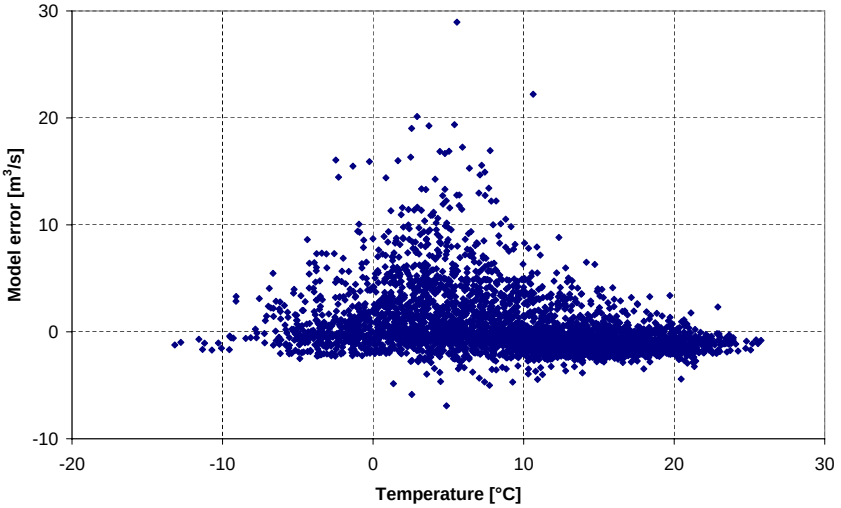

Figure 6.1: Scatterplot showing heteroskedasticity of model error with respect to temperature at Höfen.

Uncertainty estimation methods which do not incorporate these features can be significantly biased. Therefore, a generic error model is proposed here which considers temporally variable input and processes uncertainty. It can be used in calibration to normalize the model residuals and leads to more realistic uncertainty estimates than simple additive or multiplicative error models. In this error model, the uncertainty is quantified using a combined procedure. A stochastic simulation method is used for the uncertainty of discharge due to meteorological input. To quantify the effect of process representation and parametrisation, a sensitivity analysis is carried out. It is assumed that the model error due to process uncertainty is proportional to the sensitivity. The final model error variance can thus be calculated from the stochastic errors and the process sensitivities. The coefficients used for the quantification are estimated simultaneously with the model parameters.

The presented methodology produces a Gaussian error series which is representative of the varying importance of different processes in time. It is based on a scaled composition of plausible error contributions from several uncertainty sources which represents the time-variant importance of different processes. This uncertainty time series is used as a weighting factor to normalize the model residuals during calibration such that the assumptions of least squares optimization are fulfilled. The uncertainty estimation is demonstrated by an example application to the distributed HBV model of three sub-watersheds of the Neckar basin. The model residual distributions are presented and compared to a standard calibration method. Further, it is shown that the new, heteroskedastic methodology leads to more realistic confidence intervals for model simulations. Although applied to the HBV model as an example, the method is general and can be applied to any model also in conjunction with other uncertainty estimation techniques. In the following sections the main steps of this heteroskedastic uncertainty analysis methodology are introduced.

6.1 Methodology

The error of the modelled discharge on day t is considered to be a random variable $\varepsilon_Q(t)$. This random error is supposed to be the sum of random errors due to input (e.g. precipitation $\varepsilon_P(t)$ and temperature $\varepsilon_T(t)$) and process description $\varepsilon_{\theta_i}(t)$, e.g. snow accumulation and melt processes, soil properties, runoff generation and infiltration, as well as internal storage.

$$\varepsilon_Q(t) = \varepsilon_P(t) + \varepsilon_T(t) + \sum_i \varepsilon_{\theta_i}(t) \tag{6.1}$$

With θ_i being the respective group of model parameters that control the processes mentioned above. If one assumes that these random variables are independent then the variance of the sum is the sum of the variances (Bárdossy and Götzinger, 2007a):

$$\mathrm{Var}\left[\varepsilon_Q(t)\right] = \mathrm{Var}\left[\varepsilon_P(t)\right] + \mathrm{Var}\left[\varepsilon_T(t)\right] + \sum_i \mathrm{Var}\left[\varepsilon_{\theta_i}(t)\right] \tag{6.2}$$

The assessment of these variances is not a trivial task. While for the meteorological variables one can assume that the errors on successive days are independent this assumption does not hold for the errors due to the inevitably simplifying process descriptions and effective model parameters θ_i (Kuczera et al., 2006; Schaefli et al., 2007).

6.2 Meteorological sources of uncertainty

Rainfall and temperature are the most frequent meteorological inputs for hydrological models. They are usually observed at a selected number of points and have to be estimated for the whole catchment. Meteorological data can be interpolated using geostatistical methods such as ordinary or external drift kriging (EDK) (Ahmed and de Marsily, 1987). For this study both precipitation and temperature were interpolated using EDK. For temperature topographical elevation was used as external drift as temperature changes linearly with topography. For precipitation the square

root of elevation was used as external drift, as the increase in precipitation weakens with altitude. Interpolation leads to an artificial picture of the real meteorological conditions as it is an estimation with minimum error variance. Therefore, per definition, the true variability of the real fields is smoothed out. In order to account for the effect of spatial variability simulation methods can be used to quantify the uncertainty due to meteorological input data.

6.2.1 Conditional precipitation and temperature simulation

In contrast to the objective of interpolation (minimum error variance), the goal of simulation methods is to create a series of realisations of a variable which show the same variability as the observations. Conditional simulation additionally preserves the observations at the measurement locations as far as possible. The four main groups are Monte Carlo, turning band, sequential and Markov chain simulations (Bárdossy, 2002).

Despite their popularity in geostatistics, simulation methods have not been used as extensively in hydrology as the related interpolation approaches. Haberlandt and Gattke (2004) apply simulated annealing to generate precipitation fields as stochastic input for a Nash cascade model of the Lippe basin. They found a considerable variability of the runoff hydrographs due to simulated precipitation but the excessive simplicity of the hydrological model prevented further analysis.

The method used here is related to the Modified Turning Band model of Mellor (1996), Mellor and O'Connell (1996) and Mellor and Metcalfe (1996). As the original turning band method, this space-time rainfall model is based on the generation of stochastic processes along three lines with prescribed angels. The features of these processes are projected perpendicular into the area to reproduce storm features like raincells, clusters and rainbands. The three papers describe the parameter estimation process from radar data and provide an outlook on the generation of stochastic fields from observation stations.

The applied Meta-Gaussian approach which is described in Bárdossy and Götzinger (2007b) is characterised by the following features:

- Normal score transformation of positive values (zero for negative ones)
- Covariance function of the Normal score transform calculated
- Monotonisation algorithm (PAVA)
- Automatically fitted and validated
- Conditional Simulation (using Gaussian copulas)
- Probability score calculated
- Full conditional distribution for any location
- Back transformation to the marginal of the precipitation

Figure 6.2 (left) shows an example of precipitation data interpolated with external drift kriging that is typically used in environmental models. The unrealistically

smooth gradients following elevation and distance from observations are clearly visible. The right picture shows an example of the simulated precipitation fields for the same day which exhibits a similar spatial structure determined by elevation and observations but with a much higher spatial variability (standard deviation of 17 mm compared to 8 mm in the interpolation). The mean of all simulated realisations which is shown in Figure 6.3 should therefore resemble the interpolated field. In the present example the variability in the interpolated field is already relatively high as a dense station network is available (294 stations for 14 100 km^2). In most situations fewer stations exist and interpolations are even more smooth.

A similar comparison can be done for temperature. Figure 6.4 shows again an example of EDK-interpolated (left) and simulated temperature (right). Elevation is the only source of spatial variability between the stations in the interpolation, whereas the simulated field provides a more realistic representation of the true temperature distribution. The mean of the ensemble of realisations comes again close to the interpolation which indicates that the systematic error introduced by the simulations is small (Figure 6.5).

This assumption was investigated by comparing statistics for other individual days throughout the seasons and long-term mean values for precipitation and temperature. Furthermore, analysis of discharges modelled with the simulated time series showed that on average the temperature simulations did not introduce a significant bias into the simulated discharges compared to interpolated temperatures. Depending on the time of the year some individual realisations produce larger others smaller discharges but their long-term ensemble mean matches the interpolations sufficiently well. Figure 6.6 shows the mean of the differences between interpolation and simulation as well as temperature at Höfen for 4.5 years.

In winter when temperatures are around 0°C the discharges vary significantly if precipitation falls depending on the form of precipitation (snow or rain). A positive peak in the curve is always followed by a negative one and vice versa as snow can only melt once and a smaller snowpack subsequently leads to reduced discharges. The impact in summer is small and the long-term mean of the series is zero proving that no systematic error is introduced by the temperature simulations. Looking at the standard deviation of the discharge differences mentioned above as a measure of uncertainty in the input data, one can expect a strong seasonality, which is shown in Figure 6.7. Here, a 30-day moving average of the 10-year mean daily discharge difference standard deviation and temperature are plotted. As expected, when the mean temperature is below 5°C there is a significant spread in the discharges of the different temperature simulations which also means a greater uncertainty from temperature input data than during summer.

The precipitation simulation on the other hand was shown to overestimate rainfall by about 35 mm (4%) per year and therefore also produced systematically larger discharges. This is due to the non-linearity of the Normal score transformation and the skewness of the precipitation. Accordingly, precipitation input uncertainty was determined based on the ensemble mean of the simulations instead of the interpolations. The mean of the differences between ensemble mean and realisations in this case is zero per definition. Figure 6.8 shows the standard deviation of the discharge differences between the individual realisations and the ensemble mean. Again, the 30-day moving average of the 10-year mean daily discharge difference standard devi-

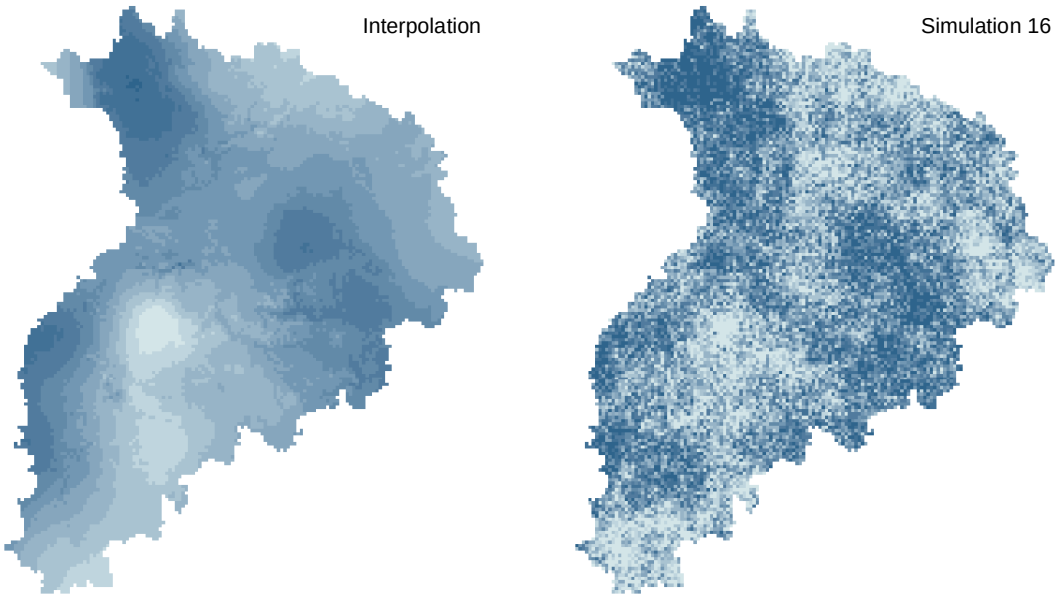

Figure 6.2: Example of an EDK-interpolated (left) and a simulated (right) precipitation field for 01.12.1981.

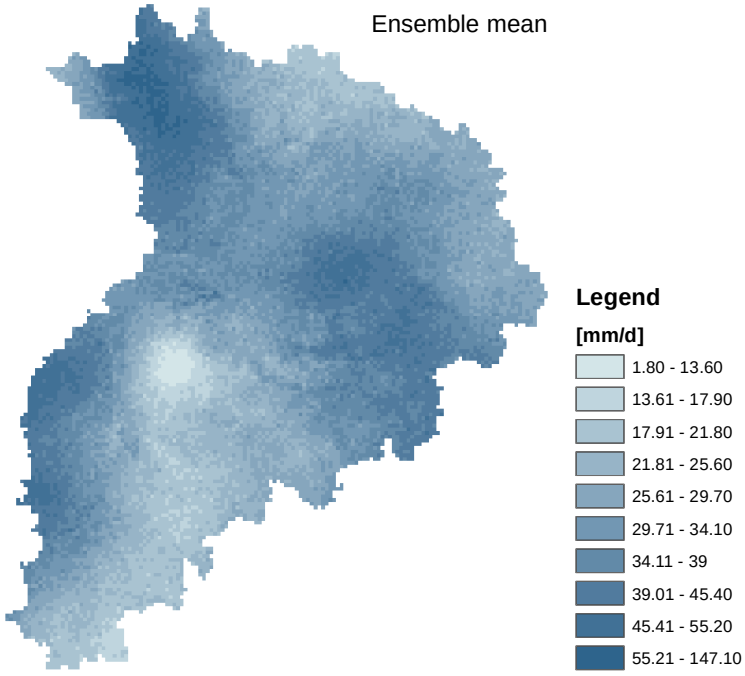

Figure 6.3: Ensemble mean of 50 simulated precipitation fields for 01.12.1981.

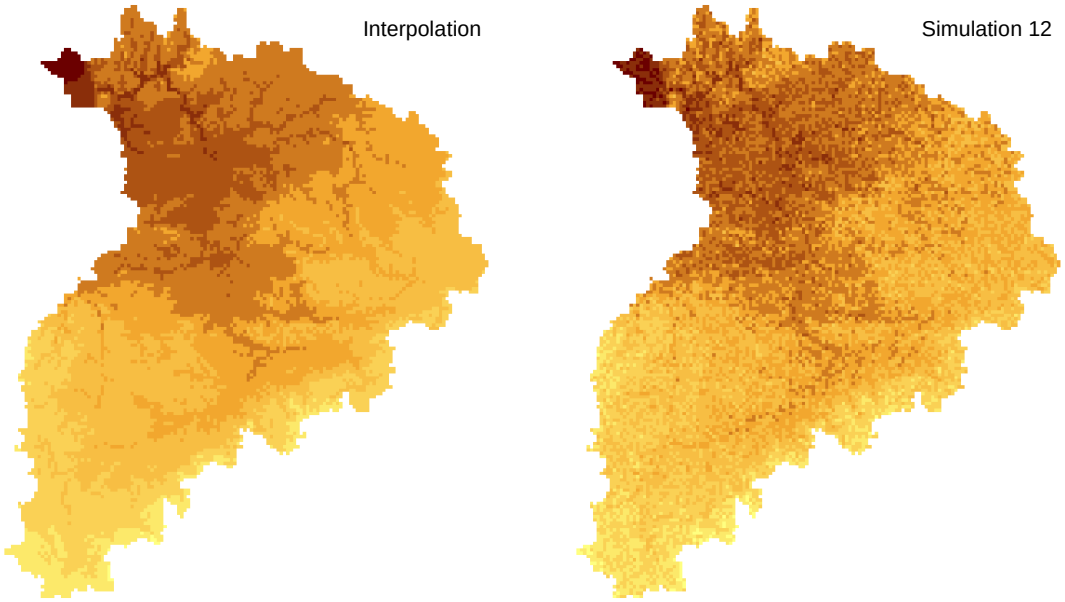

Figure 6.4: Example of an EDK-interpolated (left) and a simulated (right) temperature field for 18.03.1980.

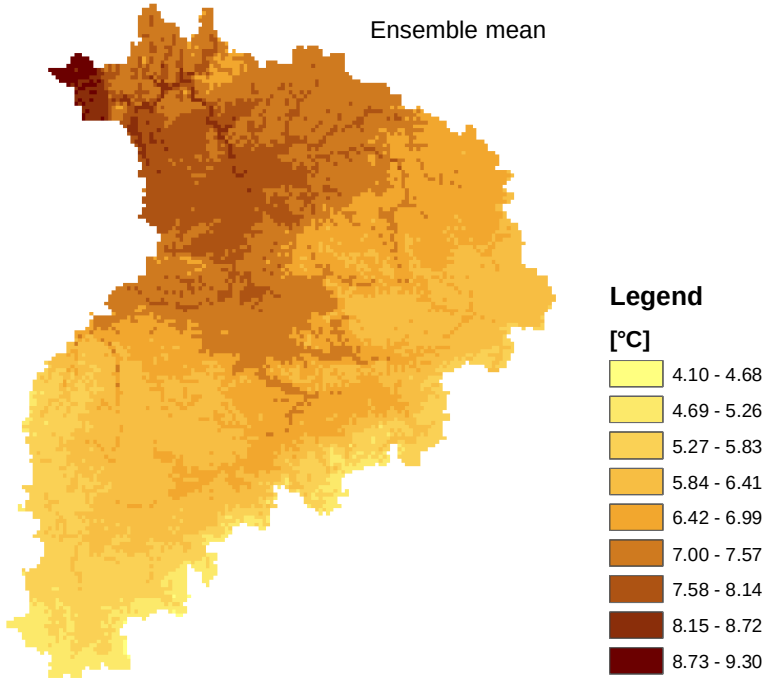

Figure 6.5: Ensemble mean of 50 simulated temperature fields for 18.03.1980.

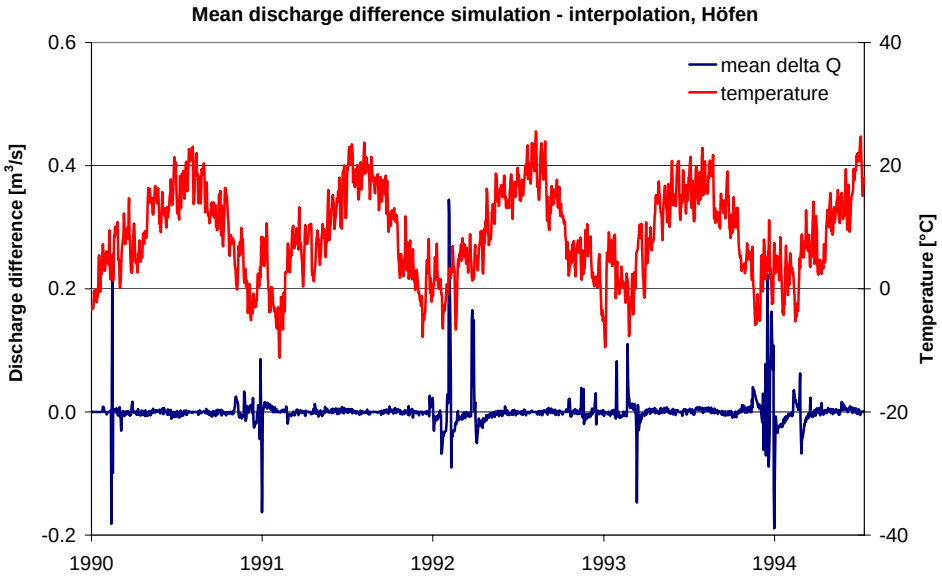

Figure 6.6: Mean differences between discharges modelled with interpolated and simulated temperatures at Höfen.

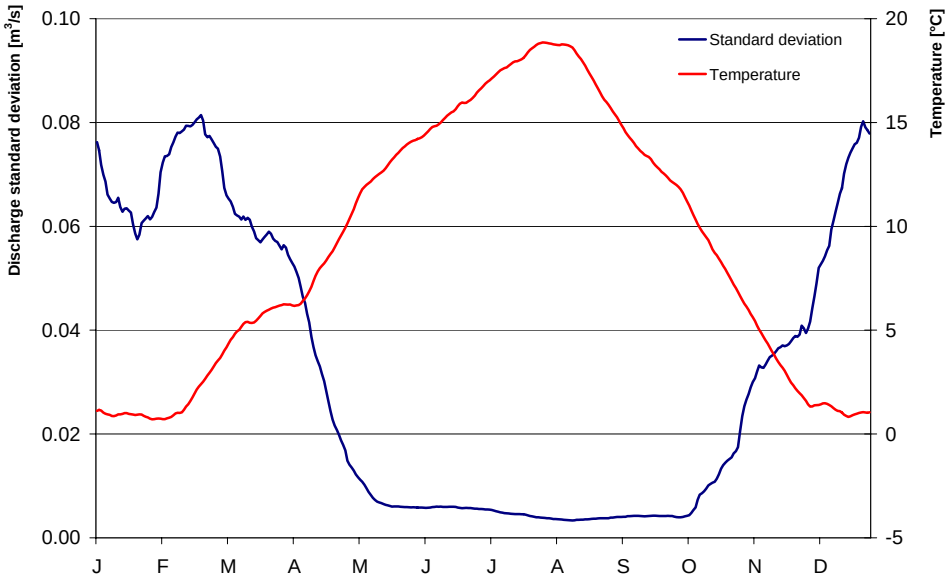

Figure 6.7: Annual cycle of daily standard deviation of discharge differences (interpolation - realisations modelled with simulated temperatures) at Höfen (30 day moving average).

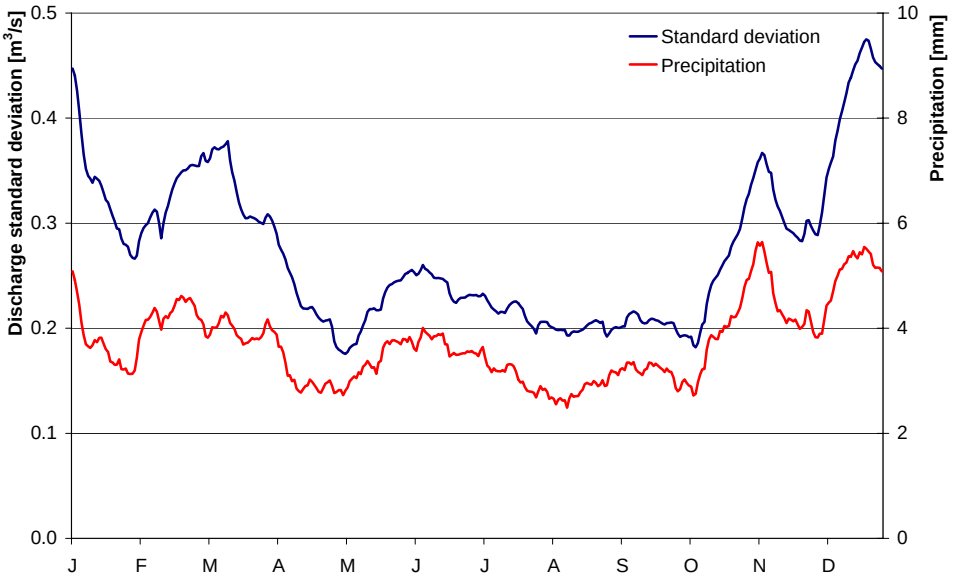

Figure 6.8: Annual cycle of daily standard deviation of discharge differences (ensemble mean - realisations) modelled with simulated precipitation at Höfen (30 day moving average).

ation and precipitation are plotted.

To estimate the uncertainty in discharge due to meteorological input data the standard deviation of the differences between modelled discharges using interpolated and simulated temperature was calculated for each day. For rainfall uncertainty the differences between the ensemble mean and the individual realisations of simulated precipitation were used. These uncertainty time series can now be combined with the process uncertainties to estimate the total model uncertainty due to input and process description.

6.3 Process and parameter related uncertainty

Process representation and process parameters play a very important role in the uncertainty of hydrological models. It is obvious that their contribution depends on the actual conditions. For example the contribution of snow accumulation and melt processes under summer conditions in Germany is negligible while in winter it may play a central role. The same applies to other processes too which under certain conditions contribute more or less to the runoff process. The sensitivity of the calculated discharge on a given day with respect to a parameter group θ can be calculated as $\frac{\partial Q}{\partial \theta}(t)$. Figure 6.9 shows an example of the determined discharge sensitivity time series.

Whereas the snow module parameters show a significant sensitivity only during winter, runoff generation and concentration processes are important throughout the whole year. The former are most sensitive during large precipitation events and in summer when the soils are more or less dry. The latter determine runoff most significantly during floods but also have a remarkable influence in the following recession

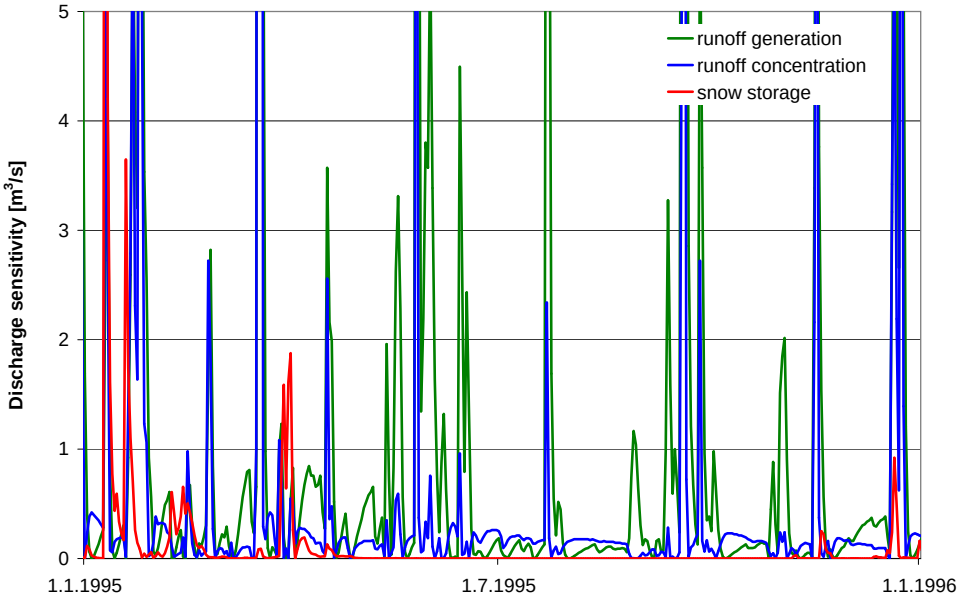

Figure 6.9: Time-variant discharge sensitivities with respect to different processes (parameter groups) at Neuenstadt.

periods by controlling the retention in the basin.

One can assume that the standard deviation of the random contribution of a certain process to the total uncertainty is proportional to its sensitivity (Bárdossy and Götzinger, 2007a).

$$\mathrm{Std}\left[\varepsilon_{\theta_i}(t)\right] = a_i \frac{\partial Q}{\partial \theta_i}(t) \tag{6.3}$$

This in combination with Equation 6.2 leads to:

$$\mathrm{Var}\left[\varepsilon_Q(t)\right] = \mathrm{Var}\left[\varepsilon_P(t)\right] + \mathrm{Var}\left[\varepsilon_T(t)\right] + \sum_i \left[a_i \frac{\partial Q}{\partial \theta_i}(t)\right]^2 \tag{6.4}$$

Because the coefficients, a_i, are unknown, the above equation does not yield an explicit estimation of the error variance. The coefficients have to be estimated via calibration. Model calibration in this case can be considered as a simultaneous estimation of the model parameters, θ_i, and the parameters of the calculated output error model, a_i. Assuming that the errors are normally distributed this task can be carried out using a maximum likelihood method or a bi-objective optimization. Therefore, for both cases the normalized errors are calculated:

$$\eta(t) = \frac{Q_o(t) - Q_m(t)}{\mathrm{Std}\left[\varepsilon_Q(t)\right]} \tag{6.5}$$

with:

$Q_o(t)$, $Q_m(t)$	Observed and modelled discharge on day t, respectively $[m^3/s]$
$\eta(t)$	Normalized model error $[-]$

The rationale behind this normalization is that the model should be more correct on a day when uncertainty is small (e.g. when fewer processes are active) and we should not force the model to be correct on a day when the input is already quite uncertain, because it would be for the wrong reason. In the maximum likelihood method, the likelihood of a normal distribution is:

$$L(\mathbf{x}|\mu,\sigma) = \prod \Phi(x) \tag{6.6}$$

In this case the likelihood of the model parameters, θ_i, and the error model parameters, a_i, is:

$$L(\theta,\mathbf{a}|0,\sigma(t)) = \prod_{t=1}^{T} \Phi(Q_o(t) - Q_m(t)) \tag{6.7}$$

If each data point, x_i, has its own standard deviation, σ_i, Equation 6.6 can be transformed leading to the log likelihood:

$$\ln L(\mathbf{x}|\mu,\sigma_i) = -\sum_i \frac{(x_i-\mu)^2}{2\sigma_i^2} - \sum_i \ln\sigma_i - \frac{1}{2}n\ln(2\pi) \tag{6.8}$$

Setting $(Q_o(t) - Q_m(t))$ for x_i, $\mathrm{Std}\,[\varepsilon_Q(t)]$ for σ_i and $\mu = 0$ gives:

$$\ln L(\theta,\mathbf{a}) = -\sum_{t=1}^{T} \frac{(Q_o(t)-Q_m(t))^2}{2\mathrm{Var}\,[\varepsilon_Q(t)]} - \sum_{t=1}^{T} \ln\left(\mathrm{Std}\,[\varepsilon_Q(t)]\right) - \frac{1}{2}T\ln(2\pi) \tag{6.9}$$

Maximizing the log likelihood function leads to the optimal model parameters, $\theta, \mathbf{a}$.

An alternative is to minimize the sum of the estimation variances:

$$\sum_{t=1}^{T} \mathrm{Var}\,[\varepsilon_Q(t)] \tag{6.10}$$

under the condition

$$\sum_{t=1}^{T} \eta(t)^2 = 1 \tag{6.11}$$

or the condition that $\eta(t)$ is normally distributed (bi-objective optimization). This condition can be ensured by minimizing the Kolmogoroff-Smirnoff D-statistic which measures the maximum distance between an empirical cumulative frequency distribution and a given theoretical distribution, in this case the normal distribution:

$$D_{test} = \sqrt{n}\,|F(x_i) - \Phi(X_i)|_{max} \tag{6.12}$$

with $F(x_i)$ being the relative cumulative frequency distribution of x_i and $\Phi(X_i)$ being the value of the normal distribution for this X_i.

Other assumptions about the error distributions may be reasonable and could be readily included into the described methodology.

Table 6.1: Key figures of the three watersheds.

	Süßen	Höfen	Neuenstadt
Elevation [m above sea level]	360-860	360-900	170-520
Area [km^2]	340	217	140
Mean annual precipitation [mm, 1990-99]	876	1375	983
Mean discharge [m^3/s, 1990-99]	5.3	4.7	1.3

6.4 Case Study

The methodology is demonstrated by application to the distributed, conceptual HBV model of three meso-scale watersheds of the central European Neckar basin. The three watersheds represent the major landscape units of the basin: The Swabian Jura in the South-East (gauge Süßen), the Black Forest in the West (gauge Höfen) and the plains in the North (gauge Neuenstadt). The climate can be characterised as temperate humid. Table 6.1 summarizes the properties of the basins.

The modified HBV model based on 1 km^2 grid cells as primary hydrological units which is described in Chapter 4.1 was used for this case study. The two snow related parameters are kept constant in each basin. The two parameters controlling the soil moisture, *beta* and k_{perc}, and the three storage coefficients, *alpha*, k_1 and k_2, are allowed to vary from cell to cell. As free calibration of such a large number of parameters is expected to introduce significant uncertainty the presented study tries to quantify this uncertainty and proposes a new, heteroskedastic calibration methodology for such distributed or lumped models. The model has been calibrated twice for the three basins using the time period 1990 to 1999: First, using a composition of Nash-Sutcliffe coefficients on daily, weekly and annual scale (standard calibration) and second, using the approach presented in Section 6.3. The traditionally measured model efficiency of both calibration runs was acceptable (mean Nash-Sutcliffe coefficient of 0.58 in both cases).

First, the distributions of the model residuals are compared. Therefore, the final model residuals of each calibration run are transformed by dividing through their standard deviation: directly in the case of the standard calibration and by taking the ratio of model residual to uncertainty in the case of the maximum likelihood methodology. Figure 6.10 shows the results for the three basins compared to a normal distribution. The standard calibration model residuals are biased, skewed and their standard deviation and kurtosis are too large. Key figures for both methodologies are presented in Table 6.2. Note that standardized model residuals are compared here. The absolute errors of the maximum likelihood calibration are not larger than the standard approach although the histograms are wider.

The maximum likelihood calibration yields approximately Gaussian error distributions which are only slightly biased and skewed. At all three stations the two classes of outliers ($<$ -3 and $>$ 3, respectively) contain a considerable number of time-steps (1.5%, 1.1% and 1.1%, respectively) where the model could not simulate the discharge approximately correctly, although it was expected to do so. This indicates additional weaknesses in the data or model structure which could not be properly addressed with this methodology. The frequency of outliers is nevertheless smaller

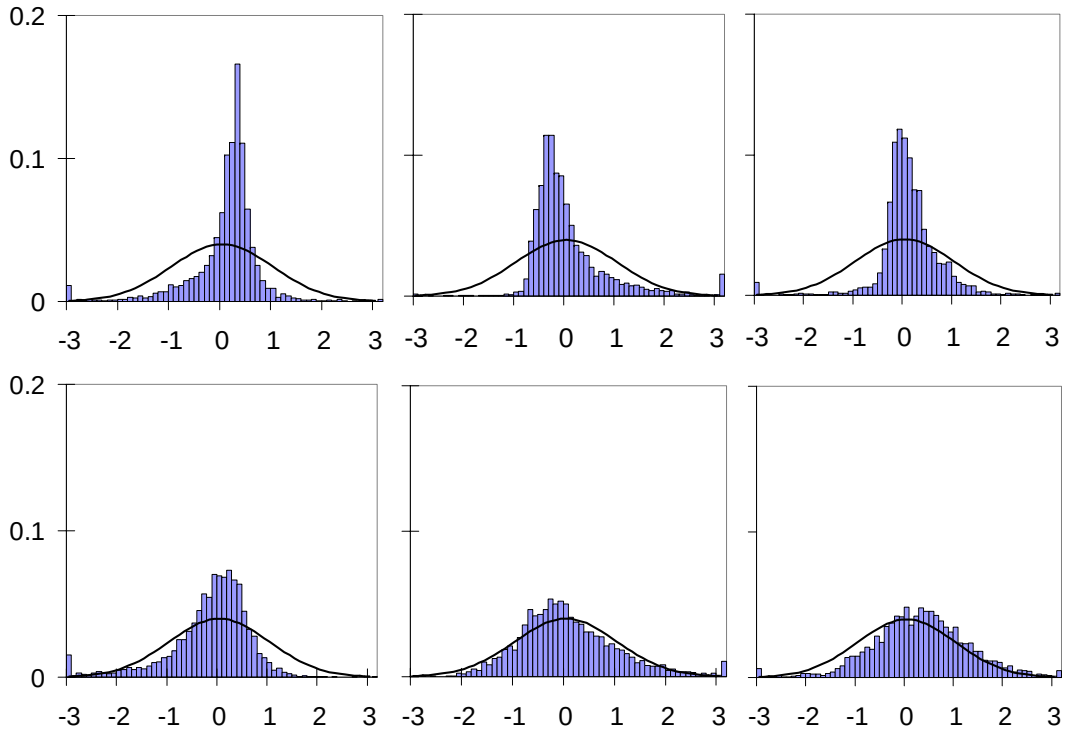

Figure 6.10: Standardized classified relative frequency distributions of model error using the standard (upper row) and maximum likelihood calibration methodology (lower row) for the basins Süßen, Höfen and Neuenstadt, respectively; normal distribution for comparison. Note that the upper and lower class contain all values greater and less than 3 and -3, respectively.

than in the standard calibration approach (1.3%, 1.7% and 1.1%, respectively).

In contrast to the standard calibration, the mean of the distribution in Höfen is zero but in Süßen and Neuenstadt it is still considerably biased. The standard deviations of all three distributions are sufficiently close to one and their kurtosis resembles the normal distribution. Therefore, despite the bias all three are much more suitable for optimization methods assuming Gaussian errors than their standard calibration equivalents.

Table 6.2: Mean, standard deviation and Kolmogoroff-Smirnoff D-statistics of the model error distributions for standard and maximum likelihood calibration.

	Standard calibration			Maximum likelihood calibration		
	Mean	Standard deviation	D_{test}	Mean	Standard deviation	D_{test}
Süßen	-0.02	2.92	11.43	-0.24	0.87	11.25
Höfen	0.67	3.21	9.5	0	0.99	4.29
Neuenstadt	0.29	1	21.1	0.25	0.99	7.18

Assuming all distributions were sufficiently normal, one can derive confidence in-

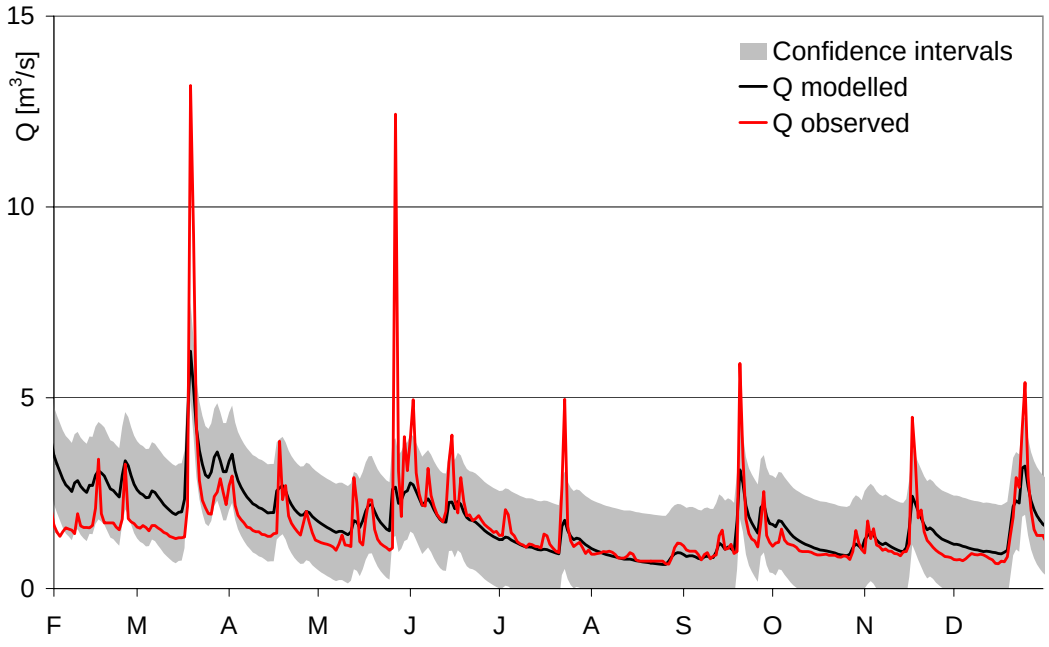

Figure 6.11: Standard calibration confidence intervals for an additive error model.

tervals for the simulated discharge by taking the inverse of the normal residual distribution and adding an expected deviation corresponding to a selected confidence limit to the calibrated discharge values. For the case of the standard calibration we have to assume a certain error model of the simulation. This can be additive (a fixed value for each discharge) or multiplicative (relative to the simulated discharge). Figure 6.11 and Figure 6.12 show two examples for the gauge Neuenstadt, calculated for a confidence level of 80%.

The confidence intervals can be validated by comparison with observed discharges. Intervals which are too wide will contain too many observations and the predictions are also very uncertain. If the intervals are too small they will not include as many observations as they theoretically should, which indicates weaknesses in the chosen methodology (Beven and Binley, 1992). As the intervals are derived from a certain confidence level, one can easily judge their value by comparing the number of points inside the limits with the chosen confidence level (Montanari and Brath, 2004).

An additive error confidence interval is like a fixed width band around the simulated values (Figure 6.11). Therefore, all low and medium flows are included but the model has little predictive power for those situations. Almost all higher discharge values on the other hand fall outside the range which shows that the methodology is not appropriate for that case either. Multiplicative error intervals can be derived by transforming the discharges and calculating the uncertainty bounds in the logarithmic domain. In a sense, these confidence limits are more realistic because many instruments show relative errors. However, uncertainty also increases in low flow situations, because it is also difficult to measure and model small quantities precisely. Therefore, these confidence limits are useful for some of the medium floods but also miss some low flow observations (Figure 6.12).

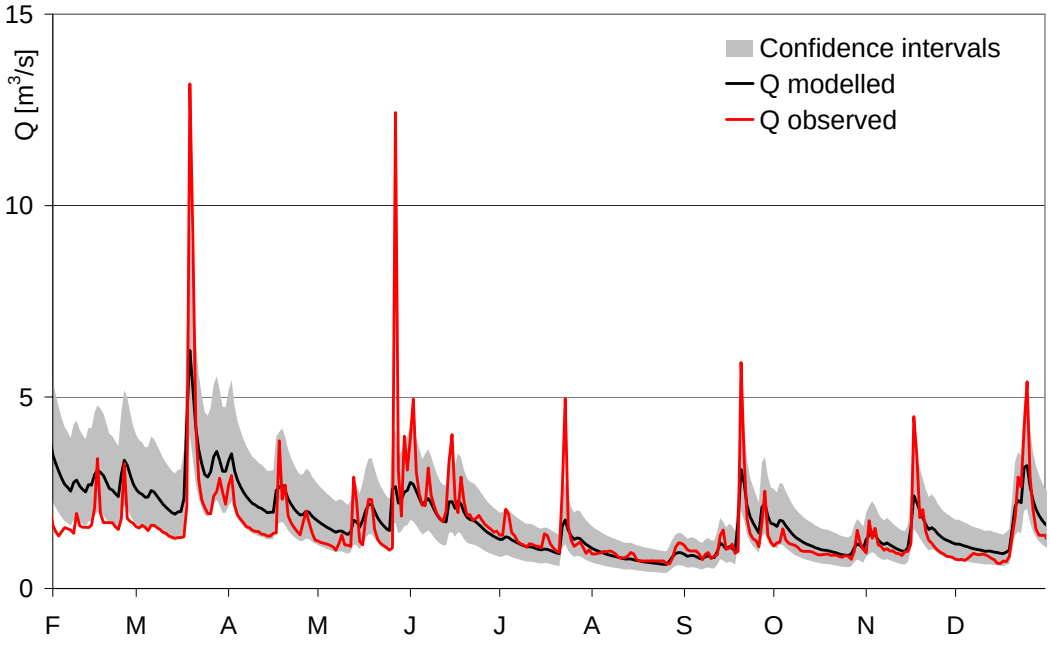

Figure 6.12: Standard calibration confidence intervals for a multiplicative error model.

Table 6.3: Data points within 80% confidence limits of the three error models [%].

	Additive error	Multiplicative error	Heteroskedastic error model
Süßen	94	77	90
Höfen	91	81	84
Neuenstadt	94	71	82

The heteroskedastic error model provides confidence intervals which represent the time-variant uncertainty of the discharge simulations more realistically (Figure 6.13). It is large during floods and in all cases where several processes are active simultaneously. It is smaller during recessions and in less complex situations, e.g. when soils are either completely wet or dry. No parts of the hydrograph are systematically missed and four of the six small floods are contained within the confidence bands which shows that they are suitable for all discharge ranges. At the same time, the error model has much more predictive power than an additive or multiplicative error model as it is smaller when the model should, in fact, be more precise.

A statistical comparison of all three error models is given in Table 6.3. As can be seen the additive error model overestimates and the multiplicative one underestimates the uncertainty of the simulations in five of the six cases. If the error distributions were perfectly normal, exactly 80% of the points would lie inside the confidence bounds. Because the distribution of the heteroskedastic methodology in Süßen deviates most from this assumption, this limit is also largely exceeded.

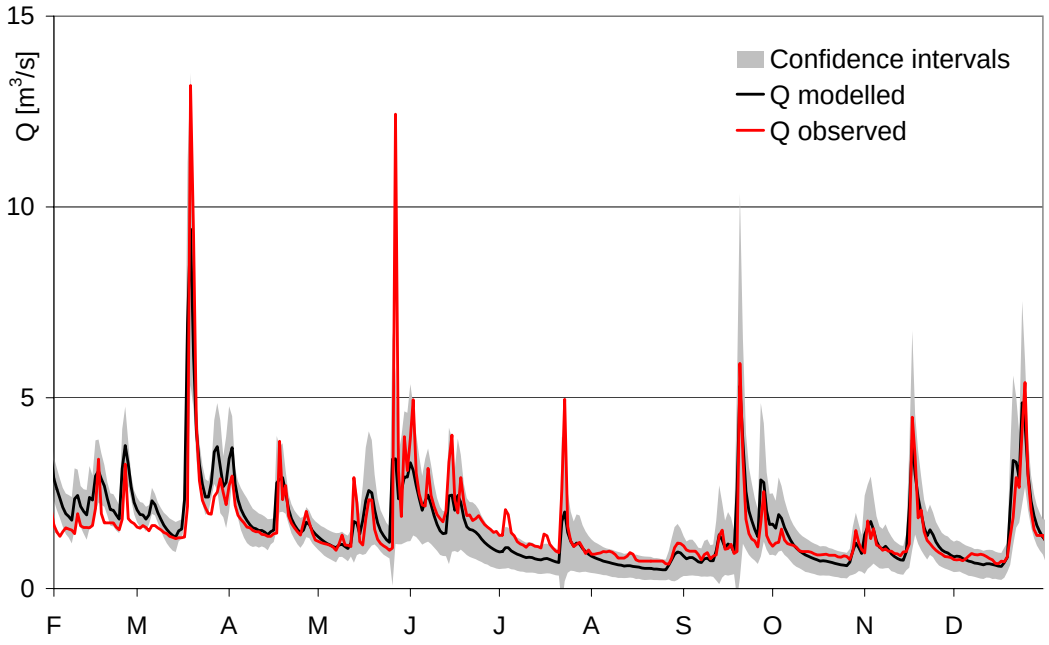

Figure 6.13: Maximum likelihood calibration confidence intervals using the heteroskedastic error model.

6.4.1 Comparison of maximum likelihood and bi-objective optimization

The maximum likelihood method presented in Section 6.3 yields the optimal model and error model parameters if all assumptions behind its application are valid. Unfortunately, *a posteriori* analysis shows that the means of the standardized model error distributions can be slightly biased. The bi-objective optimization provides the possibility to give more weight to the normality criterion during calibration. Therefore, the results of its application are now presented and compared to the maximum likelihood method. The sum of the error variances and the Kolmogoroff-Smirnoff D-statistic scaled by a constant factor of 100 have been summed up as objective function in this calibration.

As expected, Figure 6.14 shows that the standardized error distributions resemble the normal distribution more closely than those of the maximum likelihood calibration (Figure 6.10). Nevertheless, also the bi-objective calibration distributions show a considerable number of outliers, especially in Süßen and Höfen. The absolute errors of the bi-objective are larger than those of the maximum likelihood calibration which results from the larger weight which was put on the normality condition during optimization.

Table 6.4 supports these statements. Except for Höfen, where the maximum likelihood method has also achieved very good results, the Kolmogoroff-Smirnoff D-statistics show that the bi-objective calibration yields much more Gaussian distributions. At the price of reduced model precision because the absolute errors are larger and therefore the confidence intervals are also wider on average which is shown in Figure 6.15 (compared to Figure 6.13).

Note the extremely large uncertainty on the first of April which is a good example

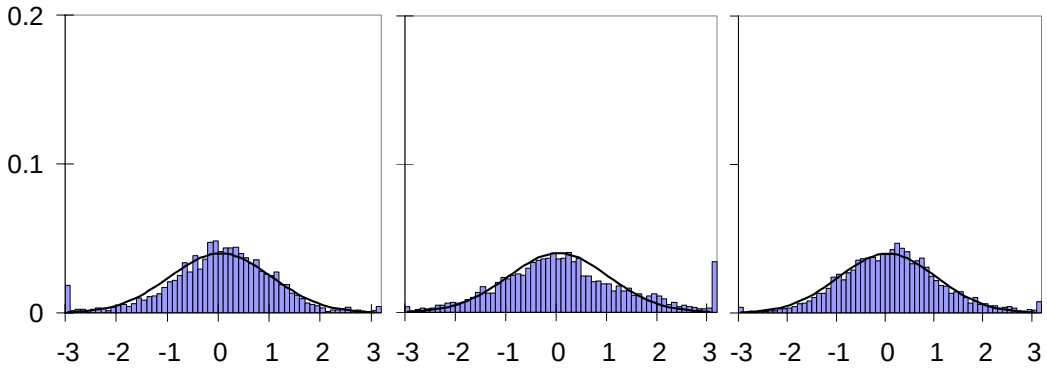

Figure 6.14: Standardized classified relative frequency distributions of model error using the bi-objective calibration methodology for the basins Süßen, Höfen and Neuenstadt, respectively; normal distribution for comparison.

Table 6.4: Mean, standard deviation and Kolmogoroff-Smirnoff D-statistics of the model error distributions for the maximum likelihood and bi-objective calibration methodologies.

	Maximum likelihood			Bi-objective calibration		
	Mean	Standard deviation	D_{test}	Mean	Standard deviation	D_{test}
Süßen	-0.24	0.87	11.25	-0.07	1.16	1.35
Höfen	0	0.99	4.29	0.09	1.37	4.29
Neuenstadt	0.25	0.99	7.18	0.04	1.03	1.27

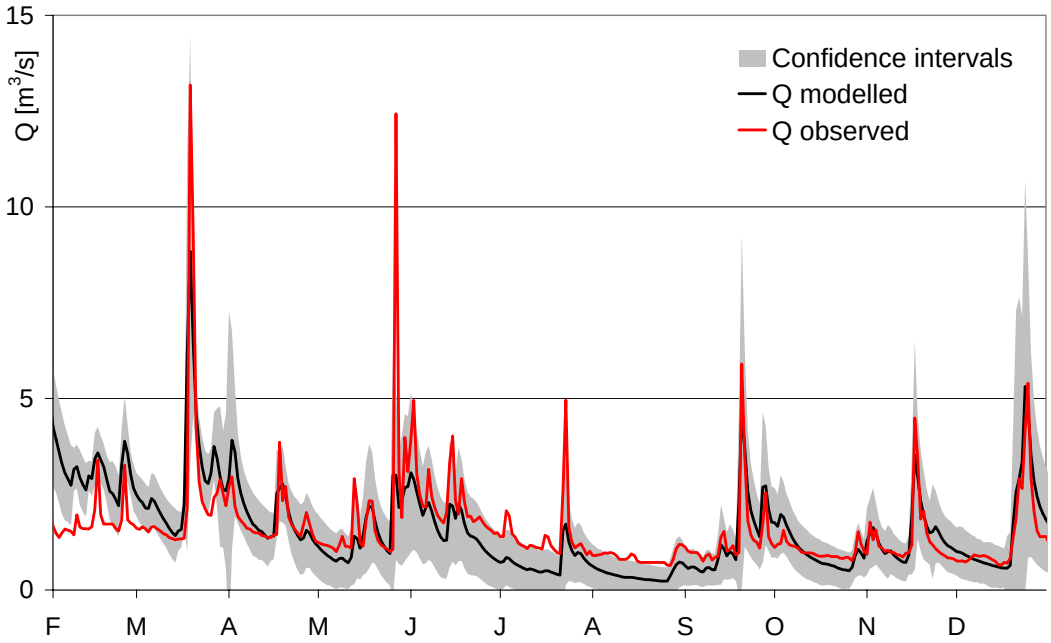

Figure 6.15: Bi-objective calibration confidence intervals using the heteroskedastic error model.

Table 6.5: Data points within the 80% confidence limits of the maximum likelihood and bi-objective calibration of the heteroskedastic error model [%].

	Maximum likelihood	Bi-objective calibration
Süßen	90	82
Höfen	84	71
Neuenstadt	82	81

of the benefit of the methodology in general. The high uncertainty stems from snow storage modelling. Whether or not the snow cover in the basin has already melted or not, precipitation on this day will fall on snow or directly on soil. On the other hand, if the air temperature is below the threshold temperature, it will fall as snow; if it is above, it will fall as rain. The possible combinations of both conditions lead to very different discharge simulations. Obviously, a process with a substantial error memory together with a purely stochastic one creates a situation which critically depends on the state and input into the system.

A statistical comparison of both calibration methods is given in Table 6.5. As can be seen the maximum likelihood method overestimates and the bi-objective underestimates the uncertainty of the simulations in three of the six cases (Süßen and Höfen, respectively). In general, the maximum likelihood method is recommended as it yields theoretically optimal results. If *a posteriori* analysis shows significant violations of the underlying assumptions the bi-objective calibration can be used to enforce normality. In that case, the exact weighting of both criteria should be optimized to reduce the loss in accuracy.

6.4.2 Validation

Because the maximum likelihood optimization has been identified as an appropriate method to determine model and error model parameters simultaneously, the transferability of both parameter sets to a different time period was analysed. Therefore, the time period 1980 to 1989 was simulated. The traditionally measured model efficiency was acceptable (mean NS-coefficient: 0.66). In addition, the rainfall and temperature variance time series have been calculated using another model parameter set to test the transferability of the input uncertainty. Table 6.6 summarizes the results of this test.

It shows that although the normality of the distributions deteriorates slightly, the transferability of parameters and input uncertainty time series is still given.

Table 6.6: Mean, standard deviation, Kolmogoroff-Smirnoff D-statistics, and points within 80% confidence intervals for the validation period.

	Mean	Standard deviation	D_{test}	Points within confidence limits
Süßen	-0.25	0.93	12.67	89
Höfen	-0.14	0.83	8.94	90
Neuenstadt	0.08	0.85	7.73	89

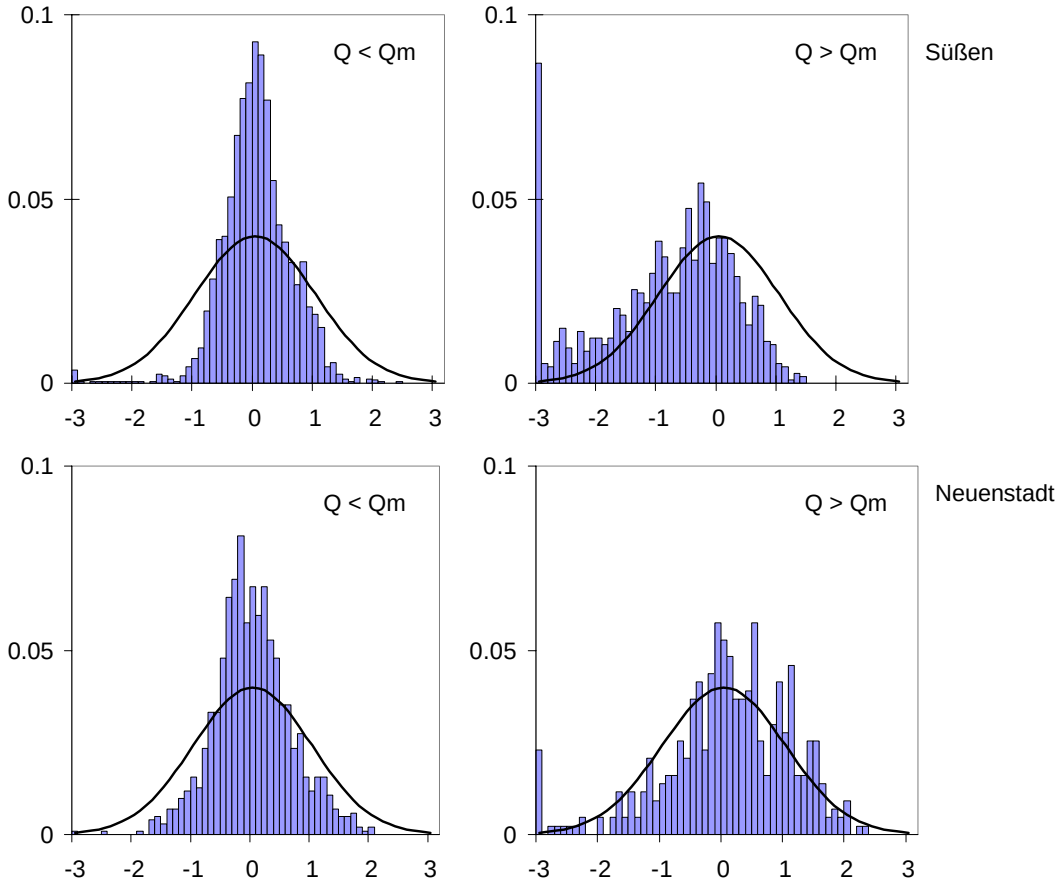

Figure 6.16: Standardized classified relative frequency distributions of model error during low and high flow situations for Süßen and Neuenstadt.

Nevertheless, the confidence limits appear to be systematically too large. An analysis of input uncertainty time series from several models showed that although being highly correlated they can be slightly biased. In the presented case this lead to the overestimation of model uncertainty in the validation period which was demonstrated by the excessive confidence intervals.

Another possibility is the internal validation of underlying assumptions. By separating observations and simulations into a low (smaller than mean discharge) and a high flow regime (larger than mean discharge), one can check if the distributions of the resulting sub-populations are also sufficiently Gaussian. In Figure 6.16 this is shown for the stations Süßen and Neuenstadt. The number of observations in the validation period at Höfen is too small to separate it into meaningful subsets.

The variance of the errors in the low flow regime is too small in both cases, however, the distributions do not deviate excessively from the normal distribution. During high flows the distributions are obviously biased and skewed, especially in Süßen, because the model is underestimating a large number of observations. This indicates internal weaknesses in the process description of the model which can not and should not be compensated for by the error model. Therefore, this analysis can be a valuable diagnostic tool in checking the models performance during different flow situations.

Table 6.7 provides the relevant statistics for both flow regimes.

A similar analysis can be performed regarding the seasonal behaviour of the model. Therefore, the observations and simulations are split into winter (from November to April) and summer periods (from May to October) and the model error distributions are plotted for each sub-population individually (Figure 6.17).

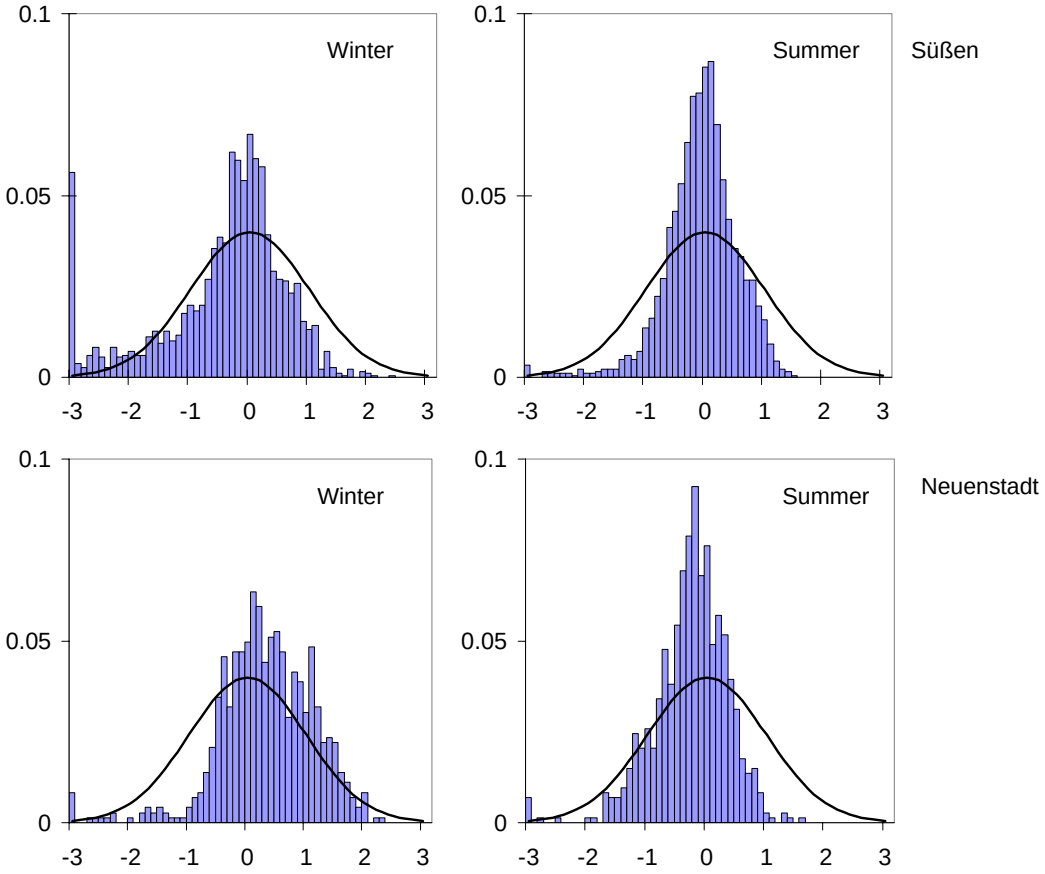

Figure 6.17: Standardized classified relative frequency distributions of model error from winter and summer periods for Süßen and Neuenstadt.

All four distributions deviate significantly from the normal distribution. The comparison of winter and summer simulations shows, that the model performs better in summer. This may be due to the reduced complexity in summer, because fewer

Table 6.7: Mean, standard deviation, and Kolmogoroff-Smirnoff D-statistics for the low and high flow regime of Süßen and Neuenstadt.

	Low flow regime			High flow regime		
	Mean	Standard deviation	D_{test}	Mean	Standard deviation	D_{test}
Süßen	-0.03	0.60	7.96	-1.05	1.55	9.69
Neuenstadt	-0.05	0.65	4.22	-0.01	1.18	1.53

Table 6.8: Mean, standard deviation, and Kolmogoroff-Smirnoff D-statistics from winter and summer periods in Süßen and Neuenstadt.

	Winter			Summer		
	Mean	Standard deviation	D_{test}	Mean	Standard deviation	D_{test}
Süßen	-0.58	1.40	8.05	-0.12	0.61	7.35
Neuenstadt	0.25	0.93	4.99	-0.32	0.64	6.99

processes are active and soils are mostly dry. The higher rainfall uncertainty in convective precipitation seems to be compensated by the standardized model error. Again, winter storms are mostly underestimated, especially in Süßen, which is dominated by snowmelt events. This systematic bias indicates weaknesses in the process representation. Table 6.8 shows the statistical key figures for both seasons.

The presented analysis of simulation subsets shows, that the model is not ergodic, which means that sub-populations behave different than the complete population. Ergodicity is an important prerequisite for the transferability of the results to other time periods (validation). Therefore, further research is needed to improve the validity of the methodology.

6.5 Results and discussion

The uncertainty from input data, model parameters and process description were estimated using a combined procedure for calibration and uncertainty estimation. The key points of the presented methodology are summarized in the following list.

- Hydrological model error is assumed to be a combination of random components from input variables and process representation errors.
- The uncertainty of the calculated discharge can be different for each time step depending on the uncertainty of the input and the processes contributing at (and before) the given time.
- The standard deviation of the random error corresponding to a given process (and parameter group) is assumed to be proportional to the sensitivity of simulated discharge with respect to the selected parameter group.
- From this an error model corresponding to a given parameter set can be created.
- Model parameters and the parameters of the error model can be estimated simultaneously using a maximum likelihood or bi-objective optimization procedure. The objective of model accuracy is the minimization of the normed deviation between modelled and observed discharge. The objective of the error model parameter estimation is to obtain normally distributed random errors.
- Because both objectives are coupled only a joint optimization can be successful.

- The framework developed in this paper yields a heteroskedastic model error, which can be used to derive plausible, time-variant, process-dependant confidence limits for hydrological simulations.

Nevertheless, the estimation of predictive uncertainty depends on the purpose of modelling. Therefore, different implementations of the presented method are necessary for simulation, forecasting or climate change impact studies as the input uncertainty varies significantly. The advantage of the presented approach is that process and parameter uncertainty are separated successfully from all other sources. The meteorological uncertainty can be added depending on the given situation. Therefore, different models may very well be optimal for different purposes depending on the data availability and quality (forecast, radar or climate scenarios).

A simple example demonstrates this effect. From a precipitation forecast or during a storm only a smaller number of rainfall observations may be available. The reduced resolution of model input has a significant effect on input uncertainty. This is demonstrated by using only every fourth rainfall station (69 instead of 294) during the conditional simulation of rainfall realisations. Figure 6.18 shows the calculated standard deviation of the differences between ensemble mean and the individual realisations based on the reduced station set which is used to estimate the input uncertainty. A comparison with Figure 6.8 indicates that the reduced data density approximately doubles the rainfall uncertainty and also changes the seasonal distribution of rainfall and discharge standard deviation. Therefore, in such cases the predictive uncertainty needs to be calculated again. However, as the error model parameters and process uncertainties were shown to be sufficiently independent one only needs to reassess the contribution of precipitation to the total uncertainty. This separation of the error sources is a significant advantage of the proposed method. Nevertheless, in the case of a forecast not the resolution but the bias of the forecast will constitute the greatest problem. This effect was not within the scope of this thesis but should be addressed in the future.

In fact, model resolution is expected to be just as important. It was shown above that input uncertainty is reduced when more observations are available at a given model resolution. On the other hand one can assume that process uncertainty increases with finer model resolutions for a given input data density. Therefore, an optimal model resolution could be found for each observation network which balances both effects and ideally exploits the available information.

Another aspect is the randomness of the calculated normalized model errors. Significant autocorrelation in the error time series (0.83, 0.91 and 0.74 for Süßen, Höfen and Neuenstadt, respectively) shows that the process-based error memory may be overestimated in the heteroskedastic error model. Additional analysis could prove if the time series can nevertheless be treated as quasi-random.

In Chapter 2.6 model structure and output were mentioned as additional sources of predictive uncertainty. The former is represented by the process uncertainties as the discharge sensitivity of each parameter group corresponding to a certain process of a given model structure is used. Therefore, the simplification by the model is implicitly taken into account. Finally, we are interested in the question how wrong the discharge can be with the given model structure and not how wrong the model structure is itself. This hypothesis can be verified by comparing several model structures as

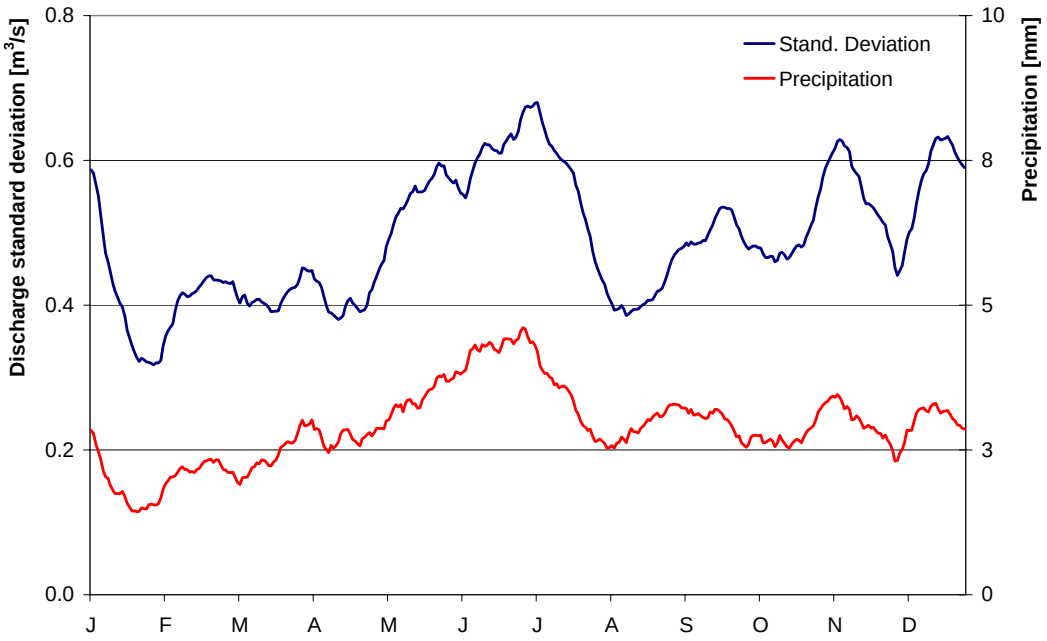

Figure 6.18: Annual cycle of daily standard deviation of discharge differences (ensemble mean - realisations) modelled with simulated precipitation using the reduced station set at Höfen (30 day mean).

discussed above for model resolution.

The output uncertainty, in this case discharge, can be derived from the analysis of rating curves and easily incorporated as an additional term into the methodology. The contribution is usually expected to be much smaller than input and process uncertainty but further analysis was not within the scope of this thesis. Therefore, additional research is needed to prove these hypotheses.

7 Summary and conclusions

In the following sections the four main research questions posed in the introduction are revisited.

7.1 Can we model the impact of global change on the water resources and what kind of models are necessary to predict the effect of land use change on the water balance of a catchment?

The HBV model concept was modified to run on 1 km^2 raster cells and generate distributed predictions of water balance components. This modification, but also the need for prediction at ungauged sites and the possibility to simulate the impact of land use change, required the development of a regionalisation method for parameter estimation from readily available catchment characteristics. In general, all four presented methods were capable of estimating reasonable parameter sets for the regionalisation catchments.
The first method using transfer functions turned out to be the most challenging in terms of prior process knowledge and optimisation. The other two methods that use conditions imposed on the parameters during simultaneous calibration are much more flexible especially in the following adaptation of suitable regression relationships. The modified Lipschitz condition produced the most efficient simulations of observed discharges in the regionalisation at the cost of some inconsistencies in the physical interpretation of the resulting relationships. The monotony condition preserved the assumed trends in the functions between cell properties and model parameters but produced sharp jumps which are not considered plausible. These jumps also resulted in slightly weaker regression relationships in the regionalisation. The combination of both methods seems to be the most promising because it produced equally good regionalisation results with much more consistent regression relationships. The approach can reproduce the derived trends with much more realistic variations in slope and the resulting relationships match our understanding of how the underlying processes are represented in the model.

The results support the findings of Vogel (2005), Parajka et al. (2005), Lee et al. (2005) and Beldring et al. (2003). The uncertainty from input data, model structure and parameter interaction results in many equally good parameter sets which significantly disturbs *a posteriori* regression analysis. The reduction of the available parameter space of distributed models through the link to catchment characteristics can crucially decrease these uncertainties and yield better regionalisation results if applied to ungauged catchments. A possible subdivision of the area according to geology and river regulations might improve the methodology.
The application of the combined conditions in the Ouémé catchment showed that the

methodology is transferable and works even under data sparse conditions although the result is strongly deteriorated by the lower data availability. The model efficiencies themselves are acceptable but from an operational perspective the variability of the discharge of the Ouémé is not modelled very well. The strong seasonality already explains a large part of the variance (and the Nash-Sutcliffe coefficient). But the model was not able to simulate all additional short-term fluctuations and the full extent of the dry season. Nevertheless, it was shown that the model parameters of this modified HBV model can be successfully linked to catchment characteristics which makes it suitable for global change impact studies.

7.2 Is it possible to integrate models on the regional scale to simulate and evaluate interdisciplinary water management scenarios?

The integration of a hydrological and a groundwater model has shown that groundwater presents a significant contribution to the water balance of the Neckar catchment, especially in low flow periods. The comparison of simulated groundwater recharge with SVAT model results and its use as input to the groundwater model demonstrated that hydrological models can provide realistic estimations of this inflow to the groundwater system. The groundwater runoff simulated with a groundwater model reacted faster and was smaller than the one simulated with the two hydrological models. Theory and other studies indicate that, even on this scale, groundwater flow can be simulated with more reliance by a physical groundwater model than a conceptual linear storage reservoir (Rojanschi et al., 2006). Integrating these models, however, extends the demands on them but also the possibilities to verify the model concepts. Despite reduced simulation efficiency, this improved our trust in the transferability of the models for the simulation of future climate or land use change impact scenarios. The presented examples have shown that model integration on the meso-scale is possible but brings up new problems which are currently being addressed in more detail. However, it also opens up possibilities to improve models by multi-response validation and provides helpful insights into internal processes and model conceptualizations.

In the Ouémé basin, the HBV model could successfully provide estimates of discharge, evapotranspiration, soil moisture and groundwater recharge for various management scenarios including the construction of irrigation and hydropower reservoirs. These data were used, among others, to simulate water supply, water quality and agro-economic figures like the length of the growing period under the scenario assumptions. A direct integration with a groundwater model was not attempted as the hydrogeologic situation in Benin does not favor regional groundwater modelling (absence of regionally connected aquifers).

7.3 What will be the impact of climate and land use change?

It was shown that higher precipitation in the climate scenarios may lead to higher discharges in the Neckar, especially in winter. Groundwater recharge on the contrary, was slightly reduced because of a simultaneous increase especially in winter temperatures. Two urbanisation scenarios with very moderate settlement growth rates did not show any effect on the water balance. Two benchmark scenarios for EU policies considering a drastic reduction of agricultural area could reduce the mean discharge in the Neckar by 15%, again with a stronger impact in winter.

The Ouémé will probably see a much stronger effect in the future. The monthly mean discharge in the rainy season could drop by almost 50% of the mean of the 1990's resulting from precipitation decrease and a temperature increase from global climate change. On the other hand, the drastic growth of population, settlements and agricultural area that has been simulated yields only a small surplus of discharge by reduced evapotranspiration and infiltration. Also the inclusion of two small-scale irrigation schemes did not endanger the water balance, but the construction of larger hydropower reservoirs could regulate the discharge and provide additional benefits to the local population.

7.4 How can we quantify uncertainties?

A general methodology has been introduced to quantify uncertainties associated with environmental simulations which is not only valid in this special case but also in a more generic framework. Based on the two sources input and process uncertainty as examples, it was shown how the total uncertainty can be derived for any desired combination of model and data. To quantify meteorological input uncertainty, simulation methods based on a modified turning band approach were used. With these methods, 50 ensemble fields of temperature and precipitation were generated and used in the hydrological model to simulate discharge time series. The standard deviation of the time-variant distribution of differences between the simulations using these individual realisations and interpolated temperature as well as the precipitation ensemble mean was used as a measure of predictive uncertainty due to input data. Process uncertainty was quantified using scaled contributions from individual parameter groups representing independent processes. The individual contributions were estimated from the time-variant discharge sensitivities of the respective parameter groups. Summed up together with the meteorological input uncertainty the scaled process sensitivities yield the total error variance. This error variance is a measure of the inherent model uncertainty and was used to normalize the model errors. Constant weights for the scaling of the sensitivities were estimated during a maximum likelihood and a bi-objective calibration yielding Gaussian normalized model errors. Both, maximum likelihood calibration as well as minimizing the error variance under the normality condition produced suitable parameter sets for the model and the corresponding error model. Reasonable quantiles of predictive uncertainty (confidence limits) were derived for the simulations with these sets and validated by comparison with observations.

7.5 Outlook

All of the developed methods and described results are only a snapshot of the current state of the art. Research on regionalisation and PUB must and will continue to improve our present ideas, views and models of the environment. The combination of Lipschitz and monotony condition is currently being tested with a semi-distributed model version of HBV in a masters thesis project by Shailesh Singh. It would be interesting to test it on other models, basins and climates to support or modify the findings of this thesis.

The integration of sectoral sub-models is also a continuing field of research, here and internationally. Another study by Johanna Jagelke is focussing on the groundwater model and a common vision is to define a strategy for improved model integration in the Neckar basin building on the presented results. This strategy should include a way to deal with the various methods to calculate groundwater recharge and baseflow. Ideally, it could further provide a map of groundwater exchange flows between surface water basins which would be an enormous help in the calibration of hydrological models. In general, our sectoral models must improve their common interfaces and address uncertainty in order to improve model integration. The most significant question within this context may be the scale differences between measurements, models and interfaces.

With the release of the IPCC fourth Assessment Report the debate on climate change has received considerable public attention. Many new research projects were advertised and launched also including adaptation measures and policy interventions. It is crucial to update the presented results continuously with new models and scenarios in order to improve the acceptance by stakeholders and society. Again, addressing and if possible reducing uncertainty is the major task for the future. Hydrological models are a suitable test bed for climate scenarios to improve climate models and downscaling methods. The mean and variability of such scenarios need to be analysed carefully in order to make reasonable impact predictions. To improve the societal relevance of the presented results a new project proposal was submitted to the EU which continues the process started in RIVERTWIN and focusses on capacity building and adaptation policy implementation in Germany, Benin, Peru and Brazil.

As mentioned above, the most promising opportunities remain in the field of uncertainty estimation. The exact implementation of the presented estimation methodology depends on the purpose of modelling, and it will be different for simulation, forecasting or climate change impact studies. Further research is needed to demonstrate the feasibility, potential and implications for these applications. It is necessary to test the method also on other basins and models, hydrological and from other fields. As it is very general in its foundations, it could also be modified, combined and compared with other uncertainty estimation methods to support and improve its assumptions. An important option would be the introduction and testing of non-Gausian error distributions.

In a changing world such as today, all the fields of research mentioned above are relevant for society and policy. It is also our task as scientists and engineers to emphasize and address the most important challenges for a more sustainable development.

Bibliography

Aarts, E. and Korst, J.: Simulated annealing and Boltzmann machines: a stochastic approach to combinatorial optimization and neural computing, J. Wiley, Hoboken, N. J., 1989.

Abbott, M. B., Bathurst, J. C., Cunge, J. A., O'Connell, P. E., and Rasmussen, J.: An introduction to the European Hydrological System – Système Hydrologique Européen, "SHE", 2: History and philosophy of a physically-based, distributed modelling system, Journal of Hydrology, 87, 45–59, 1986a.

Abbott, M. B., Bathurst, J. C., Cunge, J. A., O'Connell, P. E., and Rasmussen, J.: An introduction to the European Hydrological System – Système Hydrologique Européen, "SHE", 2: Structure of a physically-based, distributed modelling system, Journal of Hydrology, 87, 61–77, 1986b.

Ahmed, S. and de Marsily, G.: Comparison of geostatistical methods for estimating transmissivity using data on transmissivity and specific capacity, Water Resources Research, 23(9), 1717–1737, 1987.

Armbruster, V.: Grundwasserneubildung in Baden-Württemberg, Freiburger schriften zur hydrologie, University of Freiburg, 2002.

ASCE: Artificial neural networks in hydrology. I: Preliminary concepts, J. Hydrologic Engrg., Volume 5, 115–123, 2000a.

ASCE: Artificial neural networks in hydrology. II: Hydrologic applications, J. Hydrologic Engrg., Volume 5, 124–137, 2000b.

Ashagrie, A. G., de Laat, P. J. M., de Wit, M. J. M., Tu, M., and Uhlenbrook, S.: Detecting the influence of land use changes on Floods in the Meuse River Basin - the predictive power of a ninety-year rainfall-runoff relation, Hydrology and Earth System Sciences Discussions, 3, 529–559, 2006.

Bárdossy, A.: Introduction to Geostatistics, compendium, Institute for Hydraulic Engineering, Universitaet Stuttgart, 2002.

Bárdossy, A. and Götzinger, J.: Hydrological model uncertainty, Working paper, 2007a.

Bárdossy, A. and Götzinger, J.: Quantification of model uncertainty due to meteorological input, Working paper, 2007b.

Bárdossy, A., Barthel, R., Jagelke, J., and Götzinger, J.: Coupled and adapted model for surface water resources and groundwater in the Neckar basin, RIVERTWIN Deliverable D10, Universität Stuttgart, Institute for Hydraulic Engineering, http://www.rivertwin.de/assets/publications/d10_hbv_neckar.pdf, 2006.

Beldring, S., Engeland, K., Roald, L., Sælthun, N., and Voksø, A.: Estimation of parameters in a distributed precipitation-runoff model for Norway, Hydrology and Earth System Sciences, 7, 304–316, 2003.

Bergström, S.: The HBV model, in: Computer models of watershed hydrology, edited by Singh, V., pp. 443–476, Water Resources Pub., 1995.

Beven, K.: Changing Ideas in Hydrology: The Case of Physically-Based Models, Journal of Hydrology, 105, 157–172, doi:doi:10.1016/0022-1694(89)90101-7, 1989.

Beven, K.: A manifesto for the equifinality thesis, Journal of Hydrology, 320, 18–36, doi:10.1016/j.jhydrol.2005.07.007, 2006.

Beven, K. and Binley, A.: The Future of Distributed Models: Model Calibration and Uncertainty Prediction, Hydrological Processes, 6, 279–298, 1992.

Beven, K. and Kirkby, M.: A physically based, variable contributing area model of basin hydrology, Hydrological Sciences Bulletin, 24, 43–69, 1979.

Beven, K. J.: Rainfall-Runoff Modelling - the Primer, Wiley, Chichester, 2001.

Biswas, A. K.: Integrated water resources management: a reassessment - a water forum contribution, Water International, 29, 248–256, 2004.

Blöschl, G.: Rainfall-runoff modelling of ungauged catchments, in: Encyclopedia of Hydrological Sciences, edited by Anderson, M. G., chap. 133, pp. 2061–2080, Wiley, Chichester, 2005.

Bremicker, M.: Das Wasserhaushaltsmodell LARSIM - Modellgrundlagen und Anwendungsbeispiele, Ph.D. thesis, University of Freiburg, 2000.

Bremicker, M. and Gerlinger, K.: Operational application of the water balance model LARSIM in the Neckar basin, in: Proceedings of the International Workshop"Runoff Generation and Implications for River Basin Modelling", vol. 13 of *Freiburger Schriften zur Hydrologie*, pp. 306 – 312, Institut für Hydrologie der Universität Freiburg, Freiburg, Germany, 2000.

Bronstert, A., Carrera, J., Kabat, P., and Lütkemeier, S., eds.: Coupled models for the hydrological cycle, Springer, Heidelberg, Germany, 2005.

Brown, A. E., Zhang, L., McMahon, T. A., Western, A. W., and Vertessy, R. A.: A review of paired catchment studies for determining changes in water yield resulting from alterations in vegetation, Journal of Hydrology, 310, 28–61, 2005.

Crawford, N. H. and Linsley, R. K.: Digital simulation in hydrology: Stanford Watershed Model IV, vol. 39 of *Technical Report*, Stanford University, Palo Alto, Ca., 1966.

DIN: DIN 4049 Wasserwesen. Begriffe, Normen., German Institute for Standardization, Beuth, Berlin, 1996.

DKRZ: IPCC AR4 Simulations, Press release of MPI-M, DKRZ and the Model and Data group (M&D) (15.02.2005):, http://www.dkrz.de/dkrz/news/IPCC_AR4?setlang=en_US, 2005.

Engeland, K., Gottschalk, L., and Tallaksen, L.: Estimation of regional parameters in a macro scale hydrological model, Nordic Hydrology, 32, 161–180, 2001.

Enke, W., Schneider, F., and Deutschländer, T.: A novel scheme to derive optimized circulation pattern classifications for downscaling and forecast purposes, Theor. Appl. Climatol., 82, 51–63, doi:10.1007/s00704-004-0116-x, 2005.

EU: Directive 2000/60/EC of the European Parliament and of the Council establishing a framework for the Community action in the field of water policy, Official Journal of the European Communities, http://ec.europa.eu/environment/water/water-framework/index_en.html, 2000.

Falkenmark, M. and Lannerstad, M.: Consumptive water use to feed humanity - curing a blind spot, Hydrology and Earth System Sciences, 9, 15–28, 2005.

Freeze, R. A. and Harlan, R. L.: Blueprint for a physically-based, digitally-simulated hydrologic response model, Journal of Hydrology, 9, 237–258, 1969.

Gaiser, T., Graef, F., and Cordeiro, J.: Water retention characteristics of soils with contrasting clay mineral composition in semi-arid tropical regions, Australian Journal of Soil Research, 38 (3), 523–536, 2000.

Gaiser, T., Araújo, J. C., Frischkorn, H., and Krol, M., eds.: Global change and regional impacts: water availability and vulnerability of ecosystems and society in semi-arid Northeast of Brazil, Springer, Heidelberg, Germany, 2003.

Gaiser, T., Printz, A., Schwarz-von Raumer, H.-G., Schneider, M., Lange, F.-M., Götzinger, J., Barthel, R., Henseler, M., Bárdossy, A., Kaule, G., and Stahr, K.: Das EU-Projekt RIVERTWIN-Neckar: Ein Beitrag zum integrierten Flussgebietsmanagement, in: 3. KLIWA Symposium, 2006.

Gallagher, M. and Doherty, J.: Predictive error analysis for a water resource management model, Journal of Hydrology, 334, 513–533, 2007.

Giertz, S., Junge, B., and Diekkrüger, B.: Assessing the effects of land use change on soil physical properties and hydrological processes in the sub-humid tropical environment of West Africa, Physics and Chemistry of the Earth, 30, 485–496, 2005.

Giertz, S., Diekkrüger, B., and Steup, G.: Physically-based modelling of hydrological processes in a tropical headwater catchment in Benin (West Africa) - process representation and multi-criteria validation, Hydrology and Earth System Sciences, 3, 1–57, http://www.copernicus.org/EGU/hess/hessd/3/595/, 2006.

Götzinger, J. and Bárdossy, A.: Integration and calibration of a conceptual rainfall-runoff model in the framework of a decision support system for river basin management, Advances in Geosciences, 5, 31–35, 2005.

Götzinger, J. and Bárdossy, A.: Comparison of four regionalisation methods for a distributed hydrological model, Journal of Hydrology, 333, 374–384, 2007.

Götzinger, J., Jagelke, J., Barthel, R., and Bárdossy, A.: Integration of water balance models in RIVERTWIN, Advances in Geosciences, 9, 85–91, http://www.copernicus.org/EGU/adgeo/9/1/85.htm, 2006.

Gupta, H., Bastidas, L., Vrugt, J., and Sorooshian, S.: Multiple criteria global optimization for watershed model calibration, in: Calibration of Watershed Models, edited by Duan, Q., Gupta, H. V., Sorooshian, S., Rousseau, A. N., and Turcotte, R., vol. 6, pp. 125–132, AGU Water Science and Applications Series, 2003.

Gupta, H. V., Beven, K. J., and Wagener, T.: Model Calibration and Uncertainty Estimation, in: Encyclopedia of Hydrological Sciences, chap. Part 11. Rainfall-Runoff Modeling, John Wiley & Sons, Ltd, doi:10.1002/0470848944.hsa138, 2005.

GWP: Integrated water resources management, TAC Background Papers 4, Stockholm: Global Water Partnership Secretariat, 2000.

Haberlandt, U. and Gattke, C.: Spatial interpolation versus simulation of precipitation, for rainfall-runoff modelling-a case study in the Lippe River Basin, Germany., in: Hydrology: science and practice for the 21st century. Proceedings of the British Hydrological Society International Conference, vol. 1, pp. 120–127, British Hydrological Society London, UK, Imperial College, London, 2004.

Hargreaves, G. H. and Samani, Z. A.: Reference crop evapotranspiration from temperature, Applied Engineering in Agriculture, 1, 96–99, 1985.

Harmoni-CA: Harmonised Modelling Tools for Integrated Basin Management, Website, http://www.harmoni-ca.info, 2006.

Houghton, J., Ding, Y., Griggs, D., Noguer, M., van der Linden, P., Dai, X., Maskell, K., and Johnson, C., eds.: Climate change 2001: the Scientific Basis. Contributions of Working Group I to the Third Assessment Report of the Intergovernmental Panel on Climate Change, Cambridge University Press, 2001.

Hundecha, Y.: Regionalization of parameters of a conceptual rainfall-runoff model, Ph.D. thesis, University of Stuttgart, 2005.

Hundecha, Y. and Bárdossy, A.: Modeling of the effect of land use changes on the runoff generation of a river basin through parameter regionalization of a watershed model, Journal of Hydrology, 292, 281–295, doi:10.1016/j.jhydrol.2004.01.002, 2004.

IH: Flood estimation handbook, Institute of Hydrology, Wallingford, UK, 1999.

Ihringer, J.: Softwarepaket für Hydrologie und Wasserwirtschaft, Department Water Resources Management and Rural Engineering, 1999.

Kämäri, J.: BMW - Benchmark Models for the Water Framework Directive, Website, http://www.environment.fi/default.asp?contentid=116046\&lan=EN#a1, 2005.

Kaule, G.: Integrated model as decision support system for public authorities in the Neckar River basin, RIVERTWIN Deliverable D16, University of Stuttgart, Institute for Landscape Planning and Ecology, http://www.rivertwin.de/assets/publications/D16_MOSDEW.pdf, 2006.

Kavetski, D., Franks, S., and Kuczera, G.: Confronting input uncertainty in environmental modelling, in: Calibration of Watershed Models, edited by Duan, Q., Gupta, H. V., Sorooshian, S., Rousseau, A. N., and Turcotte, R., pp. 49–68, AGU Water Science and Applications Series, http://www.eng.newcastle.edu.au/~cegak/kavetski/, 2002.

KLIWA: Klimaveränderung und Wasserwirtschaft, Website, http://www.kliwa.de/en/index.html, 2006.

Krause, P., Boyle, D., and Bäse, F.: Comparison of different efficiency criteria for hydrological model assessment, Advances in Geosciences, 5, 89–97, 2005.

Kuczera, G. and Mroczkowski, M.: Assessment of hydrologic parameter uncertainty and the worth of multiresponse data, Water Resources Research, 34, 1481–1490, doi:10.1029/98WR00496, 1998.

Kuczera, G., Kavetski, D., Franks, S., and Thyer, M.: Towards a Bayesian total error analysis of conceptual rainfall-runoff models: Characterising model error using storm-dependent parameters, Journal of Hydrology, 331, 161–177, 2006.

Lee, H., McIntyre, N., Wheater, H., and Young, A.: Selection of conceptual models for regionalisation of the rainfall-runoff relationship, Journal of hydrology, 312, 125–147, doi:10.1016/j.jhydrol.2005.02.016, 2005.

Lindström, G., Johansson, B., Persson, M., Gardelin, M., and Bergström, S.: Development and test of the distributed HBV-96 hydrological model, Journal of Hydrology, 201, 272–288, doi:10.1016/S0022-1694(97)00041-3, 1997.

Mahe, G., Paturel, J.-E., Servat, E., Conway, D., and Dezetter, A.: The impact of land use change on soil water holding capacity and river flow modelling in the Nakambe River, Burkina-Faso, Journal of Hydrology, 300, 33–43, 2005.

Mantovan, P. and Todini, E.: Hydrological forecasting uncertainty assessment: Incoherence of the GLUE methodology, Journal of Hydrology, In Press, 1–14, doi:10.1016/j.jhydrol.2006.04.046, 2006.

Maréchal, D. and Holman, I. P.: Development and application of a soil classification-based conceptual catchment-scale hydrological model, Journal of Hydrology, 312, 277–293, doi:10.1016/j.jhydrol.2005.02.018, 2005.

McDonald, M. G. and Harbaugh, A. W.: A modular three-dimensional finite-difference ground-water flow model, Technical report, U.S. Geol. Survey, Reston, VA. USA, 1988.

Mellor, D.: The modified turning bands (MTB) model for space-time rainfall. I. Model definition and properties, Journal of Hydrology, 175, 113–127, 1996.

Mellor, D. and Metcalfe, A.: The Modified Turning Bands (MTB) model for space-time rainfall. III. Estimation of the storm/rainband profile and a discussion of future model prospects, Journal of Hydrology, 175, 161–180, 1996.

Mellor, D. and O'Connell, P.: The modified turning bands (MTB) model for space-time rainfall. II. Estimation of raincell parameters, Journal of Hydrology, 175, 129–159, 1996.

Meyer, W. B. and Turner II, B. L.: Human population growth and global landuse/land-cover change, Annual Rev. Ecol. Systems, 23, 39–61, 1992.

Montanari, A. and Brath, A.: A stochastic approach for assessing the uncertainty of rainfall-runoff simulations, Water Resources Research, 40, 1–11, doi:10.1029/2003WR002540, 2004.

Mulvany, T. J.: On the use of self-registering rain and flood gauges in making observations of the relations of rain fall and flood discharges in a given catchment, in: Transactions and Minutes of the Proceedings of the Institute of Civil Engineers of Ireland, Session 1850-1, v.IV, pt. II, Dublin, Ireland, 1851.

NASA: Shuttle Radar Topography Mission, website, http://www2.jpl.nasa.gov/srtm/, 2006.

Parajka, J., Merz, R., and Blöschl, G.: A comparison of regionalisation methods for catchment model parameters, Hydrology and Earth System Sciences, 2, 509–542, 2005.

Rawls, W., Brakensiek, C., and Saxton, K.: Estimation of soil water properties., Transactions - American Society of Agricultural Engineers, 25 (5), 1316–1320, 1328, 1982.

Refsgaard, J. C.: State-of-the-art report on quality assurance in modelling related to river basin management, Tech. rep., HarmoniQuA Report, D-WP1-1, Copenhagen, Denmark, 2002.

Rieland, M.: Das BMBF-Programm GLOWA: Instrumente für ein vorausschauendes Management großer Flusseinzugsgebiete, Hydrologie und Wasserbewirtschaftung (Hydrology and Water Resources Management), 48, 83–84, 2004.

Roeckner, E., Oberhuber, J., Bacher, A., Christoph, M., and Kirchner, I.: ENSO variability and atmospheric response in a global coupled atmosphere-ocean GCM, Clim. Dyn., 12, 737–754, 1996.

Schaefli, B., Talamba, D., and Musy, A.: Quantifying hydrological modeling errors through a mixture of normal distributions, Journal of Hydrology, 332, 303–315, 2007.

Seibert, J.: Multi-criteria calibration of a conceptual runoff model using a genetic algorithm, Hydrology and Earth System Sciences, 4, 215–224, 2000.

Singh, V. and Woolhiser, D.: Mathematical Modeling of Watershed Hydrology, Journal of Hydrologic Engineering, 7, 270–292, 2002.

Singh, V. P.: Computer models of watershed hydrology, Water Resources Publications, Highlands Ranch, Colorado, USA, 1995.

Sivapalan, M., Takeuchi, K., Franks, S. W., Gupta, V. K., Karambiri, H., Lakshmi, V., Liang, X., McDonnell, J. J., Mendiondo, E. M., O'Connell, P. E., Oki, T., Pomeroy, J. W., Schertzer, D., Uhlenbrook, S., and Zehe, E.: IAHS Decade on predictions in Ungauged Basins (PUB), 2003-2012: Shaping an exciting future for the hydrological sciences, Hydro. Sci. J., 48(6), 857–880, 2003.

Stahr, K.: Bioclimatic conditions in Southern Benin, in: Adapted Farming in West Africa: Issues, Potentials and Perspectives, edited by F. Graef, P. L. and von Oppen, M., pp. 205–210, Ulrich E. Grauer, Stuttgart, Germany, 2000.

Stock, M., ed.: KLARA Klimawandel - Auswirkungen, Risiken, Anpassung, no. 99 in PIK Report, Potsdam Institute for climate impact research (PIK), Potsdam, Germany, 2005.

Thornton, P. K., Jones, P. G., Owiyo, T., Kruska, R. L., Herrero, M., Kristjanson, P., Notenbaert, A., Bekele, N., and Omolo, A.: Mapping climate vulnerability and poverty in Africa. Report to the Department for International Development, Tech. rep., International Livestock Research Institute (ILRI), Nairobi, Kenya, 2006.

Tomasella, J. and Hodnett, M.: Estimating unsaturated hydraulic conductivity of Brazilian soils using soil-water retention data, Soil Science, 162 (10), 703–712, 1997.

Tomasella, J. and Hodnett, M.: Estimating soil water retention characteristics from limited data in Brazilian Amazonia, Soil Science, 163 (3), 190–202, 1998.

Uhlenbrook, S., Roser, S., and Tilch, N.: Hydrological process representation at the meso-scale: the potential of a distributed, conceptual catchment model, Journal of Hydrology, 291, 278–296, doi:10.1016/j.jhydrol.2003.12.038, 2004.

UNDP: Human development report 2003 millennium development goals: a compact among nations to end human poverty, Oxford University Press, New York, 2003.

Vogel, R. M.: Regional calibration of watershed models, in: Watershed Models, edited by Singh, V. and Frevert, D., pp. 47–71, CRC Press, 2005.

Vrugt, J. A., Gupta, H. V., Bouten, W., and Sorooshian, S.: A Shuffled Complex Evolution Metropolis Algorithm for Estimating the Posterior Distribution of Watershed Model Parameters, in: Calibration of Watershed Models, edited by Duan, Q., Gupta, H. V., Sorooshian, S., Rousseau, A. N., and Turcotte, R., vol. 6, AGU Water Science and Applications Series, doi:DOI:10.1029/006WS07, 2003.

Wagener, T., McIntyre, N., Lees, M., Wheater, H., and Gupta, H.: Towards reduced uncertainty in conceptual rainfall-runoff modelling: dynamic identifiability analysis, Hydrological Processes, 17, 455–476, 2003.

Xie, Z., Su, F., Liang, X., Zeng, Q., Hao, Z., and Guo, Y.: Applications of a surface runoff model with Horton and Dunne runoff for VIC, Advances in Atmospheric Sciences, 20, 165–172, 2003.

Xu, C.: Testing the transferability of regression equations derived from small subcatchments to a large area in central Sweden, Hydrology and Earth System Sciences, 7, 317–324, http://folk.uio.no/chongyux/papers/hess-7-317.pdf, 2003.

Yang, W. and Bárdossy, A.: Highly resoluted climate scenarios from stochastic model until 2030 for the Neckar River basin, RIVERTWIN Deliverable D3, University of Stuttgart, Institute for Hydraulic Engineering, http://www.rivertwin.de/assets/publications/D03_downscaled_highly_resolution_Neckar.pdf, 2005.

Yang, W. and Bárdossy, A.: Highly resoluted climate scenarios from stochastic model until 2030 for the Ouémé River basin, RIVERTWIN Deliverable D21, University of Stuttgart, Institute for Hydraulic Engineering, http://www.rivertwin.de/assets/publications/, 2006.

Yapo, P., Gupta, H., and Sorooshian, S.: Multi-objective global optimization for hydrologic models, Journal of Hydrology, 204, 83–97, 1998.

Young, P. C.: Data-based mechanistic and topdown modelling, in: Proceedings International Environmental Modelling and Software Society Conference, vol. I, pp. 363–374, Lugano, Switzerland, 2002.

Zehe, E. and Bárdossy, A.: Hydrological impact of climate change on the river Rhine, Final report irma-sponge development of flood management strategies for the rhine and meuse basins in the context of integrated river management, University of Stuttgart, 2002.

Zhao, R. J.: Flood forecasting method for humid regions in China, Tech. rep., East China Institute of Hydraulic Engineering, Nanjing, China, 1977.

Curriculum vitae

28. March 1977	born in Landstuhl, Germany
1987 - 1996	Gymnasium Landstuhl
1997 - 2003	Environmental Engineering Study (Dipl.-Ing.), Universitaet Stuttgart
2000 - 2001	Exchange student at the Department of Earth Science, University of Waterloo
2000 - 2003	Master of Science (M.Sc.) in Water Resources Engineering and Management (WAREM), Universität Stuttgart
2002 - 2003	Student employee at Fritz Spieth Consulting Engineers, Esslingen
2003	Master thesis at Fritz Spieth Consulting Engineers, Esslingen
since 2003	Research Assistant at the Institute for Hydraulic Engineering, Universität Stuttgart

Institut für Wasserbau
Universität Stuttgart

Pfaffenwaldring 61
70569 Stuttgart (Vaihingen)
Telefon (0711) 685 - 64717/64741/64752/64679
Telefax (0711) 685 - 67020 o. 64746 o. 64681
E-Mail: iws@iws.uni-stuttgart.de
http://www.iws.uni-stuttgart.de

Verzeichnis der Mitteilungshefte

5 Plate, Erich: *Beitrag zur Bestimmung der Windgeschwindigkeitsverteilung in der durch eine Wand gestörten bodennahen Luftschicht*,
und
Röhnisch, Arthur; Marotz, Günter: *Neue Baustoffe und Bauausführungen für den Schutz der Böschungen und der Sohle von Kanälen, Flüssen und Häfen; Gestehungskosten und jeweilige Vorteile*, sowie Unny, T.E.: *Schwingungsuntersuchungen am Kegelstrahlschieber*, 1967

6 Seiler, Erich: *Die Ermittlung des Anlagenwertes der bundeseigenen Binnenschiffahrtsstraßen und Talsperren und des Anteils der Binnenschiffahrt an diesem Wert*, 1967

7 *Sonderheft anläßlich des 65. Geburtstages von Prof. Arthur Röhnisch mit Beiträgen von* Benk, Dieter; Breitling, J.; Gurr, Siegfried; Haberhauer, Robert; Honekamp, Hermann; Kuz, Klaus Dieter; Marotz, Günter; Mayer-Vorfelder, Hans-Jörg; Miller, Rudolf; Plate, Erich J.; Radomski, Helge; Schwarz, Helmut; Vollmer, Ernst; Wildenhahn, Eberhard; 1967

8 Jumikis, Alfred: *Beitrag zur experimentellen Untersuchung des Wassernachschubs in einem gefrierenden Boden und die Beurteilung der Ergebnisse*, 1968

9 Marotz, Günter: *Technische Grundlagen einer Wasserspeicherung im natürlichen Untergrund*, 1968

10 Radomski, Helge: *Untersuchungen über den Einfluß der Querschnittsform wellenförmiger Spundwände auf die statischen und rammtechnischen Eigenschaften*, 1968

11 Schwarz, Helmut: *Die Grenztragfähigkeit des Baugrundes bei Einwirkung vertikal gezogener Ankerplatten als zweidimensionales Bruchproblem*, 1969

12 Erbel, Klaus: *Ein Beitrag zur Untersuchung der Metamorphose von Mittelgebirgsschneedecken unter besonderer Berücksichtigung eines Verfahrens zur Bestimmung der thermischen Schneequalität*, 1969

13 Westhaus, Karl-Heinz: *Der Strukturwandel in der Binnenschiffahrt und sein Einfluß auf den Ausbau der Binnenschiffskanäle*, 1969

14 Mayer-Vorfelder, Hans-Jörg: *Ein Beitrag zur Berechnung des Erdwiderstandes unter Ansatz der logarithmischen Spirale als Gleitflächenfunktion*, 1970

15 Schulz, Manfred: *Berechnung des räumlichen Erddruckes auf die Wandung kreiszylindrischer Körper*, 1970

16 Mobasseri, Manoutschehr: *Die Rippenstützmauer. Konstruktion und Grenzen ihrer Standsicherheit*, 1970

17 Benk, Dieter: *Ein Beitrag zum Betrieb und zur Bemessung von Hochwasserrückhaltebecken*, 1970

18 Gàl, Attila: *Bestimmung der mitschwingenden Wassermasse bei überströmten Fischbauchklappen mit kreiszylindrischem Staublech*, 1971, vergriffen

19 Kuz, Klaus Dieter: *Ein Beitrag zur Frage des Einsetzens von Kavitationserscheinungen in einer Düsenströmung bei Berücksichtigung der im Wasser gelösten Gase*, 1971, vergriffen

20 Schaak, Hartmut: *Verteilleitungen von Wasserkraftanlagen*, 1971

21 *Sonderheft zur Eröffnung der neuen Versuchsanstalt des Instituts für Wasserbau der Universität Stuttgart mit Beiträgen von* Brombach, Hansjörg; Dirksen, Wolfram; Gàl, Attila; Gerlach, Reinhard; Giesecke, Jürgen; Holthoff, Franz-Josef; Kuz, Klaus Dieter; Marotz, Günter; Minor, Hans-Erwin; Petrikat, Kurt; Röhnisch, Arthur; Rueff, Helge; Schwarz, Helmut; Vollmer, Ernst; Wildenhahn, Eberhard; 1972

22 Wang, Chung-su: *Ein Beitrag zur Berechnung der Schwingungen an Kegelstrahlschiebern*, 1972

23 Mayer-Vorfelder, Hans-Jörg: *Erdwiderstandsbeiwerte nach dem Ohde-Variationsverfahren*, 1972

24 Minor, Hans-Erwin: *Beitrag zur Bestimmung der Schwingungsanfachungsfunktionen überströmter Stauklappen*, 1972, vergriffen

25 Brombach, Hansjörg: *Untersuchung strömungsmechanischer Elemente (Fluidik) und die Möglichkeit der Anwendung von Wirbelkammerelementen im Wasserbau*, 1972, vergriffen

26 Wildenhahn, Eberhard: *Beitrag zur Berechnung von Horizontalfilterbrunnen*, 1972

27 Steinlein, Helmut: *Die Eliminierung der Schwebstoffe aus Flußwasser zum Zweck der unterirdischen Wasserspeicherung, gezeigt am Beispiel der Iller*, 1972

28 Holthoff, Franz Josef: *Die Überwindung großer Hubhöhen in der Binnenschiffahrt durch Schwimmerhebewerke*, 1973

29 Röder, Karl: *Einwirkungen aus Baugrundbewegungen auf trog- und kastenförmige Konstruktionen des Wasser- und Tunnelbaues*, 1973

30 Kretschmer, Heinz: *Die Bemessung von Bogenstaumauern in Abhängigkeit von der Talform*, 1973

31 Honekamp, Hermann: *Beitrag zur Berechnung der Montage von Unterwasserpipelines*, 1973

32 Giesecke, Jürgen: *Die Wirbelkammertriode als neuartiges Steuerorgan im Wasserbau*, und Brombach, Hansjörg: *Entwicklung, Bauformen, Wirkungsweise und Steuereigenschaften von Wirbelkammerverstärkern*, 1974

33 Rueff, Helge: *Untersuchung der schwingungserregenden Kräfte an zwei hintereinander angeordneten Tiefschützen unter besonderer Berücksichtigung von Kavitation*, 1974

34 Röhnisch, Arthur: *Einpreßversuche mit Zementmörtel für Spannbeton - Vergleich der Ergebnisse von Modellversuchen mit Ausführungen in Hüllwellrohren*, 1975

35 *Sonderheft anläßlich des 65. Geburtstages von Prof. Dr.-Ing. Kurt Petrikat mit Beiträgen von*: Brombach, Hansjörg; Erbel, Klaus; Flinspach, Dieter; Fischer jr., Richard; Gàl, Attila; Gerlach, Reinhard; Giesecke, Jürgen; Haberhauer, Robert; Hafner Edzard; Hausenblas, Bernhard; Horlacher, Hans-Burkhard; Hutarew, Andreas; Knoll, Manfred; Krummet, Ralph; Marotz, Günter; Merkle, Theodor; Miller, Christoph; Minor, Hans-Erwin; Neumayer, Hans; Rao, Syamala; Rath, Paul; Rueff, Helge; Ruppert, Jürgen; Schwarz, Wolfgang; Topal-Gökceli, Mehmet; Vollmer, Ernst; Wang, Chung-su; Weber, Hans-Georg; 1975

36 Berger, Jochum: *Beitrag zur Berechnung des Spannungszustandes in rotationssymmetrisch belasteten Kugelschalen veränderlicher Wandstärke unter Gas- und Flüssigkeitsdruck durch Integration schwach singulärer Differentialgleichungen*, 1975

37 Dirksen, Wolfram: *Berechnung instationärer Abflußvorgänge in gestauten Gerinnen mittels Differenzenverfahren und die Anwendung auf Hochwasserrückhaltebecken*, 1976

38 Horlacher, Hans-Burkhard: *Berechnung instationärer Temperatur- und Wärmespannungsfelder in langen mehrschichtigen Hohlzylindern*, 1976

39 Hafner, Edzard: *Untersuchung der hydrodynamischen Kräfte auf Baukörper im Tiefwasserbereich des Meeres*, 1977, ISBN 3-921694-39-6

40 Ruppert, Jürgen: *Über den Axialwirbelkammerverstärker für den Einsatz im Wasserbau*, 1977, ISBN 3-921694-40-X

41 Hutarew, Andreas: *Beitrag zur Beeinflußbarkeit des Sauerstoffgehalts in Fließgewässern an Abstürzen und Wehren*, 1977, ISBN 3-921694-41-8, vergriffen

42 Miller, Christoph: *Ein Beitrag zur Bestimmung der schwingungserregenden Kräfte an unterströmten Wehren*, 1977, ISBN 3-921694-42-6

43 Schwarz, Wolfgang: *Druckstoßberechnung unter Berücksichtigung der Radial- und Längsverschiebungen der Rohrwandung*, 1978, ISBN 3-921694-43-4

44 Kinzelbach, Wolfgang: *Numerische Untersuchungen über den optimalen Einsatz variabler Kühlsysteme einer Kraftwerkskette am Beispiel Oberrhein*, 1978, ISBN 3-921694-44-2

45 Barczewski, Baldur: *Neue Meßmethoden für Wasser-Luftgemische und deren Anwendung auf zweiphasige Auftriebsstrahlen*, 1979, ISBN 3-921694-45-0

46 Neumayer, Hans: *Untersuchung der Strömungsvorgänge in radialen Wirbelkammerverstärkern*, 1979, ISBN 3-921694-46-9

47 Elalfy, Youssef-Elhassan: *Untersuchung der Strömungsvorgänge in Wirbelkammerdioden und -drosseln*, 1979, ISBN 3-921694-47-7

48 Brombach, Hansjörg: *Automatisierung der Bewirtschaftung von Wasserspeichern*, 1981, ISBN 3-921694-48-5

49 Geldner, Peter: *Deterministische und stochastische Methoden zur Bestimmung der Selbstdichtung von Gewässern*, 1981, ISBN 3-921694-49-3, vergriffen

50 Mehlhorn, Hans: *Temperaturveränderungen im Grundwasser durch Brauchwassereinleitungen*, 1982, ISBN 3-921694-50-7, vergriffen

51 Hafner, Edzard: *Rohrleitungen und Behälter im Meer*, 1983, ISBN 3-921694-51-5

52 Rinnert, Bernd: *Hydrodynamische Dispersion in porösen Medien: Einfluß von Dichteunterschieden auf die Vertikalvermischung in horizontaler Strömung*, 1983, ISBN 3-921694-52-3, vergriffen

53 Lindner, Wulf: *Steuerung von Grundwasserentnahmen unter Einhaltung ökologischer Kriterien*, 1983, ISBN 3-921694-53-1, vergriffen

54 Herr, Michael; Herzer, Jörg; Kinzelbach, Wolfgang; Kobus, Helmut; Rinnert, Bernd: *Methoden zur rechnerischen Erfassung und hydraulischen Sanierung von Grundwasserkontaminationen*, 1983, ISBN 3-921694-54-X

55 Schmitt, Paul: *Wege zur Automatisierung der Niederschlagsermittlung*, 1984, ISBN 3-921694-55-8, vergriffen

56 Müller, Peter: *Transport und selektive Sedimentation von Schwebstoffen bei gestautem Abfluß*, 1985, ISBN 3-921694-56-6

57 El-Qawasmeh, Fuad: *Möglichkeiten und Grenzen der Tropfbewässerung unter besonderer Berücksichtigung der Verstopfungsanfälligkeit der Tropfelemente*, 1985, ISBN 3-921694-57-4, vergriffen

58 Kirchenbaur, Klaus: *Mikroprozessorgesteuerte Erfassung instationärer Druckfelder am Beispiel seegangsbelasteter Baukörper*, 1985, ISBN 3-921694-58-2

59 Kobus, Helmut (Hrsg.): *Modellierung des großräumigen Wärme- und Schadstofftransports im Grundwasser*, Tätigkeitsbericht 1984/85 (DFG-Forschergruppe an den Universitäten Hohenheim, Karlsruhe und Stuttgart), 1985, ISBN 3-921694-59-0, vergriffen

60 Spitz, Karlheinz: *Dispersion in porösen Medien: Einfluß von Inhomogenitäten und Dichteunterschieden*, 1985, ISBN 3-921694-60-4, vergriffen

61 Kobus, Helmut: *An Introduction to Air-Water Flows in Hydraulics*, 1985, ISBN 3-921694-61-2

62 Kaleris, Vassilios: *Erfassung des Austausches von Oberflächen- und Grundwasser in horizontalebenen Grundwassermodellen*, 1986, ISBN 3-921694-62-0

63 Herr, Michael: *Grundlagen der hydraulischen Sanierung verunreinigter Porengrundwasserleiter*, 1987, ISBN 3-921694-63-9

64 Marx, Walter: *Berechnung von Temperatur und Spannung in Massenbeton infolge Hydratation*, 1987, ISBN 3-921694-64-7

65 Koschitzky, Hans-Peter: *Dimensionierungskonzept für Sohlbelüfter in Schußrinnen zur Vermeidung von Kavitationsschäden*, 1987, ISBN 3-921694-65-5

66 Kobus, Helmut (Hrsg.): *Modellierung des großräumigen Wärme- und Schadstofftransports im Grundwasser*, Tätigkeitsbericht 1986/87 (DFG-Forschergruppe an den Universitäten Hohenheim, Karlsruhe und Stuttgart) 1987, ISBN 3-921694-66-3

67 Söll, Thomas: *Berechnungsverfahren zur Abschätzung anthropogener Temperaturanomalien im Grundwasser*, 1988, ISBN 3-921694-67-1

68 Dittrich, Andreas; Westrich, Bernd: *Bodenseeufererosion, Bestandsaufnahme und Bewertung*, 1988, ISBN 3-921694-68-X, vergriffen

69 Huwe, Bernd; van der Ploeg, Rienk R.: *Modelle zur Simulation des Stickstoffhaushaltes von Standorten mit unterschiedlicher landwirtschaftlicher Nutzung*, 1988, ISBN 3-921694-69-8, vergriffen

70 Stephan, Karl: *Integration elliptischer Funktionen*, 1988, ISBN 3-921694-70-1

71 Kobus, Helmut; Zilliox, Lothaire (Hrsg.): *Nitratbelastung des Grundwassers, Auswirkungen der Landwirtschaft auf die Grundwasser- und Rohwasserbeschaffenheit und Maßnahmen zum Schutz des Grundwassers*. Vorträge des deutsch-französischen Kolloquiums am 6. Oktober 1988, Universitäten Stuttgart und Louis Pasteur Strasbourg (Vorträge in deutsch oder französisch, Kurzfassungen zweisprachig), 1988, ISBN 3-921694-71-X

72 Soyeaux, Renald: *Unterströmung von Stauanlagen auf klüftigem Untergrund unter Berücksichtigung laminarer und turbulenter Fließzustände*,1991, ISBN 3-921694-72-8

73 Kohane, Roberto: *Berechnungsmethoden für Hochwasserabfluß in Fließgewässern mit überströmten Vorländern*, 1991, ISBN 3-921694-73-6

74 Hassinger, Reinhard: *Beitrag zur Hydraulik und Bemessung von Blocksteinrampen in flexibler Bauweise*, 1991, ISBN 3-921694-74-4, vergriffen

75 Schäfer, Gerhard: *Einfluß von Schichtenstrukturen und lokalen Einlagerungen auf die Längsdispersion in Porengrundwasserleitern*, 1991, ISBN 3-921694-75-2

76 Giesecke, Jürgen: *Vorträge, Wasserwirtschaft in stark besiedelten Regionen; Umweltforschung mit Schwerpunkt Wasserwirtschaft*, 1991, ISBN 3-921694-76-0

77 Huwe, Bernd: *Deterministische und stochastische Ansätze zur Modellierung des Stickstoffhaushalts landwirtschaftlich genutzter Flächen auf unterschiedlichem Skalenniveau*, 1992, ISBN 3-921694-77-9, vergriffen

78 Rommel, Michael: *Verwendung von Kluftdaten zur realitätsnahen Generierung von Kluftnetzen mit anschließender laminar-turbulenter Strömungsberechnung*, 1993, ISBN 3-92 1694-78-7

79 Marschall, Paul: *Die Ermittlung lokaler Stofffrachten im Grundwasser mit Hilfe von Einbohrloch-Meßverfahren*, 1993, ISBN 3-921694-79-5, vergriffen

80 Ptak, Thomas: *Stofftransport in heterogenen Porenaquiferen: Felduntersuchungen und stochastische Modellierung*, 1993, ISBN 3-921694-80-9, vergriffen

81 Haakh, Frieder: *Transientes Strömungsverhalten in Wirbelkammern,* 1993, ISBN 3-921694-81-7

82 Kobus, Helmut; Cirpka, Olaf; Barczewski, Baldur; Koschitzky, Hans-Peter: *Versucheinrichtung zur Grundwasser und Altlastensanierung VEGAS, Konzeption und Programmrahmen*, 1993, ISBN 3-921694-82-5

83 Zang, Weidong: *Optimaler Echtzeit-Betrieb eines Speichers mit aktueller Abflußregenerierung*, 1994, ISBN 3-921694-83-3, vergriffen

84 Franke, Hans-Jörg: *Stochastische Modellierung eines flächenhaften Stoffeintrages und Transports in Grundwasser am Beispiel der Pflanzenschutzmittelproblematik*, 1995, ISBN 3-921694-84-1

85 Lang, Ulrich: *Simulation regionaler Strömungs- und Transportvorgänge in Karstaquiferen mit Hilfe des Doppelkontinuum-Ansatzes: Methodenentwicklung und Parameteridentifikation*, 1995, ISBN 3-921694-85-X, vergriffen

86 Helmig, Rainer: *Einführung in die Numerischen Methoden der Hydromechanik*, 1996, ISBN 3-921694-86-8, vergriffen

87 Cirpka, Olaf: *CONTRACT: A Numerical Tool for Contaminant Transport and Chemical Transformations - Theory and Program Documentation* -, 1996, ISBN 3-921694-87-6

88 Haberlandt, Uwe: *Stochastische Synthese und Regionalisierung des Niederschlages für Schmutzfrachtberechnungen*, 1996, ISBN 3-921694-88-4

89 Croisé, Jean: *Extraktion von flüchtigen Chemikalien aus natürlichen Lockergesteinen mittels erzwungener Luftströmung*, 1996, ISBN 3-921694-89-2, vergriffen

90 Jorde, Klaus: *Ökologisch begründete, dynamische Mindestwasserregelungen bei Ausleitungskraftwerken*, 1997, ISBN 3-921694-90-6, vergriffen

91 Helmig, Rainer: *Gekoppelte Strömungs- und Transportprozesse im Untergrund - Ein Beitrag zur Hydrosystemmodellierung-*, 1998, ISBN 3-921694-91-4

92 Emmert, Martin: *Numerische Modellierung nichtisothermer Gas-Wasser Systeme in porösen Medien*, 1997, ISBN 3-921694-92-2

93 Kern, Ulrich: *Transport von Schweb- und Schadstoffen in staugeregelten Fließgewässern am Beispiel des Neckars*, 1997, ISBN 3-921694-93-0, vergriffen

94 Förster, Georg: *Druckstoßdämpfung durch große Luftblasen in Hochpunkten von Rohrleitungen 1997*, ISBN 3-921694-94-9

95 Cirpka, Olaf: *Numerische Methoden zur Simulation des reaktiven Mehrkomponententransports im Grundwasser*, 1997, ISBN 3-921694-95-7, vergriffen

96 Färber, Arne: *Wärmetransport in der ungesättigten Bodenzone: Entwicklung einer thermischen In-situ-Sanierungstechnologie*, 1997, ISBN 3-921694-96-5

97 Betz, Christoph: *Wasserdampfdestillation von Schadstoffen im porösen Medium: Entwicklung einer thermischen In-situ-Sanierungstechnologie*, 1998, ISBN 3-921694-97-3

98 Xu, Yichun: *Numerical Modeling of Suspended Sediment Transport in Rivers*, 1998, ISBN 3-921694-98-1, vergriffen

99 Wüst, Wolfgang: *Geochemische Untersuchungen zur Sanierung CKW-kontaminierter Aquifere mit Fe(0)-Reaktionswänden,* 2000, ISBN 3-933761-02-2

100 Sheta, Hussam: *Simulation von Mehrphasenvorgängen in porösen Medien unter Einbeziehung von Hysterese-Effekten*, 2000, ISBN 3-933761-03-4

101 Ayros, Edwin: *Regionalisierung extremer Abflüsse auf der Grundlage statistischer Verfahren*, 2000, ISBN 3-933761-04-2, vergriffen

102 Huber, Ralf: *Compositional Multiphase Flow and Transport in Heterogeneous Porous Media*, 2000, ISBN 3-933761-05-0

103 Braun, Christopherus: *Ein Upscaling-Verfahren für Mehrphasenströmungen in porösen Medien*, 2000, ISBN 3-933761-06-9

104 Hofmann, Bernd: *Entwicklung eines rechnergestützten Managementsystems zur Beurteilung von Grundwasserschadensfällen*, 2000, ISBN 3-933761-07-7

105 Class, Holger: *Theorie und numerische Modellierung nichtisothermer Mehrphasenprozesse in NAPL-kontaminierten porösen Medien,* 2001, ISBN 3-933761-08-5

106 Schmidt, Reinhard: *Wasserdampf- und Heißluftinjektion zur thermischen Sanierung kontaminierter Standorte*, 2001, ISBN 3-933761-09-3

107 Josef, Reinhold:, *Schadstoffextraktion mit hydraulischen Sanierungsverfahren unter Anwendung von grenzflächenaktiven Stoffen*, 2001, ISBN 3-933761-10-7

108 Schneider, Matthias: *Habitat- und Abflussmodellierung für Fließgewässer mit unscharfen Berechnungsansätzen*, 2001, ISBN 3-933761-11-5

109 Rathgeb, Andreas: *Hydrodynamische Bemessungsgrundlagen für Lockerdeckwerke an überströmbaren Erddämmen*, 2001, ISBN 3-933761-12-3

110 Lang, Stefan: *Parallele numerische Simulation instätionärer Probleme mit adaptiven Methoden auf unstrukturierten Gittern*, 2001, ISBN 3-933761-13-1

111 Appt, Jochen; Stumpp Simone: *Die Bodensee-Messkampagne 2001, IWS/CWR Lake Constance Measurement Program 2001*, 2002, ISBN 3-933761-14-X

112 Heimerl, Stephan: *Systematische Beurteilung von Wasserkraftprojekten,* 2002, ISBN 3-933761-15-8

113 Iqbal, Amin: *On the Management and Salinity Control of Drip Irrigation,* 2002, ISBN 3-933761-16-6

114 Silberhorn-Hemminger, Annette: *Modellierung von Kluftaquifersystemen: Geostatistische Analyse und deterministisch-stochastische Kluftgenerierung,* 2002, ISBN 3-933761-17-4

115 Winkler, Angela: *Prozesse des Wärme- und Stofftransports bei der In-situ-Sanierung mit festen Wärmequellen,* 2003, ISBN 3-933761-18-2

116 Marx, Walter: *Wasserkraft, Bewässerung, Umwelt - Planungs- und Bewertungsschwerpunkte der Wasserbewirtschaftung,* 2003, ISBN 3-933761-19-0

117 Hinkelmann, Reinhard: *Efficient Numerical Methods and Information-Processing Techniques in Environment Water,* 2003, ISBN 3-933761-20-4

118 Samaniego-Eguiguren, Luis Eduardo: *Hydrological Consequences of Land Use / Land Cover and Climatic Changes in Mesoscale Catchments*, 2003, ISBN 3-933761-21-2

119 Neunhäuserer, Lina: *Diskretisierungsansätze zur Modellierung von Strömungs- und Transportprozessen in geklüftet-porösen Medien*, 2003, ISBN 3-933761-22-0

120 Paul, Maren: *Simulation of Two-Phase Flow in Heterogeneous Poros Media with Adaptive Methods*, 2003, ISBN 3-933761-23-9

121 Ehret, Uwe: *Rainfall and Flood Nowcasting in Small Catchments using Weather Radar*, 2003, ISBN 3-933761-24-7

122 Haag, Ingo: *Der Sauerstoffhaushalt staugeregelter Flüsse am Beispiel des Neckars - Analysen, Experimente, Simulationen -,* 2003, ISBN 3-933761-25-5

123 Appt, Jochen: *Analysis of Basin-Scale Internal Waves in Upper Lake Constance,* 2003, ISBN 3-933761-26-3

124 Hrsg.: Schrenk, Volker; Batereau, Katrin; Barczewski, Baldur; Weber, Karolin und Koschitzky, Hans-Peter: *Symposium Ressource Fläche und VEGAS - Statuskolloquium 2003, 30. September und 1. Oktober 2003,* 2003, ISBN 3-933761-27-1

125 Omar Khalil Ouda: *Optimisation of Agricultural Water Use: A Decision Support System for the Gaza Strip,* 2003, ISBN 3-933761-28-0

126 Batereau, Katrin: *Sensorbasierte Bodenluftmessung zur Vor-Ort-Erkundung von Schadensherden im Untergrund*, 2004, ISBN 3-933761-29-8

127 Witt, Oliver: *Erosionsstabilität von Gewässersedimenten mit Auswirkung auf den Stofftransport bei Hochwasser am Beispiel ausgewählter Stauhaltungen des Oberrheins*, 2004, ISBN 3-933761-30-1

128 Jakobs, Hartmut: *Simulation nicht-isothermer Gas-Wasser-Prozesse in komplexen Kluft-Matrix-Systemen*, 2004, ISBN 3-933761-31-X

129 Li, Chen-Chien: *Deterministisch-stochastisches Berechnungskonzept zur Beurteilung der Auswirkungen erosiver Hochwasserereignisse in Flussstauhaltungen,* 2004, ISBN 3-933761-32-8

130 Reichenberger, Volker; Helmig, Rainer; Jakobs, Hartmut; Bastian, Peter; Niessner, Jennifer: *Complex Gas-Water Processes in Discrete Fracture-Matrix Systems: Upscaling, Mass-Conservative Discretization and Efficient Multilevel Solution,* 2004, ISBN 3-933761-33-6

131 Hrsg.: Barczewski, Baldur; Koschitzky, Hans-Peter; Weber, Karolin; Wege, Ralf: *VEGAS - Statuskolloquium 2004,* Tagungsband zur Veranstaltung am 05. Oktober 2004 an der Universität Stuttgart, Campus Stuttgart-Vaihingen, 2004, ISBN 3-933761-34-4

132 Asie, Kemal Jabir: *Finite Volume Models for Multiphase Multicomponent Flow through Porous Media*. 2005, ISBN 3-933761-35-2

133 Jacoub, George: *Development of a 2-D Numerical Module for Particulate Contaminant Transport in Flood Retention Reservoirs and Impounded Rivers,* 2004, ISBN 3-933761-36-0

134 Nowak, Wolfgang: *Geostatistical Methods for the Identification of Flow and Transport Parameters in the Subsurface,* 2005, ISBN 3-933761-37-9

135 Süß, Mia: *Analysis of the influence of structures and boundaries on flow and transport processes in fractured porous media*, 2005, ISBN 3-933761-38-7

136 Jose, Surabhin Chackiath: *Experimental Investigations on Longitudinal Dispersive Mixing in Heterogeneous Aquifers,* 2005, ISBN: 3-933761-39-5

137 Filiz, Fulya: *Linking Large-Scale Meteorological Conditions to Floods in Mesoscale Catchments,* 2005, ISBN 3-933761-40-9

138 Qin, Minghao: *Wirklichkeitsnahe und recheneffiziente Ermittlung von Temperatur und Spannungen bei großen RCC-Staumauern*, 2005, ISBN 3-933761-41-7

139 Kobayashi, Kenichiro: *Optimization Methods for Multiphase Systems in the Subsurface - Application to Methane Migration in Coal Mining Areas*, 2005, ISBN 3-933761-42-5

140 Rahman, Md. Arifur: *Experimental Investigations on Transverse Dispersive Mixing in Heterogeneous Porous Media,* 2005, ISBN 3-933761-43-3

141 Schrenk, Volker: *Ökobilanzen zur Bewertung von Altlastensanierungsmaßnahmen,* 2005, ISBN 3-933761-44-1

142 Hundecha, Hirpa Yeshewatesfa: *Regionalization of Parameters of a Conceptual Rainfall-Runoff Model*, 2005, ISBN: 3-933761-45-X

143 Wege, Ralf: *Untersuchungs- und Überwachungsmethoden für die Beurteilung natürlicher Selbstreinigungsprozesse im Grundwasser,* 2005, ISBN 3-933761-46-8

144 Breiting, Thomas: *Techniken und Methoden der Hydroinformatik - Modellierung von komplexen Hydrosystemen im Untergrund*, 2006, 3-933761-47-6

145 Hrsg.: Braun, Jürgen; Koschitzky, Hans-Peter; Müller, Martin: *Ressource Untergrund: 10 Jahre VEGAS: Forschung und Technologieentwicklung zum Schutz von Grundwasser und Boden,* Tagungsband zur Veranstaltung am 28. und 29. September 2005 an der Universität Stuttgart, Campus Stuttgart-Vaihingen, 2005, ISBN 3-933761-48-4

146 Rojanschi, Vlad: *Abflusskonzentration in mesoskaligen Einzugsgebieten unter Berücksichtigung des Sickerraumes,* 2006, ISBN 3-933761-49-2

147 Winkler, Nina Simone: *Optimierung der Steuerung von Hochwasserrückhaltebecken-systemen,* 2006, ISBN 3-933761-50-6

148 Wolf, Jens: *Räumlich differenzierte Modellierung der Grundwasserströmung alluvialer Aquifere für mesoskalige Einzugsgebiete*, 2006, ISBN: 3-933761-51-4

149 Kohler, Beate: *Externe Effekte der Laufwasserkraftnutzung*, 2006, ISBN 3-933761-52-2

150 Hrsg.: Braun, Jürgen; Koschitzky, Hans-Peter; Stuhrmann, Matthias: *VEGAS-Statuskolloquium 2006,* Tagungsband zur Veranstaltung am 28. September 2006 an der Universität Stuttgart, Campus Stuttgart-Vaihingen, 2006, ISBN 3-933761-53-0

151 Niessner, Jennifer: *Multi-Scale Modeling of Multi-Phase - Multi-Component Processes in Heterogeneous Porous Media*, 2006, ISBN 3-933761-54-9

152 Fischer, Markus: *Beanspruchung eingeerdeter Rohrleitungen infolge Austrocknung bindiger Böden,* 2006, ISBN 3-933761-55-7

153 Schneck, Alexander: *Optimierung der Grundwasserbewirtschaftung unter Berücksichtigung der Belange der Wasserversorgung, der Landwirtschaft und des Naturschutzes*, 2006, ISBN 3-933761-56-5

154 Das, Tapash: *The Impact of Spatial Variability of Precipitation on the Predictive Uncertainty of Hydrological Models,* 2006, ISBN 3-933761-57-3

155 Bielinski, Andreas: *Numerical Simulation of CO_2 sequestration in geological formations*, 2007, ISBN 3-933761-58-1

156 Mödinger, Jens: *Entwicklung eines Bewertungs- und Entscheidungsunterstützungssystems für eine nachhaltige regionale Grundwasserbewirtschaftung*, 2006, ISBN 3-933761-60-3

157 Manthey, Sabine: *Two-phase flow processes with dynamic effects in porous media - parameter estimation and simulation,* 2007, ISBN 3-933761-61-1

158 Pozos Estrada, Oscar: *Investigation on the Effects of Entrained Air in Pipelines,* 2007, ISBN 3-933761-62-X

159 Ochs, Steffen Oliver: *Steam injection into saturated porous media – process analysis including experimental and numerical investigations*, 2007,
ISBN 3-933761-63-8

160 Marx, Andreas: *Einsatz gekoppelter Modelle und Wetterradar zur Abschätzung von Niederschlagsintensitäten und zur Abflussvorhersage, 2007,*
ISBN 3-933761-64-6

161 Hartmann, Gabriele Maria: *Investigation of Evapotranspiration Concepts in Hydrological Modelling for Climate Change Impact Assessment*, 2007,
ISBN 3-933761-65-4

162 Kebede Gurmessa, Tesfaye: *Numerical Investigation on Flow and Transport Characteristics to Improve Long-Term Simulation of Reservoir Sedimentation*, 2007,
ISBN 3-933761-66-2

163 Trifković, Aleksandar: *Multi-objective and Risk-based Modelling Methodology for Planning, Design and Operation of Water Supply Systems*, 2007,
ISBN 3-933761-67-0

164 Götzinger, Jens: *Distributed Conceptual Hydrological Modelling - Simulation of Climate, Land Use Change Impact and Uncertainty Analysis*, 2007,
ISBN 3-933761-68-9

Die Mitteilungshefte ab dem Jahr 2005 stehen als pdf-Datei über die Homepage des Instituts: www.iws.uni-stuttgart.de zur Verfügung.